AD_____

Award Number: **W81XWH-12-1-0511**

TITLE: **Large Extremity Peripheral Nerve Repair**

PRINCIPAL INVESTIGATOR: **Robert W. Redmond Ph.D.**

CONTRACTING ORGANIZATION: **Massachusetts General Hospital**
Boston, MA 02114

REPORT DATE: **December 2016**

TYPE OF REPORT: **Final**

PREPARED FOR: U.S. Army Medical Research and Materiel Command
Fort Detrick, Maryland, 21702-5012

DISTRIBUTION STATEMENT: Approved for Public Release;
Distribution Unlimited

The views, opinions and/or findings contained in this report are those of the author(s) and should not be construed as an official Department of the Army position, policy or decision unless so designated by other documentation.

REPORT DOCUMENTATION PAGE

Form Approved
OMB No. 0704-0188

1. REPORT DATE	2. REPORT TYPE	3. DATES COVERED
December 2016	Final	30 Sep 2012 - 29 Sep 2016

4. TITLE AND SUBTITLE
Large Extremity Peripheral Nerve Repair

5a. CONTRACT NUMBER

5a. GRANT NUMBER
W81XWH-12-1-0511

5c. PROGRAM ELEMENT NUMBER

6. AUTHOR(S)
Robert W. Redmond Ph.D.
Jonathan M. Winograd M.D.
CDR Mark E. Fleming M.D. MC, USN

E-Mail: redmond@helix.mgh.harvard.edu

5d. PROJECT NUMBER

5e. TASK NUMBER

5f. WORK UNIT NUMBER

7. PERFORMING ORGANIZATION NAME(S) AND ADDRESS(ES) AND ADDRESS(ES)
The Massachusetts General Hospital,
55 Fruit Street, Boston, MA 02114. and
Walter Reed National Military Medical Center
8901 Wisconsin Avenue, Bethesda, MD 20814

8. PERFORMING ORGANIZATION REPORT NUMBER

9. SPONSORING / MONITORING AGENCY NAME(S) AND ADDRESS(ES)
U.S. Army Medical Research and Materiel Command

Fort Detrick, Maryland 21702-5012

10. SPONSOR/MONITOR'S ACRONYM(S)

11. SPONSOR/MONITOR'S REPORT NUMBER(S)

12. DISTRIBUTION / AVAILABILITY STATEMENT
Approved for Public Release; Distribution Unlimited

13. SUPPLEMENTARY NOTES

14. ABSTRACT

In current war trauma, 20-30% of all extremity injuries and >80% of penetrating injuries being associated with peripheral nerve damage, typically involve large segmental nerve deficits. Standard repair uses autologous nerve graft, secured by suture. Outcomes are unsatisfactory, affecting quality of life and return to active duty. We have investigated a sutureless, light-activated technology for sealing nerve grafts to produce an immediate seal that optimizes the regenerating nerve environment. Our studies have shown that biocompatible chemical crosslinking of human amnion considerably strengthens and protects it from biodegradation in vivo that compromises their function as nerve wrap sealants. Rodent studies of segmental nerve deficit repair using isograft show the best performing wrap/ fixation method to be sutureless photochemical tissue bonding with the crosslinked amnion wrap. Autograft is often unavailable in wounded warriors, due to extensive tissue damage and amputation and, importantly, we also showed nerve regeneration using our approach with an acellular nerve allograft to be equivalent to standard autograft repair in rodent models. Outcomes have now been validated in a large animal (swine) model with 5 cm ulnar nerve deficit where electrophysiological outcomes for light-activated sealing of a commercial nerve graft conduit (Avance^{TM}) were equivalent to standard of care autograft.

15. SUBJECT TERMS

16. SECURITY CLASSIFICATION OF:	17. LIMITATION OF ABSTRACT	18. NUMBER OF PAGES	19a. NAME OF RESPONSIBLE PERSON
			USAMRMC

a. REPORT	b. ABSTRACT	c. THIS PAGE		94	19b. TELEPHONE NUMBER *(include area code)*
U	U	U	UU		

Table of Contents

Page

1. Introduction.

The goal of the research performed in this project is to develop a new technology for repair of peripheral nerve injuries involving significant neural deficit with improved functional outcomes for the wounded warrior. The research addresses drawbacks of current methods of suture attachment of nerve grafts and involves development of both a sutureless fixation method to place the nerve graft and an optimal wrap material to seal the endoneurial environment for regeneration. Reduction in needle trauma, reduced inflammation and scarring and sealing the endoneurial environment should all contribute to improved clinical outcomes.

2. Keywords: Nerve injury, nerve gap, nerve wrap, PTB, photosealing, Rose Bengal, amnion, nerve conduit, crosslinking, allograft, photochemistry.

3. Accomplishments:

Major Goals of the Project

Task 1– Determine mechanical properties, seal strength and resistance to biodegradation of candidate photochemical nerve wrap biomaterials. (Months 1-10)

Task 1a. Regulatory approval of use of human tissue by Partners (MGH) IRB and review and approval by USAMRMC Office of Research Protections (human amniotic membrane, HAM). (Months 1-4, MGH: Winograd/Redmond)

Regulatory approval for the use of discarded human tissue (Amniotic membrane) was obtained from both the MGH Institutional Review Board and the USAMRMC Office of Research Protections in August 2012.

Task 1b. Regulatory approval of rodent sciatic nerve for nerve wrap bond measurements by MGH IACUC and review and approval by USAMRMC Office of Research Protections (ACURO). (Months 1-4, MGH: Redmond)

Approvals for the rodent protocols to be used in Task 2 were obtained from the MGH IACUC (protocol #2012N000117) and ACURO approval on 11/19/2012.

Task 1c. Mechanical testing of AxoGuard nerve protector (Months 2-4, MGH: Redmond)

The AxoGuard nerve protector proved to be too thick for facile use in photochemical tissue bonding experiments in the rodent model. It was not possible to wrap this material around the small caliber rat sciatic nerve without undue mechanical tension on the wrap that tended to disrupt the contact between nerve and wrap. This required a search for a different source of commercial nerve wrap material, described below in Task 1i.

Task 1d. Processing of HAM and crosslinking with EDC to make xHAM. (Months 4-6, MGH: Redmond)
Task 1e. Mechanical testing (ultimate stress and Young's Modulus) of HAM and xHAM. (Months 4-6, MGH: Redmond)

We have completed processing of human amniotic membrane (HAM) and chemical crosslinking with EDC/NHS to make the crosslinked HAM (xHAM) that should resist biodegradation in vivo. A chemical crosslinking system (EDC (1-ethyl-3-(3-dimethylaminopropyl) carbodiimide), a water soluble agent used with N-hydroxysuccinimide (NHS) for coupling carboxyl groups with primary amines to form

amide bonds in proteins) was used at different concentrations under conditions of one hour incubation at room temperature and the resultant mechanical properties measured using a microtensiometer. Figures 1A and 1B show the effect of chemical crosslinker on the maximum stress and Young's modulus (stiffness) of HAM, measured using a microtensiometer. As expected, crosslinking imparts a greater strength and stiffness to the HAM, especially at the higher concentrations used.

Task 1f. Determine resistance of nerve wraps to collagenase digestion. (Months 4-6, MGH: Redmond).

Biodegradation of HAM as a function of EDC/NHS treatment was determined in the presence of 0.1% collagenase, a high concentration used in our laboratory for extraction of chondrocytes from cartilage. Two assays were used (a) time to complete dissolution and (b) rate of release of amine containing amino acids using the fluorescamine assay.

As can be seen in Figure 2, crosslinking of HAM with EDC/NHS has a large effect on the ability of HAM to resist biodegradation. Figure 2A shows that the uncrosslinked HAM is dissolved in the first hour of treatment whereas all treated samples remain intact even up to 24 h. A more detailed approach using the fluorescamine assay (Figure 2B) to detect amino-acid residues released on degradation shows that increasing EDC/NHS reduces rate and extent of degradation measured in this fashion. This is a highly positive result as a major limiting factor for use in nerve repair would be rapid degradation of the HAM wrap in vivo and this treatment affords considerable protection.

Task 1g. Rat sciatic nerve harvest from 20 Lewis rats. (Months 6-8, MGH: Randolph/Winograd)
Task 1h. Measure bonding strengths of wraps to ex vivo sciatic nerve (months 6-8, MGH: Redmond)

One of the strategies for sutureless graft fixation in this project involves photochemical bonding of a nerve wrap at the graft/nerve stump junction. Studies above show that chemical crosslinking with EDC/NHS strengthens the wrap material and increases its resistance to biodegradation. It is, however, important to evaluate whether this chemical crosslinking could interfere with the ability to *photochemically* bond the wrap material around the epineurium. Thus, rat sciatic nerves were harvested from donor rats immediately post-euthanasia (Task 1g) and bonding of the wrap around the nerve ends performed following application of 0.1% Rose Bengal dye in saline and illumination at 532 nm. The HAM wrap/nerve sample was then mounted in a microtensiometer, as shown in Figure 3, and the tensile load increased until bond failure.

The bond strength of the EDC/NHS treated HAM remains unchanged until the highest tested concentration of 8mM/2mM (EDC/NHS), when a statistically significant decrease is observed with respect to control ($p<0.05$). At this higher concentration the xHAM becomes brittle and more difficult to handle. Figure 4 shows the data for bond strength as a function of treatment parameters.

In Task 1h we focused on determining the failure strength of the bond formed between ex vivo nerve segments as a function of the fixation procedure, in preparation for the corresponding rat experiments in Task 2. Figure 5 shows the results obtained with the three fixation methods under study (a) epineurial suture, (b) fibrin glue and (c) photochemical tissue bonding (PTB) with a wrap material. All methods induced bonding between the nerve segments with bond strength in the order of suture>PTB>fibrin glue. Conventional epineurial suturing using six 10.0 nylon sutures resulted in the strongest bond. This bond was significantly greater than any of the bonds created by PTB ($p<0.05$). The strength of the bonds created by PTB were not significantly different from those created following 4-suture epineurial repair. The caliber of the rat sciatic nerve is comparable to a human digital nerve. The use of four epineurial sutures in this situation is clinically realistic and is therefore supportive of the bond strength imparted by PTB. Little difference was seen between uncrosslinked HAM or crosslinked xHAM, except at the highest crosslinker concentration used. In the rat repair model in Aim 2 we chose to use the xHAM due to its increased resistance to enzymatic degradation.

Although bond strength is not really an issue in nerve repair, which should ideally be tension-free, these results show that the PTB method can provide fixation strengths approaching that of conventional microsurgery and that the PTB repair is unlikely to be disturbed in vivo.

The results in Figure 5 were obtained with PTB parameters of 0.1% Rose Bengal with 532 nm light delivered at an irradiance of 0.5 W/cm^2 and a fluence of 60 J/cm^2. To further explore the optimal dosimetry conditions for the rat experiments in Aim 2, we performed a fluence dependence study using light delivered at an irradiance of 0.5 W/cm^2 for various durations. Figure 6 shows the fluence dependence of the bond strength formed using PTB/xHAM (4mM/1mM (EDC/NHS)) to reattach the nerve segments ex vivo. A fluence of 60 J/cm^2 resulted in superior bond strength in comparison to 30, 120 and 240 J/cm^2 ($p<0.05$). Interestingly, bond strength was significantly weaker with the highest fluence, presumably due to increasing friability of the amnion wrap. Those nerve/wrap preparations treated with no illumination predictably had negligible bond strength. An irradiance of 0.5W/cm^2 and a fluence of 60J/cm^2 equates to an illumination duration of 120 seconds (60 seconds per nerve/wrap side) and this was felt to be clinically acceptable for use in the animal studies in Aim 2.

The anatomy of HAM is shown pictorially in Figure 7. In vivo, the epithelial layer is in contact with the amniotic fluid while the spongy layer is in contact with the chorion. During preparation the amnion is de-epithelialized but there remains the question as to "which way up" the HAM should be bonded to the nerve. To that end we performed experiments where we were careful to note the surface in contact with the nerve and the resultant bond strength obtained after bonding with 60 J/cm^2 of 532 nm light delivered at an irradiance of 0.5 W/cm^2. Figure 8 shows that the bond strength between nerve and amnion was not significantly different to the epithelial and chorionic surfaces. This finding has helped simplify processing and storage of the amnion and also intra-operative handling.

The outcome of these experiments has helped confirm the following optimum conditions to apply to the in-vivo rodent survival operations in aim 2:

- Amnion cross-linked with 4mM 1-ethyl-3-(3-dimethylaminopropyl) carbodiimide (EDC)/1mM H-hydroxysuccinimide (NHS)
- Laser irradiance of 0.5 W/cm^2 and fluence of 60 J/cm^2
- Amniotic epithelial and chorionic surfaces bond equally well

Task 1i. Data analysis, conclusions and consideration of alternative wrap materials, if required (Months 6-10, MGH: Redmond)

In this task we focused on determining the best candidate commercial wrap to evaluate in PTB studies for nerve repair. As outlined in the original project proposal, our plan was to use a tubular swine intestinal submucosa (SIS) product called AxoGuard manufactured by AxoGen. Following initial trials this product was found to be unsuitable as it was too thick and possessed too much inherent shape memory to permit easy wrapping around the small diameter rat sciatic nerve. Intimate contact between tissue surfaces is an essential pre-requisite for photochemical tissue bonding. Following this discovery, we conducted a thorough search of alternative commercially available biomaterials that could satisfy our needs.

The following products were sampled and assessed for their conformability and bonding ability:

1. AxoGuard (multi-layer SIS – AxoGen)
2. NeuraGen (Collagen – Integra)
3. NeuraWrap (Collagen – Integra)
4. Tenoglide (Collagen – Integra)

5. NeuraMend (Collagen – Stryker)
6. NeuraMatrix (Collagen – Stryker)
7. Colafilm (Collagen – Innacol)
8. Amniofix (Collagen – MiMedx)
9. SurgiMend (Collagen – TEI Biosciences)
10. Oasis (Single layer SIS – HealthPoint)

Options 1-9 were also found to be unsuitable due to similar problems regarding excessive material thickness, stiffness, shape memory and inability of the material to conform satisfactorily around the rat sciatic nerve.

Option 10 is a single layer SIS product that met our requirements. Oasis is a product marketed and distributed as a wound dressing by HealthPoint. Although the material is approximately double the thickness of human amnion, it was sufficiently thin to allow circumferential nerve wrapping and close contact between wrap and epineurium. In fact, we discovered that both AxoGuard and Oasis SIS products are manufactured by Cook Medical. AxoGuard is simply a multi-layered SIS product.

Biomechanical testing of the single layer SIS material showed a Young's modulus (Fig. 9) and a maximum load to failure (Fig. 10) that were considerably greater than that that of human amnion (See Figs. 1 and 2). Similar to earlier HAM studies the chemical crosslinking of SIS with increasing concentrations of EDC/NHS, gave an increase in Young's modulus and maximum load to failure. (Figs. 9 and 10). Digestion with 0.1% collagenase showed that increasing the concentration of EDC/NHS crosslinker reduced the rate of proteolytic degradation (Fig. 11) thus, extending the longevity of the material in vivo. This finding was consistent with those results observed with HAM and satisfied our goal to increase the in-vivo survival of nerve wrap biomaterial during long periods of recovery associated with large nerve deficit reconstruction and long nerve grafts.

As with the human amnion nerve wraps, it was important for us to confirm that, in addition to increasing the resistance to enzymatic degradation, EDC/NHS crosslinking of SIS did not interfere with photochemical tissue bonding. Figure 12 shows that there was no significant drop in bond strength measured by ex-vivo tensiometer testing. Interestingly, bond strength between SIS nerve wrap and sciatic epineurium was significantly greater than that found with untreated and crosslinked human amnion.

Milestones for Task 1 included the following, with decisions taken at the joint meetings of Partnering PI's, held at MGH, WRNMMC and mutual conferences.

- *Obtain MGH and DOD approvals for all protocols*
- *Determine mechanical properties of wrap materials and establish suitability for use in PTB. Modify processing of wraps and utilize alternate wraps if necessary*
- *Determine bond strength of wraps to ex-vivo nerve and synthetic graft. Modify processing of wraps and utilize alternate wraps if necessary.*
- *Collate results and determine best nerve wraps to use in Task 2*
- *Prepare publications and presentations based on Task 1 research results*

All the above milestones have been met, as described above.

Task 2 – Determine efficacy of nerve regeneration in a rodent model of segmental nerve deficit injury as a function of wrap and fixation procedure. (Months 6-22).

Task 2a. Regulatory approval for rodent study of segmental deficit repair by MGH IACUC and review and approval by USAMRMC Office of Research Protections (ACURO). (Months 1-4, MGH: Redmond/Winograd/Randolph)

This aim involved a large study of peripheral nerve repair in a rat sciatic nerve model using isogeneic Lewis rats. The animal protocol for these experiments received IACUC approval at the Massachusetts General Hospital (protocol #2012N000117) and was also granted ACURO approval on 11/19/2012.

Task 2b. Rodent surgeries for segmental deficit and repair using isograft with 110 Lewis rats. (Months 6-8, MGH: Winograd/Randolph)

A total of 110 rodents underwent survival surgery, commencing on 2/26/2013 and completed on 5/10/2013.

Task 2c. Biweekly functional recovery testing by gait analysis in isograft study. (Months 6-14, MGH: Redmond)

Functional recovery in each rodent during the 5-month follow-up period was measured by monthly walking track analysis using the well-established Sciatic Function Index (SFI) as calculated from the paw-prints of the rodents as a function of time after surgery. As predicted, those animals in the negative control group (no repair following nerve deficit injury) experienced no functional recovery as illustrated by a complete lack of correction of the sciatic function index (-96.2+/-3.7). A value of -100 indicates zero functional recovery. Despite performing well in ex vivo experiments, those isografts wrapped with the commercially sourced SIS material performed worst out of all biological nerve wraps. In SIS+suture and SIS+PTB groups, this was statistically significant in comparison to standard repair (positive control). Isografts wrapped with cross-linked human amnion and secured with PTB (xHAM+PTB) exhibited the greatest functional recovery value although this did not reach statistical significance in comparison to the positive control group (SFI = -67.93+/-5.11 vs -71.69+/-4.80). There was no statistically significant difference between any of the remaining experimental groups compared to the positive control group. Table 1 provides a summary of the functional data.

It should be noted that although walking track analysis is a well-accepted outcome measure for functional assessment following rodent peripheral nerve surgery, the method has several recognised limitations that have been encountered. The inked footprints are rarely perfect and are open to considerable inter-observer variability. Walking track analysis is also limited by experimental hind-paw clawing. Although this was not a major problem, a small number of rodents at later time points in the majority of experimental groups were excluded from the calculation of mean SFIs due to unmeasurable footprints. Clawing results due to injury and incomplete recovery of the nerve supply to intrinsic musculature in the hind foot and may be exacerbated by the lack of physical rehabilitative measures that would ordinarily be introduced in human subjects. Although not thoroughly assessed, the presence of clawing did not seem to affect the reinnervation and retention of gastrocnemius muscle mass and therefore this problem may be limited to walking track analysis. Thus, SFI results are useful but a decision regarding which wrap and fixation method to proceed with in the next step could not be taken solely on this metric.

Task 2d. Gastrocnemius muscle harvest and muscle mass retentions in isograft study (Months 12-14, MGH: Redmond)

Following sacrifice, both experimental left sided gastrocnemius muscle and contralateral right-sided control muscle were harvested from each rodent. Wet muscle mass was recorded immediately following harvest and percentage muscle mass retention calculated. Mean muscle mass retention in the negative

control group was only 9.2% +/- 0.92. As expected, this was significantly less that achieved in the standard microsurgical repair group. Greatest muscle mass retention occurred in the xHAM+PTB group and the increase over standard microsurgical repair was statistically significant (67.3% +/- 4.44 vs 60.0% +/-5.16; p=0.02). There was no statistically significant difference between the positive control group and any of the remaining experimental groups. Wraps secured with fibrin glue performed consistently better than those secured with suture although these effects did not reach statistical significance. Table 2 provides a summary of muscle mass retention data.

Task 2e. Histomorphometric analysis of proximal and distal fibers in isograft study (Months 12-16, MGH: Redmond/Winograd)

Following sacrifice, left sciatic nerves were harvested and sent for histology. Nerves were harvested from a distance 5mm proximal to the proximal isograft neurorrhaphy site to 5mm distal to the distal neurorrhaphy. Following 24-hours of fixation, each nerve was cut into proximal, mid-graft and distal sections. Following dehydration and epoxy resin embedding, 1-micron slices of each specimen were cut and mounted for histomorphometric analysis. Axon counts and G-ratio (marker of myelination) were measured from scanned images. All histologic specimens were collected and prepared for sectioning.

Histomorphomeric analysis of all groups is shown in Table 3 and Figure 13. Axon counts at the distal section site did not differ significantly between treatment groups and positive controls. Those nerves that were repaired with crosslinked amnion and PTB (xHAM+PTB) recovered significantly greatest fiber diameter, axon diameter and myelin thickness (Table 3; Fig 13). The corrected values (G-ratio) for myelination were not significantly different. These results support earlier functional data on sciatic function index (SFI) and muscle mass retention with xHAM+PTB performing best of all repair procedures.

Task 2f. Determination of axonal migration, endoneurial scarring in isograft study. (Months 12-16, MGH: Redmond/Randolph/Winograd)

Previous studies from our lab have suggested that, in addition to creating a watertight seal at the neurorrhaphy site, photochemical tissue bonding also reduces the formation of fibrinous adhesions around the nerve. Although this is difficult to quantify, observations following rodent sacrifice in this study have supported this (Figure 14).

Task 2g. Decision on wrap/fixation method for Avance^{TM} nerve graft studies in rodent model. (Month 16, All PI's)

This decision was made based on the composite results from gait analysis, muscle mass retention and histomorphometric studies that showed that of all approaches used the best outcomes were reproducibly observed when the PTB+xHAM procedure was used (see above). This was due to statistically significant increases in gastrocnemius muscle mass retention and histomorphometric outcomes including fiber diameter, axon diameter and myelin thickness along with equivalent SFI results in comparison to standard microsurgical repair of peripheral nerve injury involving significant nerve deficit using autograft (isograft) repair. Thus, for the isograft studies the wrap/fixation method chosen was PTB+xHAM in a model of rat sciatic nerve injury with deficit.

In the original proposal, our intention was to purchase the Avance processed human allograft from AxoGen for use in this final phase of the rodent studies. After discussion with AxoGen scientists and a review of the most recent literature on the use of human versus rat allograft in rodent models, we concluded that the human-sourced nerve may not be optimal for rodent studies (due to the potential for cross-species immunoreactivity being greater than originally expected) and that for the purpose of these studies it would be better use processed rodent allograft. We then harvested, froze and stored donor rat

sciatic nerve before shipping to AxoGen for processing. A Material Transfer Agreement was agreed between MGH and AxoGen and delivery of the processed nerve was concluded in December 2013. The returned allografts were of excellent quality. Microscopic examination revealed no evidence of epineurial fragmentation and fascicular architecture appeared intact. The grafts were pliable and resembled autogenous tissue.

Task 2h. Rodent surgeries for segmental deficit and repair using rat processed allograft (MGH: Winograd/Randolph)

Surgery was completed on the remaining 2 groups (n=10) of acellular nerve allograft (ANA) repairs in rodents. ANA secured using xHAM+PTB (using optimal crosslinking conditions of 4mM/1mM EDC/NHS and 532 nm illumination at an irradiance of 0.5 W/cm^2 and fluence of 60 J/cm^2) were compared to a control group where ANA was secured using conventional 10-0 epineurial suture. The rat-processed nerve bore very close resemblance to freshly harvested autogenous nerve and was easy to handle intra-operatively. No issues were encountered when photochemically bonding the nerve. Walking track analysis, calculation of sciatic function index (SFI) (Table 4)) and measurement of gastrocnemius muscle mass retention was completed (Table 5). Histology processing of excised nerve tissue was also completed and results of histomorphometric analysis are summarized in Table 6.

Task 2i. Biweekly functional recovery testing by gait analysis in Avance® nerve graft study. (Winograd/Randolph/Redmond - Months 16-20)

While photochemically sealed ANA showed an improvement in SFI in comparison to sutured ANA (-80.3+/-4.2 vs. -78.3+/-5.0; Table 4 and Fig.15), the difference was not statistically significant. When the analogous isograft studies from this Task were included for comparison, the isograft+xHAM/PTB group recovered greatest SFI after 5-months follow-up (Table 4). This was not statistically significant in comparison to isograft+suture. ANA+suture performed statistically worse than isograft+suture (-80.3+/-4.2 vs. -71.7+/-4.8; p=0.0019; Table 1 and 4). SFI was also statistically less for ANA+xHAM/PTB in comparison to isograft+xHAM/PTB (Table 4) but not significantly different from the standard of care isograft+suture repair.

Task 2j. Gastrocnemius muscle harvest and muscle mass retentions in Avance® nerve graft study. (Winograd/Randolph/Redmond - Months 20-22)

Although ANA+xHAM/PTB displayed a trend towards greater muscle mass recovery in comparison to ANA+suture, this result was not statistically significant (55.2+/-5.5% vs. 52.9+/-4.77%; Table 5, Fig 16). When the analogous isograft repairs are considered, the isograft+xHAM/PTB recovered greatest gastrocnemius muscle mass retention and this was statistically significant in comparison to all other groups (Table 5). Muscle mass recovery was statistically poorer in ANA+suture group in comparison to isograft+suture group. Likewise, recovery of ANA+xHAM/PTB was statistically poorer than isograft+xHAM/PTB. Muscle mass retention in the ANA+xHAM/PTB group was statistically comparable to that achieved using gold standard isograft+suture.

Task 2k. Histomorphometric analysis of proximal and distal fibers in Avance® nerve graft study. (Winograd/Randolph/Redmond - Months 20-22)

Although not statistically significant, fiber diameter, axon diameter and myelin thickness in the ANA+xHAM/PTB group displayed a trend towards greater recovery in comparison to ANA+suture. When considering analogous isograft repair groups, isograft+xHAM/PTB recovered the greatest fiber

diameter, axon diameter and myelin thickness and this was statistically significant in comparison to all other groups (Table 6). Axon counts in the distal nerve stump were significantly greater for isograft+xHAM/PTB in comparison to ANA+suture. No other significant differences in axon counts or axon density existed between treatment groups. Histomorphometric recovery was poorest in the ANA+suture group and this was statistically significant in comparison to isograft+suture and isograft+xHAM/PTB. There was no significant difference between ANA+xHAM/PTB and gold standard isograft+suture (Table 6).

Task 2l. Determination of axonal migration, endoneurial scarring in Avance® nerve graft study. (Winograd/Randolph/Redmond - Months 20-22)

As with previous isograft studies, the formation of extraneural scar tissue was qualitatively less with photochemical repair in comparison to suture repair (Fig 17).

Task 2m. Decision on Avance® nerve graft procedure for large animal studies in Aim 3. (All PIs, Month 22)

This study shows that outcomes following light-activated sealing of ANA with PTB/xHAM are improved in comparison to sutured ANA, and are statistically equivalent to gold standard sutured isografts. Based on these findings, isografts that are photochemically sealed with crosslinked amnion nerve wraps have emerged as the superior reconstructive method for large gap nerve repair. However, the ability to elevate the performance of ANA to match the current gold standard is of major clinical interest when severe injuries to wounded warriors, complicated with limb loss, preclude the use of autograft. The demonstrated success of light-activated sealing of isograft coaptation sites is likely related to the creation of a water-tight seal and the subsequent containment of the neurotrophic rich milieu. It is possible that removal of Schwann cells (SC), and the neurotrophic factors they liberate, during decellularization of ANAs, may partially abrogate this effect. However, the benefit observed suggests that the technique remains advantageous. The avoidance of suture-induced inflammation and fibrosis, the exclusion of infiltrating scar tissue and the prevention of axonal escape may be responsible.

Following decellularization, ANAs consist of basal lamina scaffolds. Components of the basal lamina such as fibronectin and laminin have pro-regenerative effects on neurite outgrowth and can support axonal regeneration in the absence of SCs. Whilst this may be sufficient over short lengths of ANA, successful regeneration across longer lengths is dependent on re-population of ANA by resident SCs. This study did not assess the extent of SC re-population but it is possible that photochemical sealing may augment SC migration, further improving regeneration through long ANAs. Investigating SC repopulation in ANAs of varying length may form the basis of future investigation. When combined with cell-based therapy and tissue engineering, sealing the regenerative milieu and maintaining high levels of growth promoting factors at the repair site, may amplify this effect.

With these acellular nerve allograft studies showing equivalent nerve regeneration outcomes for photochemical sealing of ANA or standard of care sutured autograft and promise in the use of ANA in this fashion for wounded warriors that lack sufficient autograft for standard repair, we were confident in this approach to progress to large animal studies.

Milestones for Task 2 include the following, with decisions taken at the quarterly meetings of Partnering PI's, held alternately at MGH and WRNMMC.

- *Obtain MGH and DoD approvals for all protocols.*
- *Complete all rodent surgeries and repair groups for isograft study.*

- *Determine lead wrap/fixation method for best functional recovery in isograft model and proceed with this method for Avance nerve graft study*
- *Determine method for rodent acellular nerve allograft (ANA) preparation*
- *Complete all rodent surgeries and repair groups for Avance nerve graft study*
- *Analyze recovery of function, muscle mass retention and histomorphometry data.*
- *Determine animal model and best photosealing procedure for Avance nerve graft vs autograft large animal study in Task 3*
- *Prepare publications and presentations based on Task 2 research results.*

All above milestones were completed

Task 3. Explore efficacy of lead wrap/fixation approach against standard of care autograft in large animal model of large segmental nerve deficit.

Task 3a. Regulatory approval for swine study of segmental deficit repair. (Winograd, Randolph/Redmond, Months 23-34)

Rodent studies to determine the best wrap/fixation method for use in repair of large segmental nerve deficits using autograft showed the best performing repair method to be photosealing using a crosslinked human amnion wrap. In the subsequent allograft study, this method again performed well, reaching statistical equivalence to standard of care autograft repair by microsurgery. This approach therefore shows potential for improving outcomes in wounded warfighters with large nerve deficit injuries where no autograft is available due to concomitant trauma.

Large animal studies of segmental deficit repair were proposed in Phase 3 as a step towards human deployment, originally calling for repair of a 5 cm deficit in the median nerve of sheep. However, in discussion with scientists at the Axogen company regarding their Avance nerve allograft product the difference in sheep and human nerve structure rendered sheep an unsuitable model for interpositional repair with the Avance product. The consensus was to replace sheep with a swine median nerve deficit model, which is equally well-tolerated by the animals, using the Avance acellular nerve allograft (from humans). Axogen scientists did not expect immunogenicity to be an issue with these studies but we investigated the validity of this assumption with an initial pilot study in the swine model before proceeding to the full study. The protocol for these studies was submitted to the IACUC at MGH in early October 2014 and was approved on 12/23/14. The protocol was forwarded to ACURO for approval in January and ACURO approval was granted on May 26, 2015.

Following ACURO approval the challenge was to obtain MGH miniature swine for these experiments. The proposed model was initially a 5 cm defect in swine median nerve (n=10 swine, bilateral repair, n=20 repairs), representative of large nerve deficit injury typically seen in combat trauma. However, on exploratory dissection on a euthanized swine from another study it became clear that there was a considerable size mismatch between the larger median nerve and the smaller medial saphenous nerve, and that the ulnar nerve was a much better size match to the saphenous nerve graft and its more superficial anatomical location made it a superior choice for surgical access with minimal morbidity to the animal. Additionally, the flexor carpi ulnaris muscle proved to be a better choice for functional electrophysiology testing. Thus, we amended the animal protocol with the MGH IACUC and received approval on September 15, 2015 and ACURO approval on September 29, 2015. Under this protocol, injuries either underwent definitive repair using (a) Avance nerve graft and photosealing or (b) standard microsurgical suture repair with an autologous nerve graft of medial

saphenous nerve harvested intraoperatively from a hind limb. This standard of care repair serves as a positive control.

3b. Surgical procedures to create segmental deficit in swine model. (Months 35-37)
3c. Repair of nerve deficit by Avance® and autograft in swine model. (Months 35-37)

We planned and executed a pilot arm to investigate whether swine woul immunologically tolerate a human cadaveric decellularized nerve graft. Commercially available graft, Avance, is pretreated to remove cellular debris and immunogenicity. The pilot arm of our study was to perform 3 nerve repairs to determine whether there would be any significant cross-reactivity or acute rejection between species despite the decellularization process. Therefore the first group of swine (n=3 pigs, n=3 repairs) was scheduled to undergo surgical injury and immediate repair (Avance + microsurgical repair, Avance + PTB and autograft + microsurgery). After 30 days, animals were euthanized and samples harvested for histological analysis for signs of acute rejection. Surgeries were completed by October 14, 2015 and harvests by November 13, 2015. Initial H&E stained sections showed the presence of inflammatory cells in both Avance and isograft repairs (Figure 18). Sections were tested with immuno-histochemical staining for macrophages vs. lymphocytes to determine whether inflammatory response was due to the injury itself vs. acute rejection of the Avance graft in the swine model. Slides were examined for immune reactivity by Dr. Robert Colvin, Chief Emeritus of the Department of Pathology and an expert in transplantation biology. His evaluation determined that there was a prevalent T cell response in the Avance repair groups as compared to the isograft repair group.

In response to these results the animal protocol was again amended to add immunosuppression with Tacrolimus (FK506) to this large nerve graft model. In order to do so, we added the following procedures: central line placement, blood collection and Tacrolimus administration, to ensure appropriate drug administration and therapeutic serum levels. The purpose of this study was to test the hypothesis that large segmental nerve deficits injuries can be optimally repaired with AxoGen's Avance nerve grafts and photochemical sealing compared to standard microsurgical repair. In our swine model, Avance is actually a xenograft, so in order to suppress the additional inflammation due to the xenograft animals were treated with Tacrolimus 0.1 mg/kg to 0.4 mg/kg (goal serum levels 10-20 ng/mL). This regimen was determined after several discussions with senior investigators of research teams in the Center for Transplant Science (CTS) and as previously reported in the literature [Jensen JN et al. Effect of FK506 on peripheral nerve regeneration through long grafts in inbred swine. *Annals of Plastic Surgery.* 2005, 54:420-7]. The senior investigators in this study have a long history of working with immunosuppression in the MGH miniature swine model in vascularized composite allograft (VCA) studies. The placement of central venous catheters and use of infusion pump systems helped facilitate blood draws and drug administration. The infusion pump system limited the number of times the animals were handled and the central line was accessed; which in turn reduced the potential for line infections. Central lines are commonly placed into the jugular veins to administer Tacrolimus on a continuous basis through the use of osmotic pumps. This is common practice for swine in transplant studies and indwelling lines can be left in place for months, but they have also been known to become infected since swine lay in their own excrement and excrement can become aerosolized during cage washing. Meticulous line care, as performed in this study, involving triple antibiotic treatment of the line exit sites can stave off infections, but the risk is always present. Generally, when a line infection is suspected, due to loss of appetite and dehydration, the best treatment is to pull the line immediately and begin administering antibiotics. Once line infections are cleared and the animal recovers fully, new lines can be successfully re-inserted.

In a further amendment we requested an exemption to the MGH IACUC social housing policy for our swine due to the presence of indwelling catheters.

The amendment for central line placement, blood collection and Tacrolimus administration was approved by the MGH IACUC on February 5, 2016 and the amendment regarding social housing was approved on March 2, 2016. Both amendments subsequently gained ACURO approval on March 14, 2016.

Following a slight delay in swine procurement, due to high demand at MGH, six swine were procured and the first 6 procedures were performed on June, 10, 13, 14, 17, 20 and 21. At these times each swine received bilateral 5 mm ulnar nerve deficits and were repaired either using PTB/Avance (3 cm diameter, 5 cm long) or autologous nerve graft, harvested from the saphenous vein. Figure 19 shows intraoperative images of the autologous nerve repair procedure (A-C) and from the PTB/Avance repair procedure (D-F).

As outlined above, the swine were placed on an immunosuppression regimen following inconclusive histological results in our pilot studies and received Tacrolimus with a serum goal of 20-30 ng/ml. All animals underwent central venous catheter placement at the beginning of the operative procedure, inserted in external jugular vein, tunneled and exteriorized at the nape of the neck. Tacrolimus was delivered using a Q-pump (elastomeric infusion pump). A loading dose of 0.2 mg/kg was given intravenously prior to Avance placement and Tacrolimus infusion started immediately post-operatively at 0.1 mg/kg/day.

One swine began to lose its appetite on day 60, and the central line was pulled one day later. When the animal did not improve, the decision was made to euthanize this swine due to possible systemic infection caused by central line infection. It was possible, however, to collect the nerve specimens during the necropsy and histological evaluation demonstrated that the Tacrolimus had been effective in preventing immune rejection of the graft during these two months of treatment. The remaining five swine were also showing evidence of line infections and after veterinary consultation the decision was made to pull all the central lines and discontinue Tacrolimus administration at the 65-70 day time point for the remaining five animals (since the histology from the euthanized swine showed no evidence of cellular infiltrate). Histopathology at the termination of the 150 day study period showed minimal reaction towards the xenografts after the discontinuation of the Tacrolimus. Figure 20 shows representative intra-surgical images at Day 0 and Day 150 post repair of control repair (microsurgical repair with autograft) and light-activated repair (Avance nerve graft and photosealing).

3d. Electrophysiology measurements in swine. (Months 35-48)

EMGs were performed at Day 0, at the mid point (Day 75) and immediately prior to euthanasia at the end of the study (Day 150). Figure 21 shows examples of EMG readings taken as described at Day 0 and Day 150 post-repair on both forelimbs of the same animal. Both Compound Muscle Action Potential (CMAP) and Conduction Velocities were not significantly different between control autograft and photosealed Avance nerve graft at day 150 after large ulnar nerve gap repair (Figure 22).

3e. Histomorphometric analysis of proximal and distal fibers in swine study.

3f. Determination of axonal migration, endoneurial scarring in swine study.

At this time the nerve specimens have been collected and processed for histology in anticipation of performing Tasks 3e and 3f. The completed histological sections have not yet been returned from the pathology laboratory but return is imminent and tasks 3e and 3f will soon be completed

3g. Preparation of manuscript based on Task 3 studies and evaluation for recommendation for human studies.

This final task will be performed in the next few weeks when the histology slides become available and histomorphometric analysis is performed. However, on the basis of the very positive electrophysiology

results already in hand we are already anticipating an impactful publication showing improved outcomes using the photoselaed allograft to bridge large peripheral nerve deficits.

Miscellaneous Findings.

We have also performed preliminary experiments, not funded by this research but fully relevant to the topic, using a novel nerve imaging technology that will allow longitudinal visualization of important aspects of nerve regeneration for various types of nerve injury and repair procedures. We are working with Dr. Benjamin Vakoc at the Wellman Center for Photomedicine at MGH to determine rates of graft vascularization and re-establishment of blood-nerve barrier using Optical Frequency Domain Imaging (OFDI) as part of his NIH P41 grant that funds his ***Center for Biomedical OCT Research and Translation*** at Massachusetts General Hospital (P41EB015903) awarded by the National Institute of Biomedical Imaging and Bioengineering. The goals of this effort are "to develop new OCT technologies that are responsive to biomedical end-user needs, and to foster adoption and translation of new and existing OCT technologies into a diverse set of research projects and programs."

Initial experiments were performed to establish whether we could determine the rate of vascularization of processed rat nerve allograft when inserted as an interpositional graft in a rat sciatic nerve deficit model. Figure 23 shows the comparison between normal OCT structural images and OFDI images of the nerve before and 6 days after surgery after surgery. The normal OCT images do not highlight vasculature whereas the OFDI images pick up the vasculature very nicely, showing that extensive revascularization with small vessels had occurred at about 6 days post-repair. Longitudinal examination of this process supports a revascularization process that occurs to the graft from the adjacent tissue rather than by migration from the nerve stumps along the graft. With these encouraging data we plan to participate in Dr. Vakoc's upcoming P41 renewal grant proposal where we propose the development of a multimodal imaging system that can assess vasculature (OFDI), remyelination (polarization sensitive OCT) and Schwann cell migration (fluorescence) in one portable unit that can be used in the surgical suite. We anticipate that this technology will provide a unique ability to probe and understand the nerve regeneration process in greater detail than was previously possible and assess clinical interventions for future development to optimize peripheral nerve regeneration.

(b) Key Research Accomplishments:

- Demonstrated that human amniotic membrane (HAM) can be strengthened by a biocompatible crosslinking process.
- Demonstrated that crosslinking dramatically increases resistance of HAM to biodegradation, thus, increasing its longevity as a wrap for nerve graft sealing in vivo.
- Demonstrated that chemical, crosslinking of HAM does not affect its ability as a wrap for photochemical sealing over nerve graft coaptation sites.
- Demonstrated that photochemical sealing of crosslinked HAM (xHAM) over nerve graft coaptation sites can be performed in a facile manner in a rat sciatic nerve model.
- Demonstrated that commercial single layer SIS (swine intestinal submucosa, Oasis) is a stronger material than HAM and can be further strengthened by chemical crosslinking with increased resistance to biodegradation.
- Demonstrated that both SIS and HAM and their crosslinked derivatives can be used as photochemical wraps in vivo over nerve graft coaptation sites in a facile manner in a rat sciatic nerve model.

- Demonstrated improved nerve regeneration in a functional recovery model (SFI, sciatic function index) using PTB/xHAM wrap compared to standard (suture) of care microsurgery.
- Demonstrated improved nerve regeneration in a muscle mass retention model (contralateral control (unoperated) vs treated sciatic nerve graft) using PTB/xHAM wrap compared to standard (suture) of care microsurgery.
- Demonstrated improved nerve regeneration in histomorphometric outcomes using PTB/xHAM wrap compared to standard (suture) of care microsurgery.
- Determined PTB/xHAM wrap to be the optimal fixation method for nerve repair involving large segmental deficit in a rodent model.
- Demonstrated that detergent-based processing of rat nerve can provide excellent acellular nerve allograft (ANA) for study of nerve regeneration in a rodent model.
- Demonstrated improved nerve regeneration outcomes of PTB/xHAM fixation of rat ANA compared to suture fixation.
- Demonstrated regeneration outcomes using ANA + PTB/xHAM repair of segmental nerve deficit in a rodent model equivalent to standard of care autograft/suture repair.
- Demonstrated that ANA + PTB/xHAM is a potential solution to providing oprtimal nerve regeneration outcomes in wounded warriors with insufficient autograft.
- Outlined a large animal protocol for comparative study of standard of care autograft vs ANA + PTB/xHAM in nerve regeneration using electrophysiological outcomes.
- Showed that the swine ulnar nerve is a better model for studies of repair of nerve injury involving deficit than the median nerve.
- Established a short-term immunosuppression regimen that protects against immune reactivity of Avance human allograft in swine models.
- Demonstrated that nerve conduction outcomes using photosealed allograft following nerve regeneration are elevated to the level of standard of care microsurgery using autograft across a large segmental deficit in a large animal model that recapitulates serious traumatic injury.
- Investigated polarization-sensitive optical coherence tomography (PSOCT) as a sensitive imaging method to study revascularization of peripheral nerve graft following repair and image axon regeneration.

(c) Opportunities for training and professional development.

Neil G. Fairbairn BSc HON, MBChB, MD, was awarded his MD from Edinburgh University, Scotland, following submission of a thesis based on the research performed under this award. Dr. Fairbairn also had opportunities to present his research at national and international conferences to further his professional development.
Mark A. Randolph, MAS, was also promoted to the rank of Assistant Professor in the Department of Surgery at Harvard Medical School, with the DoD-funded, light-activated tissue bonding portfolio studies also contributing significantly to his eligibility for promotion.

(d) Dissemination of results to communities of interest.

This technology was featured in the Netflix Original Series entitled "*The White Rabbit Project*" in Series 1, Episode 8, where the presenters considered six different technologies that had taken ideas expressed previously in science fiction media and made them reality. Nerve repair and regeneration was one of the examples highlighted on the show, in video shot at the Massachusetts General

Hospital. This activity certainly brought the technology to the public at large, outside of clinical specialists, and enhanced public understanding of its possibilities.

(e) Plan for next reporting period.

This is the final report, thus, nothing to report

4. Impact:

(a) Impact on the development of the principal discipline(s) of the project

At the end of this project there have been some notable discoveries that may impact military health care in the near future. There is a clear need in military medicine to improve outcomes in wounded warriors that undergo severe extremity injury involving large gap peripheral nerve injury. We have demonstrated that biocompatible chemical crosslinking can be used to strengthen thin nerve wraps and increase resistance to biodegradation such that the wrap retains its sealing ability throughout the time taken for the regenerating axons to traverse the nerve graft and pass the distal coaptation site. The light-activated sealing of the nerve wrap around the coaptation sites obviates the need for suture attachment of the graft and a host of advantages result from the lack of needle injury, inflammation and scarring, possible infection and axonal scape that can reduce functional recovery and cause neuroma formation. Processed crosslinked human amnion, a thin biological membrane (< 50 micron), has demonstrated the best potential as a nerve wrap for photochemical sealing in rodent models in vivo, with other commercial nerve wraps having proven less suitable due to greater thickness and inability to conform to the dimensions of the rat sciatic nerve. Using a photosealing approach with this material we have shown significant improvement in nerve regeneration outcomes in rodent models of segmental nerve defect bridged by autologous nerve graft above and beyond regeneration seen in current standard of care microsurgery. This is a highly impactful result as photosealing could ultimately prove to be the procedure of choice, even in civilian medicine, leading to broad adoption of the technology in the clinic.

The severity of injury in wounded warriors exposed to IED blast can involve massive soft tissue damage and amputation. As such, donor autologous nerve may be unavailable for repair purposes and alternatives are sought. We focus on human allograft as a potential solution. Although allograft has proven to be less effective for nerve regeneration than autograft in clinical implementation using microsurgical attachment, we hypothesized that the photosealing benefit may improve outcomes. In the same rodent model we have demonstrated that photosealing allograft as a nerve bridge produces nerve regeneration that is not statistically different from standard of care sutured autograft. Similar equivalence between standard of care autograft attached by microsurgery and photosealed allograft was observed in a challenging large animal (swine) forelimb nerve deficit model that more accurately recapitulates the anatomical scale and deficit size seen in wounded warriors. This represents major progress in the treatment of peripheral nerve injury associated with military trauma. If these improvements translate clinically, this could result in important improvements in peripheral nerve recovery in those cases of severe trauma and limb loss where the use of nerve autograft is not possible.

We have also shown that the results obtained from this study can be compared to an analogous study where delayed repair, rather than immediate repair, was performed. Results showed no significant detriment to nerve regeneration when repair is performed in delayed fashion using light-activated photosealing. We are currently investigating a new optical technique, polarization-sensitive optical coherence tomography as a new modality to assess regeneration of peripheral nerve through both axonal advance and in revascularization of the graft following placement. We are confident that this technology may allow us to correlate longitudinal imaging with long-term functional recovery.

With refinement, and possible parallel advances in stem cell therapy and tissue engineering, this technique, when used in conjunction with acellular nerve allograft, has the potential to supplant the use of autografts following large gap injury. This approach is capable of rapid commercialization and translation into military medicine. The IP has been filed and the materials involved can be easily stored in a prolonged manner for rapid deployment.

(b) **Impact on other disciplines**

The Photochemical Tissue Bonding/Sealing technology used for nerve repair in this study has proved to be of a platform nature and has since been extended into ophthalmologic, vascular, orthopedic and GI indications. Sealing of wounds in these clinical areas has shown great promise with respect to standard of care in terms of efficacy, time, and diminishing skill level. Additionally, there has been a significant impact on the field of optical imaging where a blossoming collaboration with Dr. Benjamin Vakoc at then Wellman Center for Photomedicine has produced new non-invasive optical technologies for visualizing nerve regeneration on a longitudinal basis where regenerating axons, revascularization and re-myelination can be observed using one optical imaging platform. This novel approach was presented at the Military Health System Research Symposium in 2016.

(c) **Impact on Technology Transfer**

Nothing new to report.

(d) Impact on society beyond science and technology

Nothing new to report.

5. Changes/Problems.

Nothing new to report. All changes and problems encountered have been previously described in quarterly and annual reports.

6. Products:

Peer-Reviewed Publications (see Appendix)

1. Fairbairn NG, Randolph MA, Redmond. The clinical applications of amnion in plastic surgery. *J Plast Reconstr Aesthet Surg*. 2014; 67(5): 662-675. PMID:24560801

2. Fairbairn NG, Ng-Glazier J, Meppelink A, Randolph MA, Winograd JM, Fleming ME, Valerio IL, Redmond RW. Light-activated sealing of nerve graft coaptation sites improves outcome following large gap peripheral nerve injury. *Plast Reconstruct Surg*. 2015, 136(4): 739-750. PMID:26397251.

3. Fairbairn NG, Ng-Glazier J, Meppelink AM, Randolph MA, Winograd JM, Redmond RW. Improving outcomes in immediate and delayed nerve grafting of peripheral nerve gaps using light-activated sealing of neurorrhaphy sites with human amnion wraps. *Plast Reconstr Surg*. 2016, 137(3):887-895. PMID 26910669.

4. Fairbairn NG, Ng-Glazier J, Meppelink A, Randolph MA, Winograd JM, Fleming ME, Valerio IL, Redmond RW. Light-activated sealing of acellular nerve allografts following nerve gap injury. *J Reconstr Microsurg.* 2016, 32(6):421-430. PMID: 26878685.

Non Peer-Reviewed Periodical

1. Kochevar IE, Redmond RW. Light-activated wound healing and tissue modification. *The Biochemist*, 2016, 38(6):20-23.

Conference Presentations:

1. Fairbairn NG, Ng-Glazier J, Meppelink A, Randolph MA, Winograd JM, Fleming ME, Valerio IL, Kochevar IE, Redmond RW. Large extremity peripheral nerve repair. Military Health System Research Symposium (MHSRS) Fort Lauderdale, FL. August 12-15, 2013.
2. Fairbairn NG, Ng-Glazier J, Meppelink A, Randolph MA, Winograd JM, Fleming ME, Valerio IL, Kochevar IE, Redmond RW Treating Peripheral Nerve Injuries with Photochemical Tissue Bonding in Military and Civilians. 118th AMSUS Annual Continuing Education Meeting, Seattle, WA. November 3-8, 2013.
3. Fairbairn NG, Ng-Glazier J, Meppelink A, Randolph MA, Winograd JM, Fleming ME, Valerio IL, Kochevar IE, Redmond RW. Improved outcome following nerve graft reconstruction: The application of photochemical tissue bonding and human amnion nerve wraps in a rodent model of large deficit nerve injury. 41st Meeting of the New England Hand Society. Sturbridge MA, December 6, 2013.
4. Fairbairn NG, J Ng-Glazier, Meppelink A, Randolph MA, Winograd JM, Fleming ME, Valerio IL, Kochevar IE, Redmond RW. Annual Meeting of the American Society for Peripheral Nerve, Koloa, HI. January 10-12, 2014.
5. Fairbairn NG, Ng-Glazier J, Meppelink A, Randolph MA, Winograd JM, Fleming ME, Valerio IL, Redmond RW. Improving neuroregeneration following large deficit peripheral nerve injury: the application of human amniotic membrane scaffolds and photochemical tissue bonding (PTB). Poster presentation. 8th Symposium on Biologic Scaffolds for Regenerative Medicine, Silverado Resort, Napa, California, USA, 24-26th April, 2014.
6. Fairbairn NG, Ng-Glazier J, Meppelink A, Randolph MA, Winograd JW, Fleming ME, Valerio IL, Redmond RW. The application of Photochemical Tissue Bonding (PTB) for Large Deficit Peripheral Nerve Injury. Poster Presentation. 3rd Annual Harvard Research Day. 10th May 2014, Thomas Martin Conference Centre, Harvard Medical School, Boston, MA, USA.
7. Fairbairn NG, Ng-Glazier J, Meppelink A, Randolph MA, Winograd JM, Fleming ME, Valerio IL, Redmond RW. The application of photochemical tissue bonding for large deficit nerve repair. Oral presentation. 25th Annual Smith Day & Inaugural Jupiter International Forum. Royal Sonesta Hotel, Cambridge, MA, USA. 30th May 2014.
8. Fairbairn NG, Ng-Glazier J, Meppelink A, Randolph MA, Winograd JM, Fleming ME, Valerio IL, Redmond RW. The application of photochemical tissue bonding for large deficit nerve repair. Oral presentation. The 55th Annual meeting of the New England Society of Plastic and Reconstructive Surgeons (NESPRS), Sebasco Harbour Resort, Sebasco Harbour, Maine, USA, 6-8th June, 2014. *Joseph E Murray award for best presentation.
9. Fairbairn NG, Ng-Glazier J, Meppelink A, Randolph MA, Winograd JM, Fleming ME, Valerio IL, Redmond RW. Improving outcome following large deficit peripheral nerve injury: the application of a human amnion nerve wrap and photochemical tissue bonding (PTB). Oral presentation at the quadrennial congress of the European Society of Plastic Reconstructive and Aesthetic Surgeons (ESPRAS), Edinburgh, Scotland, UK, 6-11th July 2014.
10. Redmond RW. Clinical applications of photochemical crosslinking. Invited Talk at the Gordon Conference for Lasers in Medicine and Biology. Holderness, NH. July 13-18, 2014.
11. Fairbairn NG, Ng-Glazier JH, Meppelink AM, Randolph MA, Winograd JM, Valerio IL, Fleming ME, Redmond RW. Light activated sealing of nerve graft coaptation sites improves outcome

following large gap nerve injury. *Annual Meeting of the Orthopedic Research Society*, Las Vegas, NV, March 28-31, 2015.

12. Fairbairn NG, Ng-Glazier J, Meppelink A, Randolph MA, Winograd JM, Fleming ME, Valerio IL, Redmond RW. The application of photochemical tissue bonding and acellular nerve allograft for large gap nerve injury. *60th Annual Meeting of the Plastic Surgery Research Council*, Seattle, WA. May 14-16, 2015.
13. Nam S, Chico-Calero I, Easow JM, Villiger M, Redmond RW, Randolph, MA, Vakoc BJ. Imaging peripheral nerve graft revascularization and myelination using angiographic and polarization-sensitive OCT. *Military Health System Research Symposium (MHSRS)*. Kissimee, FL, August 15-18, 2106.
14. Goldstein R, Runyan G, Randolph MA, Easow J, Meppelink A, Fahradyan V, Winograd JM, Robert Redmond RW. Photochemical tissue bonding optimizes outcomes of large gap peripheral nerve defects repaired with acellular nerve grafts in a porcine model. *62nd Annual Meeting of the Plastic Surgery Research Council*. Durham, NC, May 4-7, 2017.
15. Goldstein R, Runyan G, Randolph MA, Easow J, Meppelink A, Fahradyan V, Winograd JM, Robert Redmond RW. Photochemical tissue bonding optimizes outcomes of large gap peripheral nerve defects repaired with acellular nerve grafts in a porcine model. *58th Annual Meeting of the New England Society of Plastic and Reconstructive Surgeons Research Council*. North Falmouth, MA Jun 2-4, 2017.

Table 1. Monthly mean SFIs. After 5-months follow-up, those nerves repaired with photochemically sealed crosslinked amnion (xHAM+PTB) recovered greatest SFI, although this was not statistically significant. The negative control and those nerves repaired using xSIS+suture and xSIS+PTB performed statistically worse than graft+suture.

Experimental group	Mean SFI				
	1-month	**2-month**	**3-month**	**4-month**	**5-month**
No Repair	-89.0+/-3.9	-94.2+/-4.7*	-89.8+/-5.1*	-89.3+/-4.8*	-96.2+/-3.7*
Standard Graft + Suture	-87.6+/-5.0	-81.1+/-4.5	-71.8+/-7.3	-74.7+/-6.3	-71.7+/-4.8
HAM+suture	-90.3+/-5.2	-85.7+/-9.8	-80.6+/-3.5*	-79.7+/-5.7	-77.9+/-6.3
HAM+fibrin	-89.2+/-4.0	-81.6+/-4.1	-80.4+/-7.2*	-79.4+/-4.3	-75.2+/-4.6
HAM+PTB	-90.0+/-5.2	-81.2+/-2.4	-72.8+/-4.6	-75.6+/-3.3	-74.5+/-4.5
xHAM+suture	-96.6+/-7.5	-82.4+/-4.8	-80.0+/-4.0*	-81.4+/-4.8	-76.8+/-2.7
xHAM+fibrin	-90.9+/-3.2	-84.1+/-3.6	-79.8+/-3.3*	-81.2+/-3.1	-75.0+/-4.0
xHAM+PTB	-88.2+/-3.9	-80.3+/-3.5	-67.2+/-3.3	-71.6+/-5.5	-67.9+/-5.1
xSIS+suture	-94.7+/-3.9	-85.6+/-4.4	-82.5+/-4.4*	-81.4+/-4.4	-80.3+/-3.2*
xSIS+fibrin	-93.2+/-4.6	-84.7+/-4.9	-82.0+/-3.7*	-81.5+/-3.9	-78.8+/-3.9
xSIS+PTB	-92.5+/-2.0	-84.7+/-5.0	-84.3+/-4.6*	-85.3+/-6.3*	-85.0+/-6.0*

Table 2: Left gastrocnemius muscle mass retention at 150 days post-repair. Those nerves repaired using xHAM+PTB recovered greatest gastrocnemius muscle mass retention. This result was statistically significant. Those nerves repaired using xSIS+suture and xSIS+PTB recovered least gastrocnemius muscle mass. *Statistically significant improvement in comparison to standard graft+suture; $p<0.05$.

Experimental group	Mean left gastrocnemius muscle mass retention (%)	SD	P value*
No Repair	9.2	0.9	<0.0001
Standard Graft + Suture	60.0	5.2	1
HAM+suture	56.0	5.6	1
HAM+fibrin	59.8	5.4	1
HAM+PTB	62.5	4.0	1
xHAM+suture	57.7	5.1	1
xHAM+fibrin	62.7	4.3	1
xHAM+PTB	67.3*	4.4	0.02*
xSIS+suture	54.9	4.5	0.68
xSIS+fibrin	58.5	5.4	1
xSIS+PTB	54.1	3.2	0.37

Table 3: Histomorphometric analysis of nerve sections 5 mm distal to distal coaptation site in all groups. No difference in axon counts existed between experimental controls and treatment groups. Nerve fiber diameter, axon diameter and myelin thickness were all significantly larger in those nerves repaired using crosslinked amnion and PTB ($p<0.05$).

Group	Total Axon Count x 10^{-3}	Axon density (mm^2 x 10^{-3})	Nerve Fiber diameter (μm)	Axon diameter (μm)	Myelin thickness (μm)	G ratio
Negative Control	0.04+/-0.05*	0.48+/-0.49*	4.25+/-1.28*	2.64+/-1.01*	1.61+/-0.55*	0.61+/-0.09
Positive Control	7.61+/-3.42	29.36+/-18.10	5.47+-1.70	3.50+/-1.44	1.96+/-0.47	0.62+/-0.08
HAM+suture	10.41+/-3.99	28.85+/-18.61	5.07+/-1.58*	3.44+/-1.39	1.63+/-0.50*	0.67+/-0.17
HAM+fibrin	10.42+/-1.54	29.95+/-14.00	5.22+/-1.67*	3.44+/-1.45	1.78+/-0.45*	0.64+/-0.09
HAM+PTB	9.31+/-4.19	30.70+/-8.94	5.19+/-1.76*	3.47+/-1.53	1.72+/-0.41*	0.65+/-0.09
xHAM+suture	9.79+/-3.35	27.12+/-9.22	5.14+/-1.66*	3.54+/-1.47	1.59+/-0.36*	0.67+/-0.08
xHAM+fibrin	10.87+/-4.32	32.12+/-20.28	5.24+/-1.68*	3.52+/-1.49	1.72+/-0.42*	0.65+/-0.09
xHAM+PTB	9.66+/-3.08	30.73+/-14.73	6.87+/-2.23*	4.51+/-1.83*	2.35+/-0.64*	0.64+/-0.08
xSIS+suture	9.36+/-2.41	30.30+/-16.46	4.83+/-1.42*	3.31+/-1.29*	1.52+/-0.38*	0.67+/-0.08
xSIS+fibrin	6.91+/-2.62	31.55+/-13.37	5.18+/-1.50*	3.58+/-1.30	1.59+/-0.52*	0.68+/-0.11
xSIS+PTB	7.84+/-2.04	30.06+/-13.38	4.81+/-1.49*	3.35+/-1.33*	1.45+/-0.34*	0.68+/-0.08

*Denotes statistical significance in comparison to standard repair group

Table 4: Mean SFI for analogous treatment groups over 5-month follow-up period. At each time point throughout recovery, no significant differences existed within each of the ANA groups.

Group	1 month	2 month	3 month	4 month	5 month
Isograft + Suture	-87.6+/-5.0	-81.1+/-4.5	-71.8+/-7.3	-74.7+/-6.3	-71.7+/-4.8
isograft+xHAM/PTB	-88.2+/-3.9	-80.3+/-3.5	-67.2+/-3.3	-71.6+/-5.5	-67.9+/-5.1
ANA+suture	-95.4+/-2.5	-90.3+/-10.6	-87.9+/-4.0	-84.1+/-3.2	-80.3+/-4.2
ANA+xHAM/PTB	-93.4+/-3.4	-91.1+/-5.4	-88.9+/-5.4	-83.4+/-4.8	-78.3+/-5.0

Table 5: Mean gastrocnemius muscle mass retention for analogous treatment groups at 150 days post-repair.

Experimental Group	Mean gastrocnemius muscle retention (%)	SD	P value*
Isograft+suture	60.0	5.2	----
Isograft+xHAM/PTB	67.3*	4.4	0.01
ANA+suture	52.9*	4.77	0.02
ANA+xHAM/PTB	55.2	5.5	0.22

*Denotes statistical significance in comparison to standard repair group

Table 6: Histomorphometric analysis of nerve sections 5 mm distal to distal coaptation site in all groups. ($p<0.05$).

Experimental Group	Total axon count ($x10^{-3}$)	Axon Density ($mm^2 \times 10^{-3}$)	Nerve fiber diameter (µm)	Axon diameter (µm)	Myelin thickness (µm)	G-ratio
Isograft+suture	7.61+/-3.42	29.36+/-18.10	5.47+-1.70	3.50+/-1.44	1.96+/-0.47	0.62+/-0.08
Isograft+xHAM/PTB	9.66+/-3.08	30.73+/-14.73	6.87+/-2.23*	4.51+/-1.83*	2.35+/-0.64*	0.64+/-0.08
ANA+suture	5.04+/-2.57	21.50+/-2.56	5.26+/-1.29	3.30+/-1.15	1.76+/-0.86	0.62+/-0.12
ANA+xHAM/PTB	6.04+/-3.20	22.03+/-5.15	5.38+/-1.22	3.41+/-0.99	1.97+/0.69	0.63+/-0.11

*Denotes statistical significance in comparison to standard repair group

Figure 1A: Effect of EDC/NHS crosslinker concentration on maximum stress of HAM (n=5, * p<0.1, ** p<0.05).

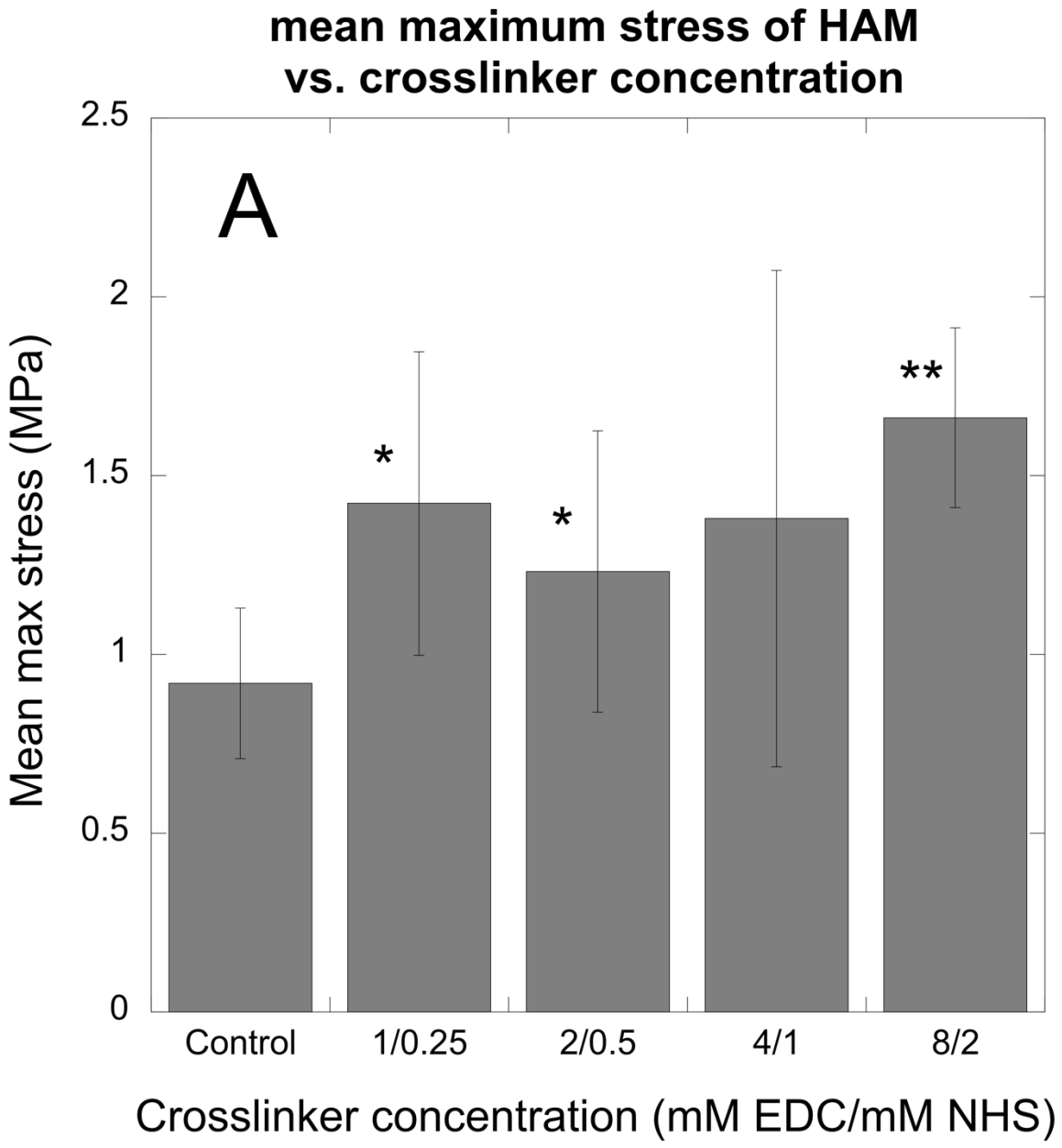

Figure 1B: Effect of EDC/NHS crosslinker concentration on Young's Modulus of HAM (n=5, * $p<0.1$, ** $p<0.05$).

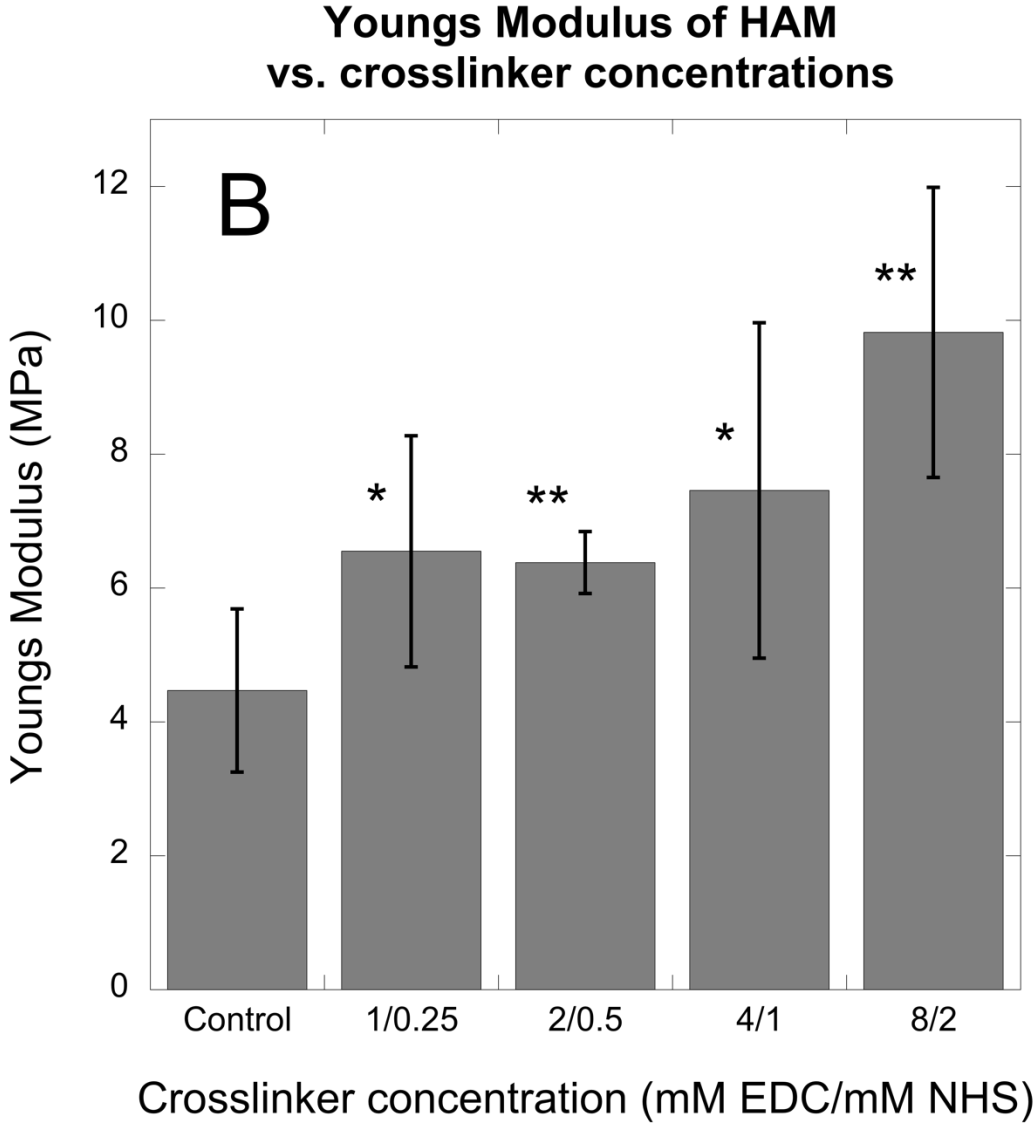

Figure 2A: Effect of EDC/NHS crosslinking on gross degradation time on incubation of control and crosslinked HAM samples with 0.1% collagenase in PBS at 37^{o}C.

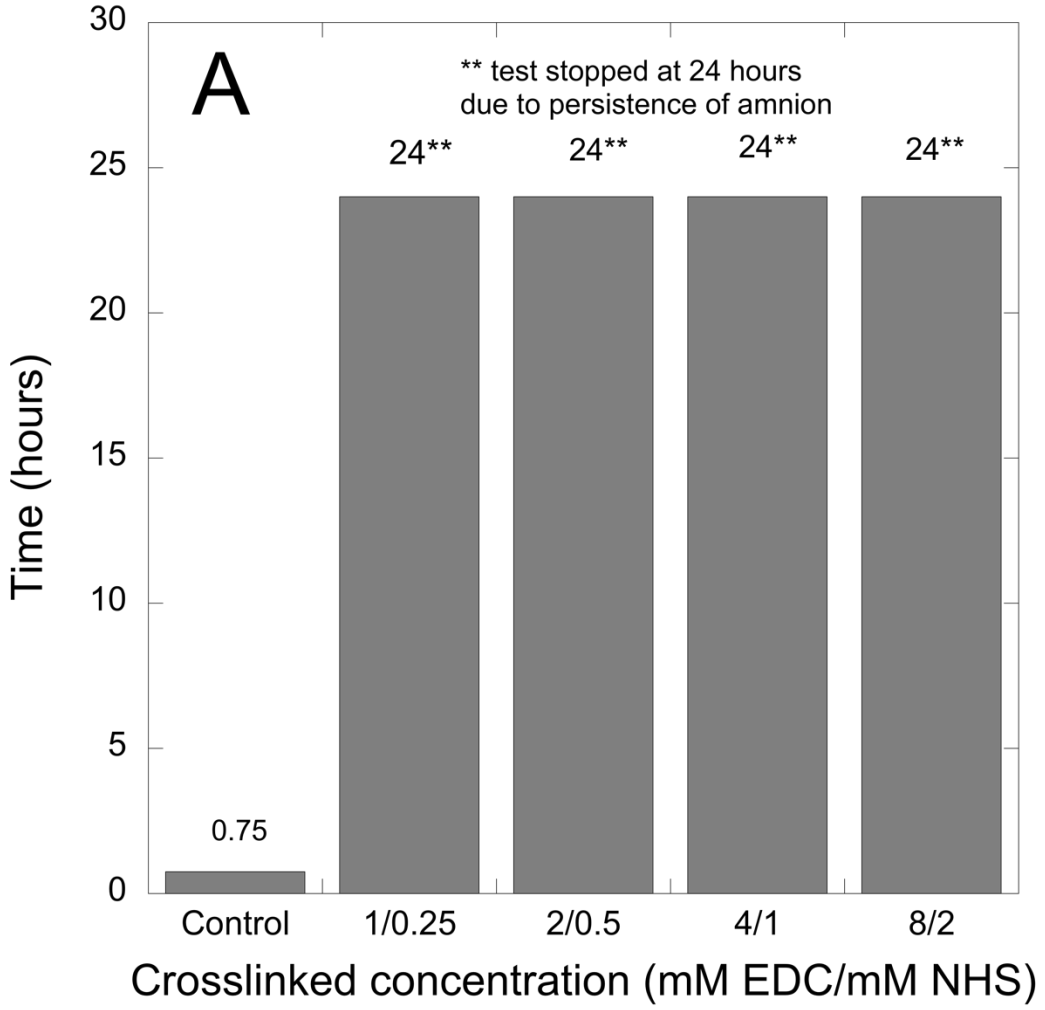

Figure 2B: Effect of EDC/NHS crosslinker concentration on amine containing amino-acid release detected by fluorescamine assay on incubation of control and crosslinked HAM samples with 0.1% collagenase in PBS at 37C.

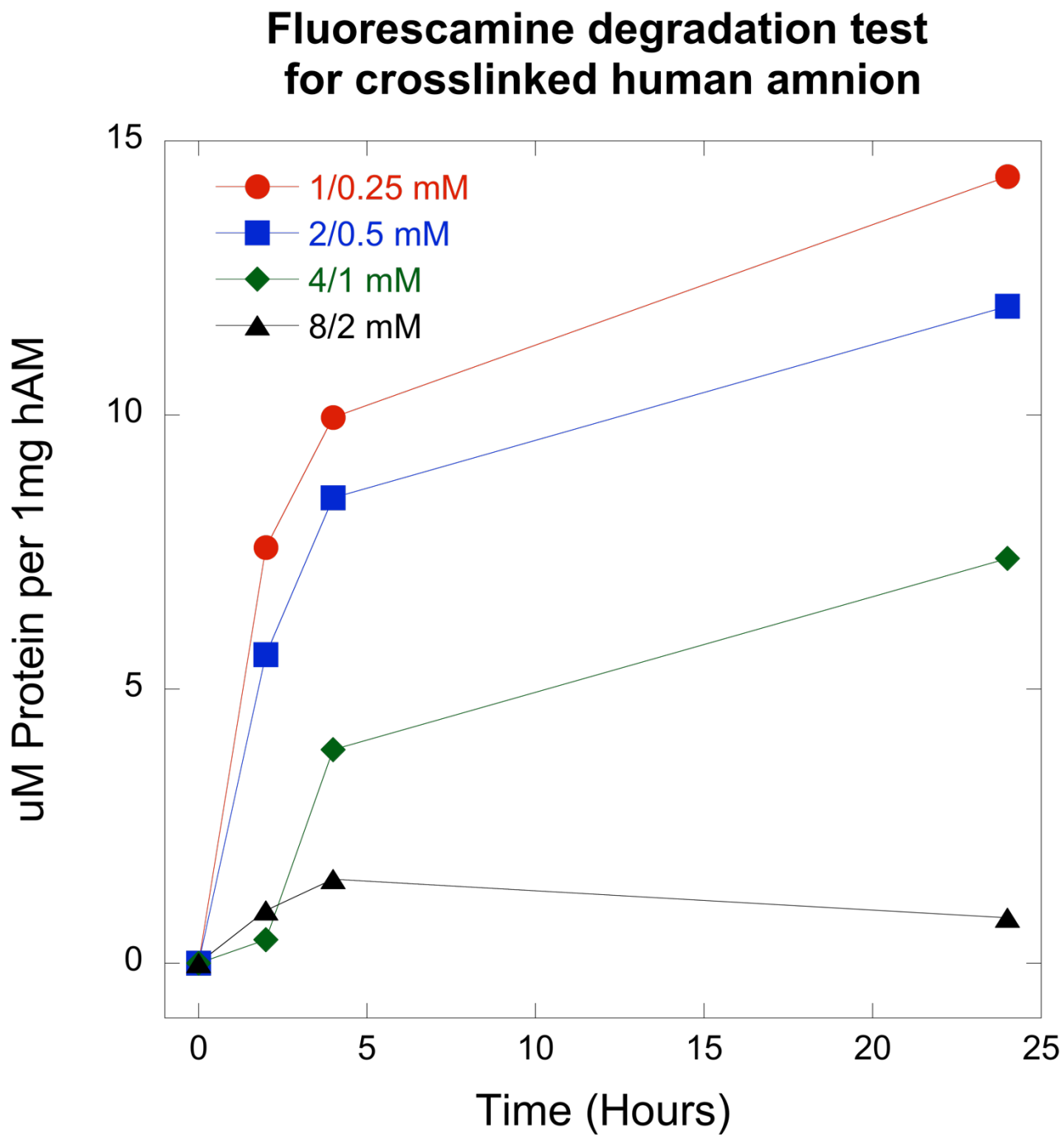

Figure 3: Schematic cartoon of wrap/nerve complex secured in the grips of the mechanical testing device.

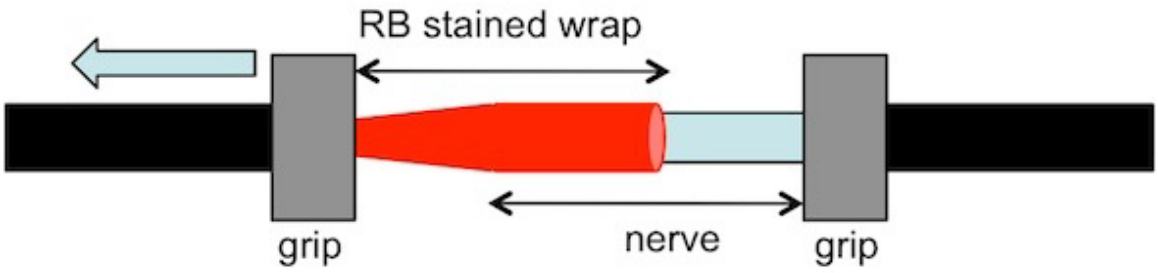

Figure 4: Bond strength between rat sciatic nerve ex vivo and HAM wrap as a function of crosslinking with photochemical bonding using 532 nm light delivered at 0.5 W/cm^2 and a total flence of 60 J/cm^2 (n=5, ** p<0.5).

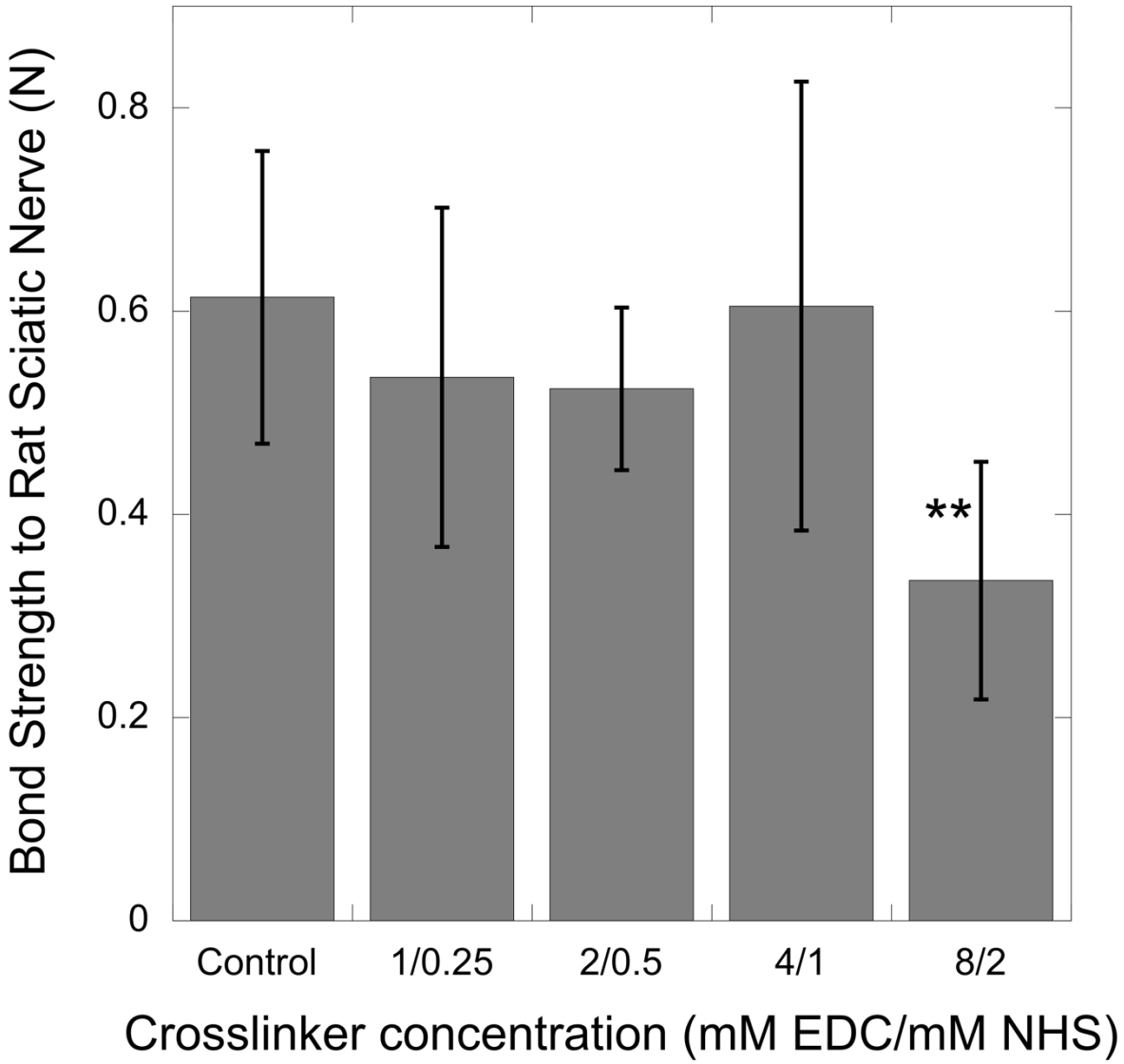

Figure 5: nerve-amnion bond strength as a function of fixation method using 532 nm light delivered at 0.5 W/cm^2 and a total fluence of 60 J/cm^2 (n=5).

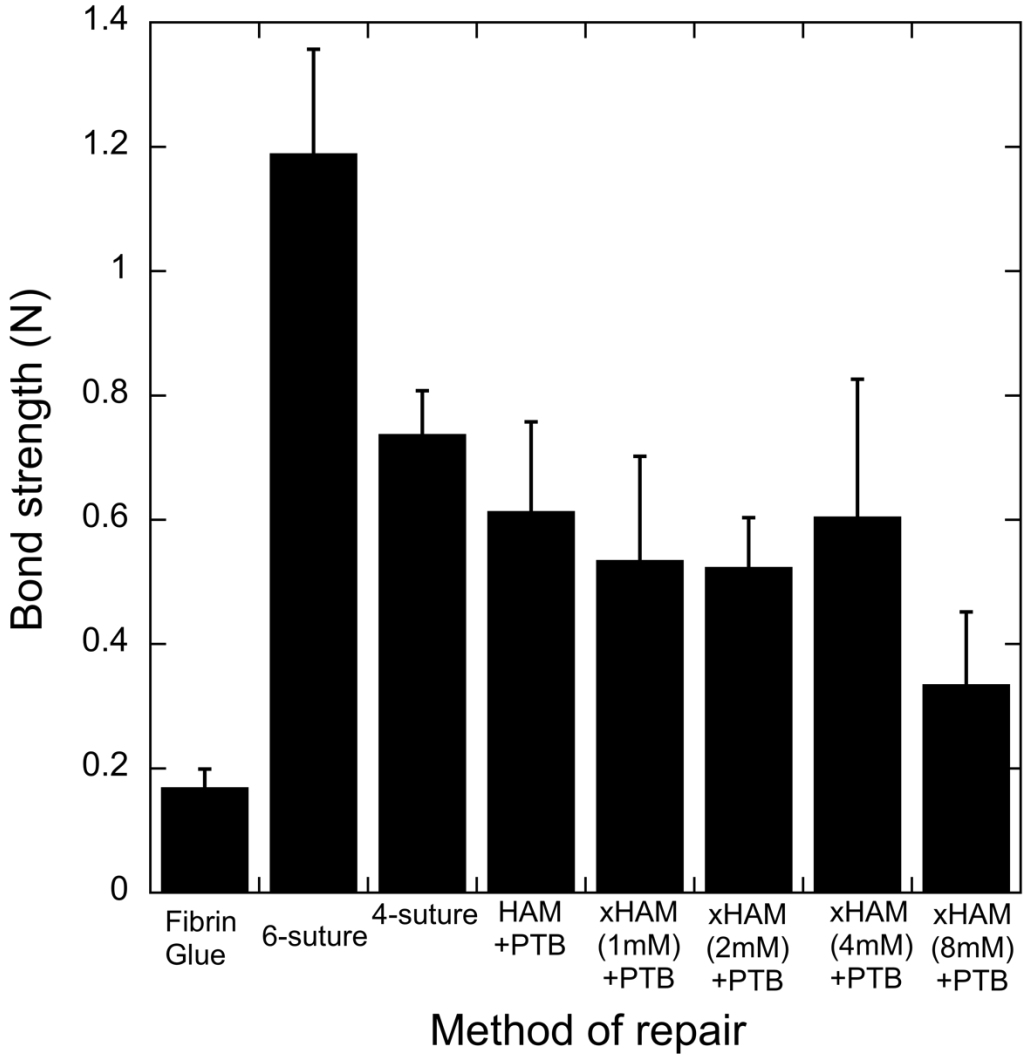

Figure 6: Nerve-amnion bond strength using PTB as a function of fluence (J/cm^2) using 532 nm light delivered at 0.5 W/cm^2 (n=5, ** p<0.5).

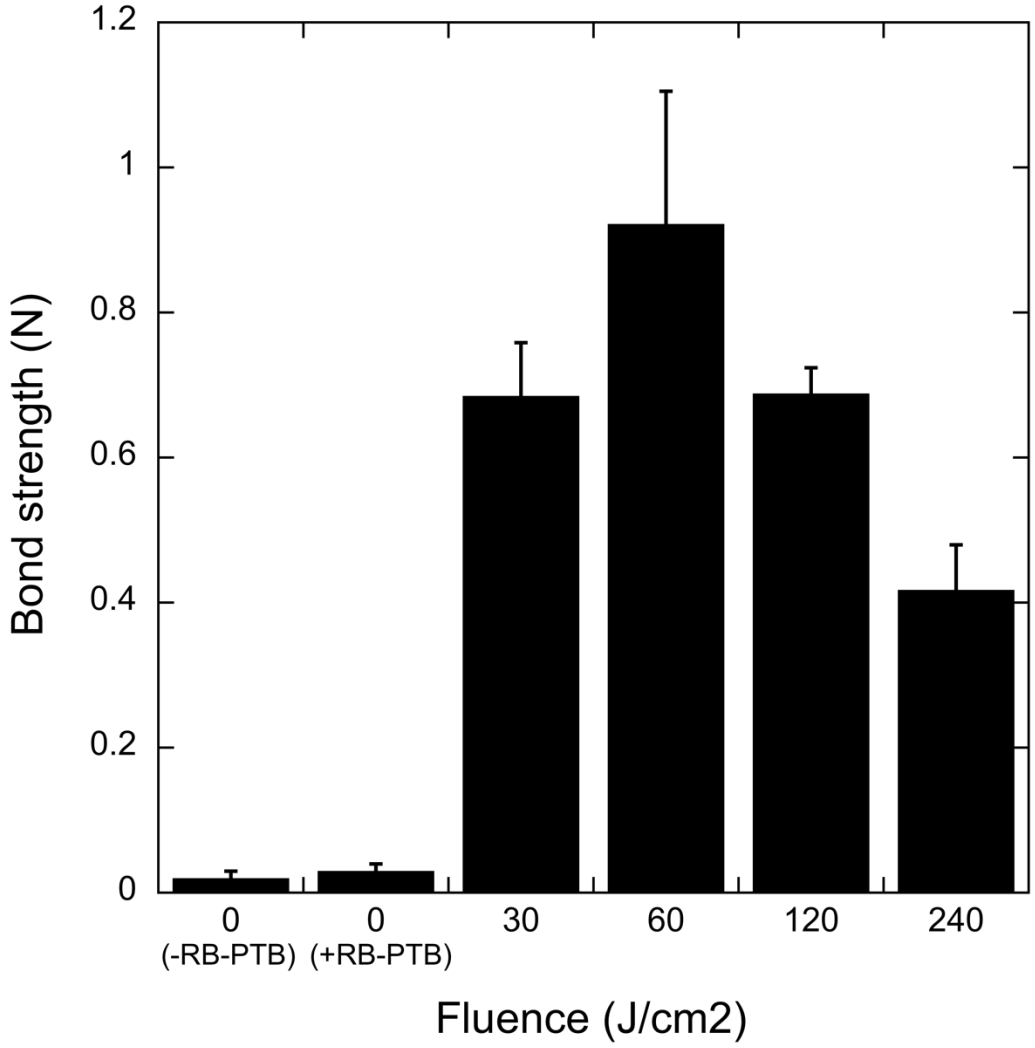

Figure 7: Schematic representation of the anatomy of human amniotic membrane (HAM)

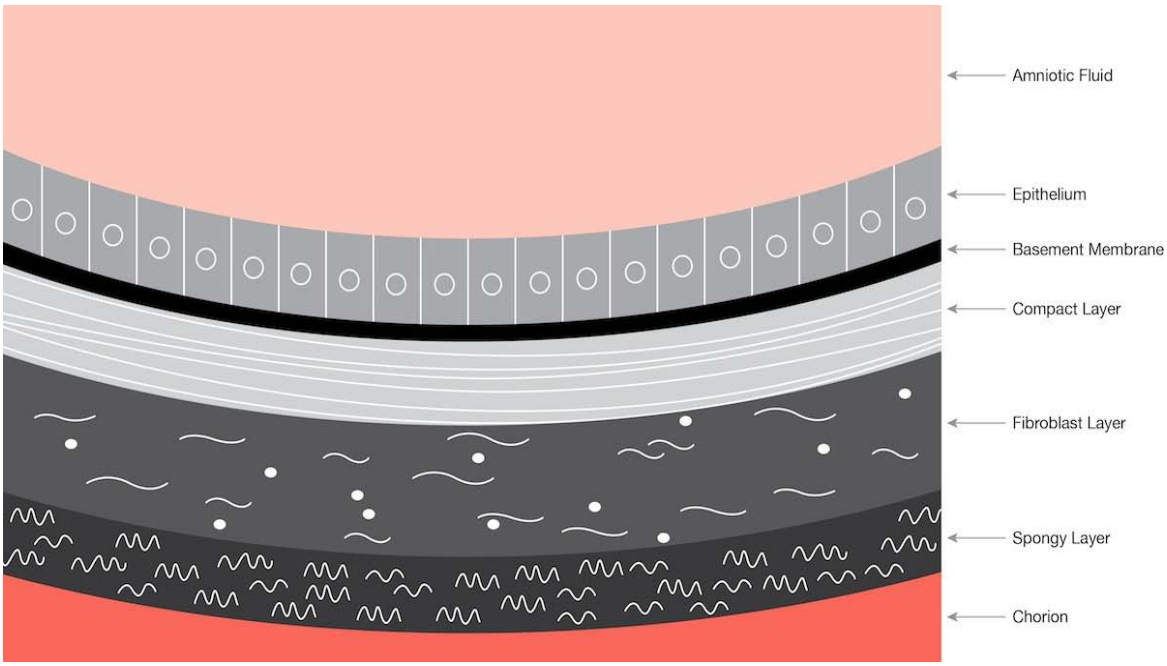

Figure 8: Amnion-nerve bond strength via PTB as a function of which surface was used as interface with nerve using 532 nm light delivered at 0.5 W/cm^2 and a total fluence of 60 J/cm^2.

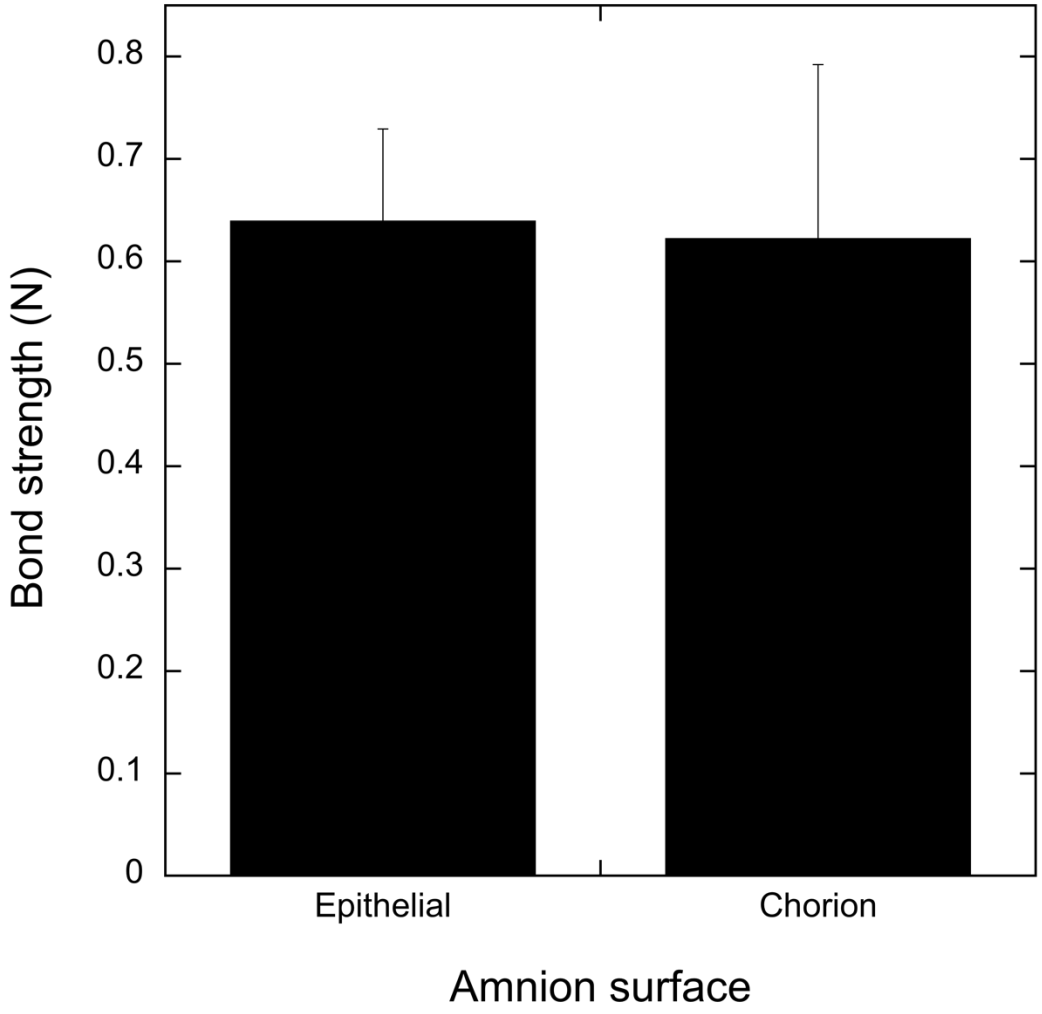

Figure 9: Effect of EDC/NHS crosslinker concentration on Young's Modulus of SIS (n=5, *p<0.5)

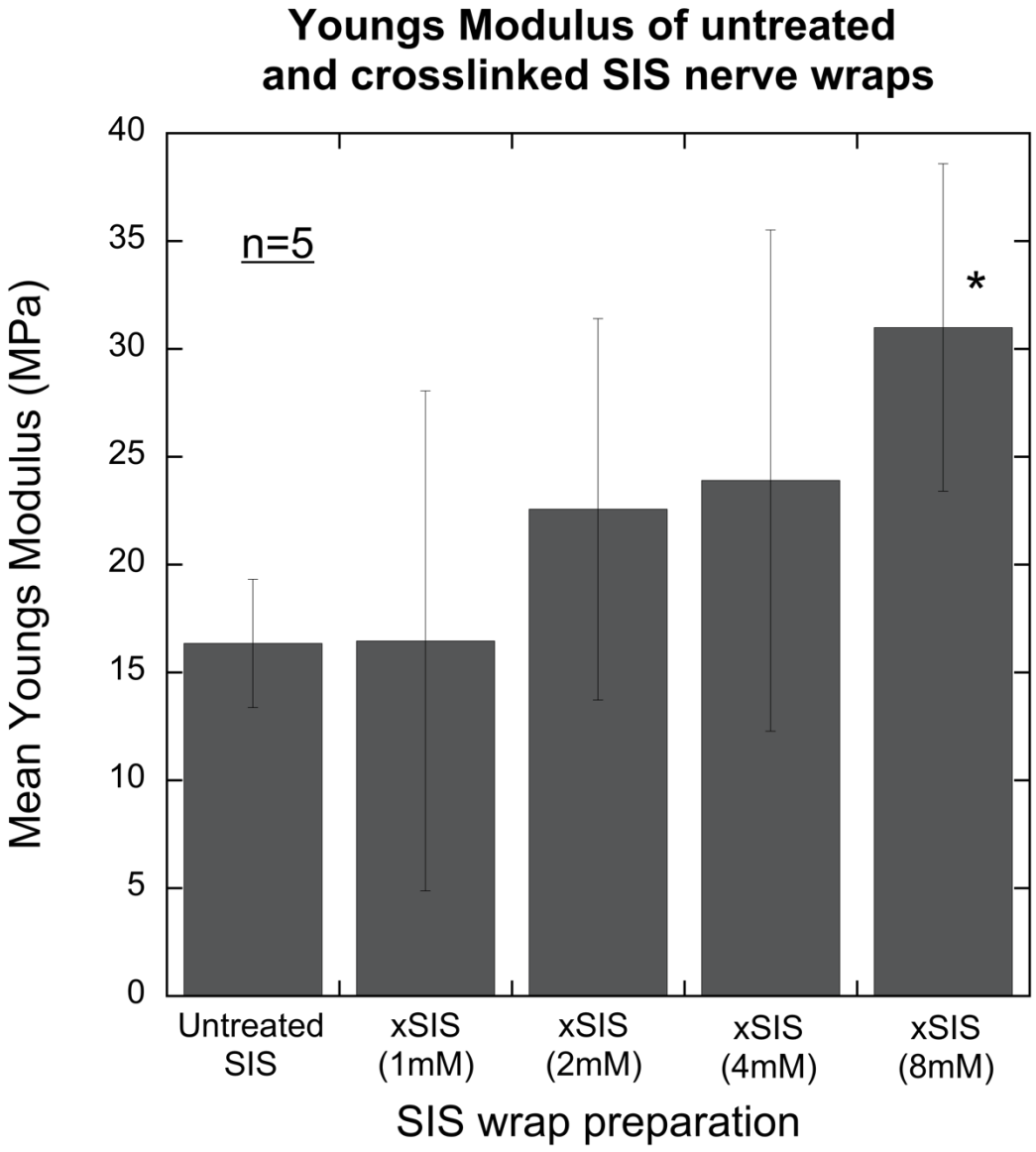

Figure 10: Effect of EDC/NHS crosslinker concentration on maximum load to failure of SIS (n=5, * p<0.5).

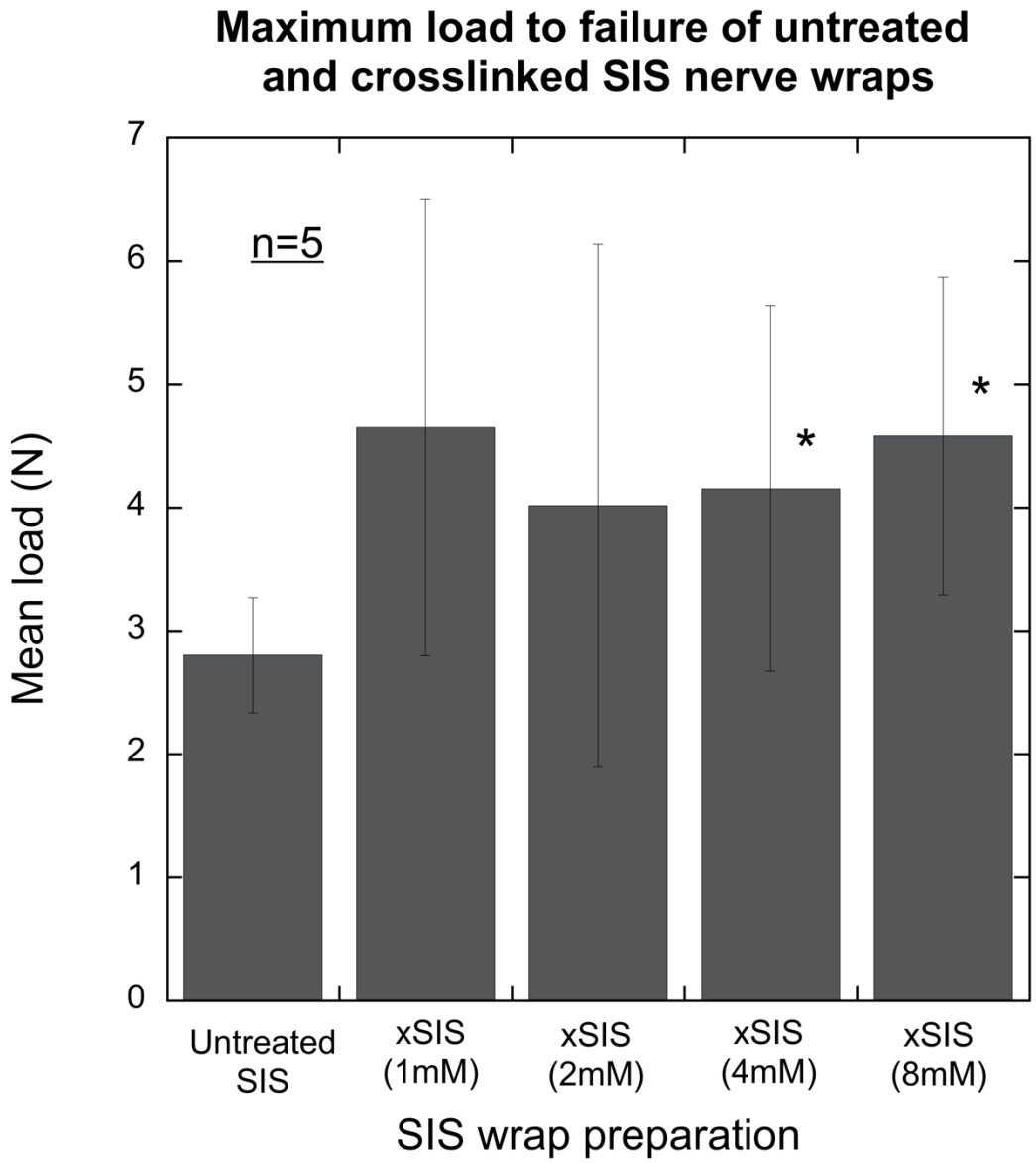

Figure 11: Digestion rates of crosslinked SIS as a function of crosslinker concentration in 0.1% collagenase solution

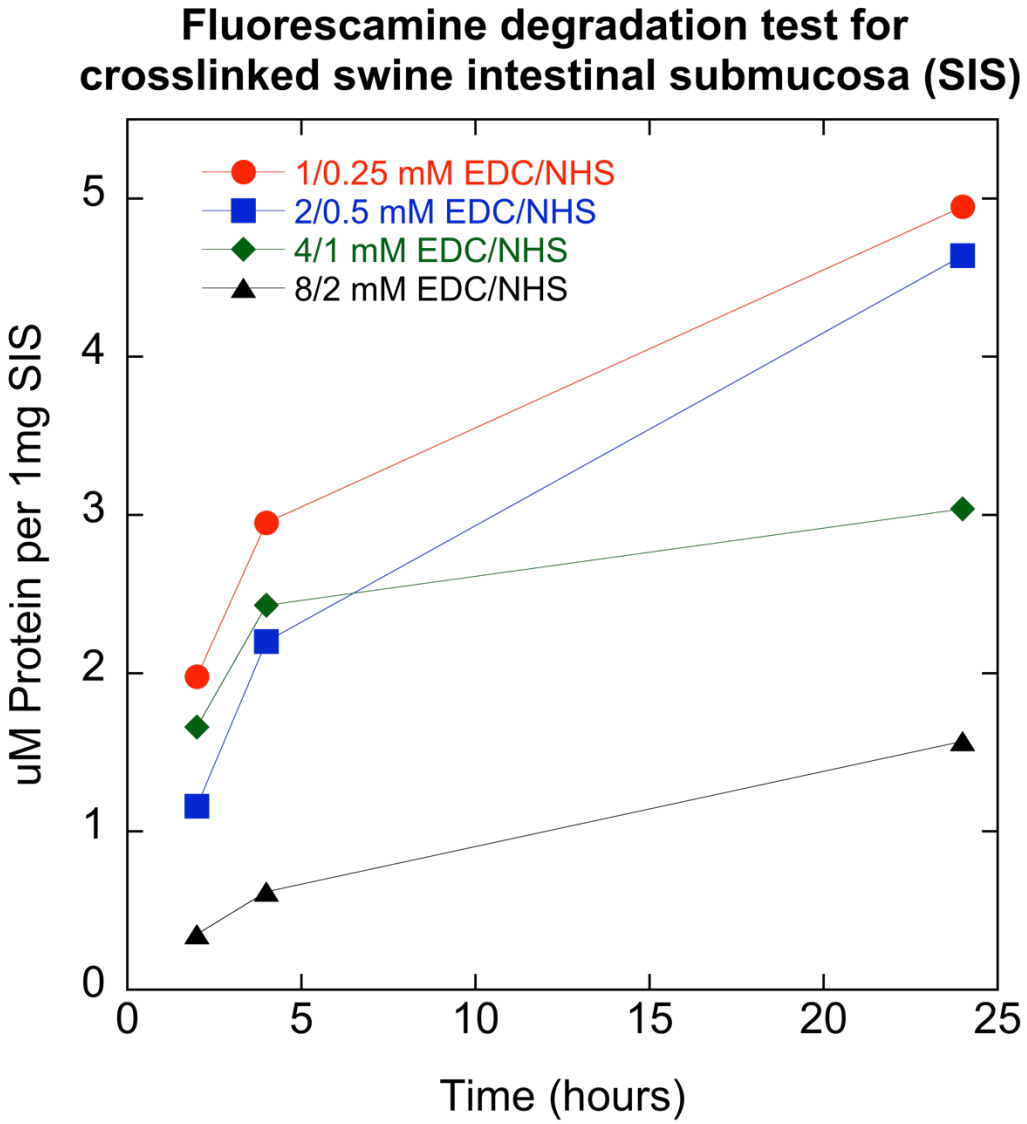

Figure 12:

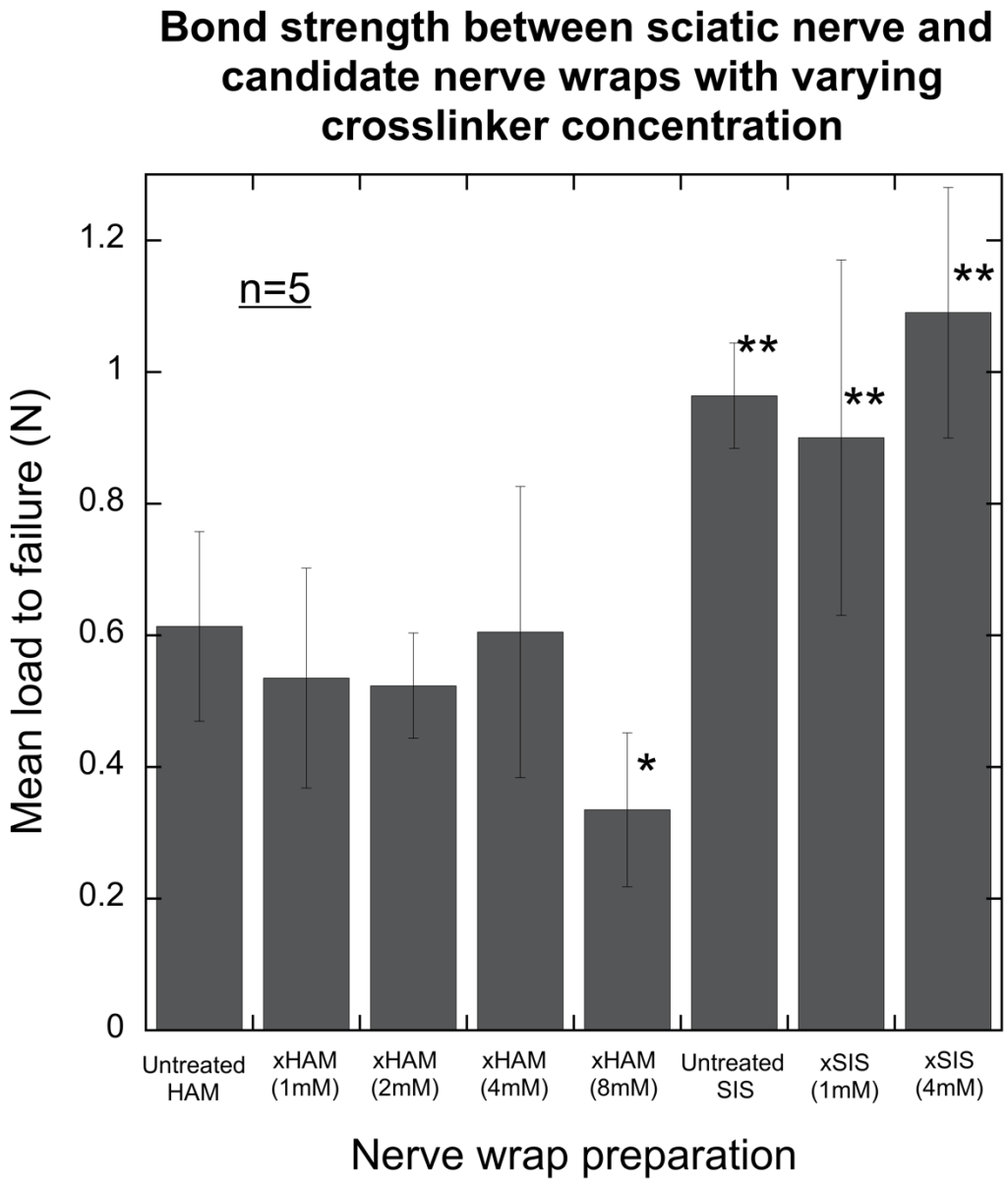
Bond strength between sciatic nerve and candidate nerve wraps with varying crosslinker concentration
n=5
Mean load to failure (N)
0
0.2
0.4
0.6
0.8
1
1.2
*
**
**
**
Untreated HAM
xHAM (1mM)
xHAM (2mM)
xHAM (4mM)
xHAM (8mM)
Untreated SIS
xSIS (1mM)
xSIS (4mM)
Nerve wrap preparation

Figure 13: Histology slides from distal nerve sites in each of the 11 treatment groups. Note the almost complete absence of axons in the no repair group. Nerves in all remaining groups successfully regenerated axons distal to the isograft. As shown in Table 3, fiber and axon size in the xHAM+PTB group were significantly greater than standard repair and other treatment groups.

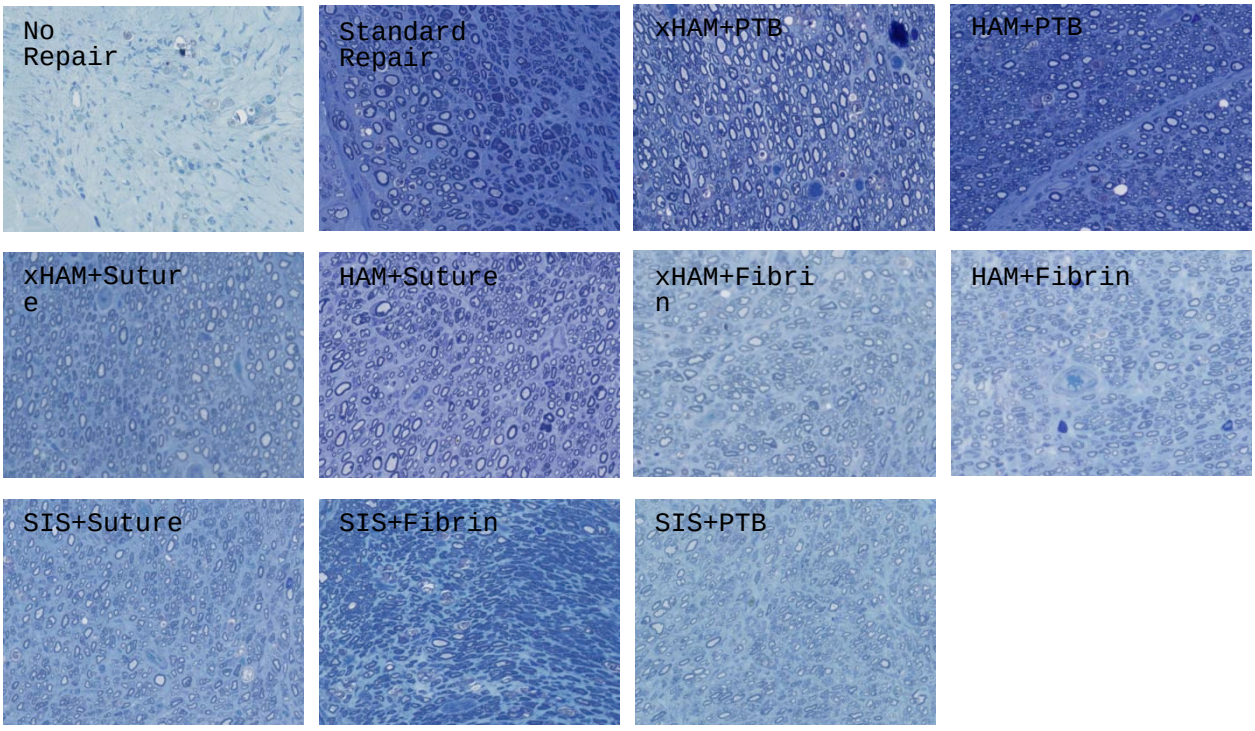

Figure 14: A. Findings following sacrifice in standard repair (positive control) group. Note the extent of fibrinous adhesions around proximal and distal neurorrhaphy sites (arrows). B. Findings following sacrifice in xHAM+PTB group. Note the relative absence of fibrinous adhesions around proximal and distal neurorrhaphy sites

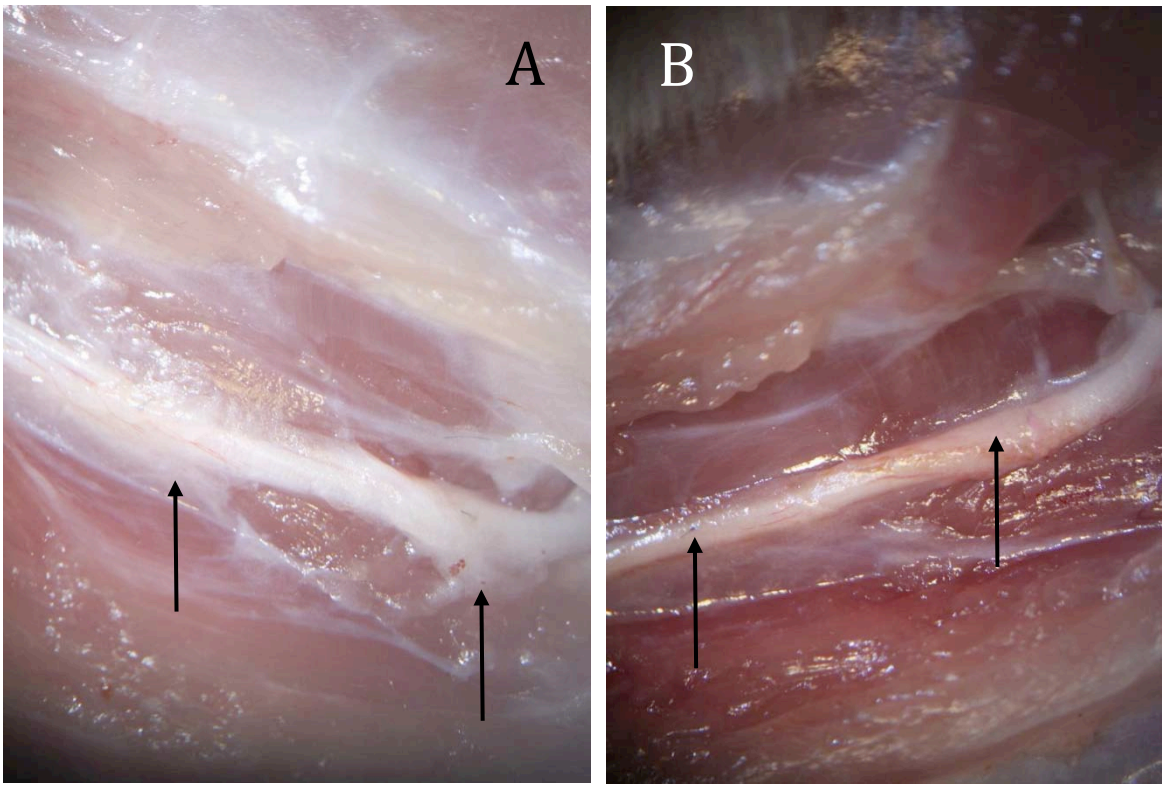

Figure 15: Sciatic Function Index for rat acellular nerve allograft secured with conventional suture vs. rat acellular nerve allograft secured with xHAM+PTB. No significant differences were found between the two groups.

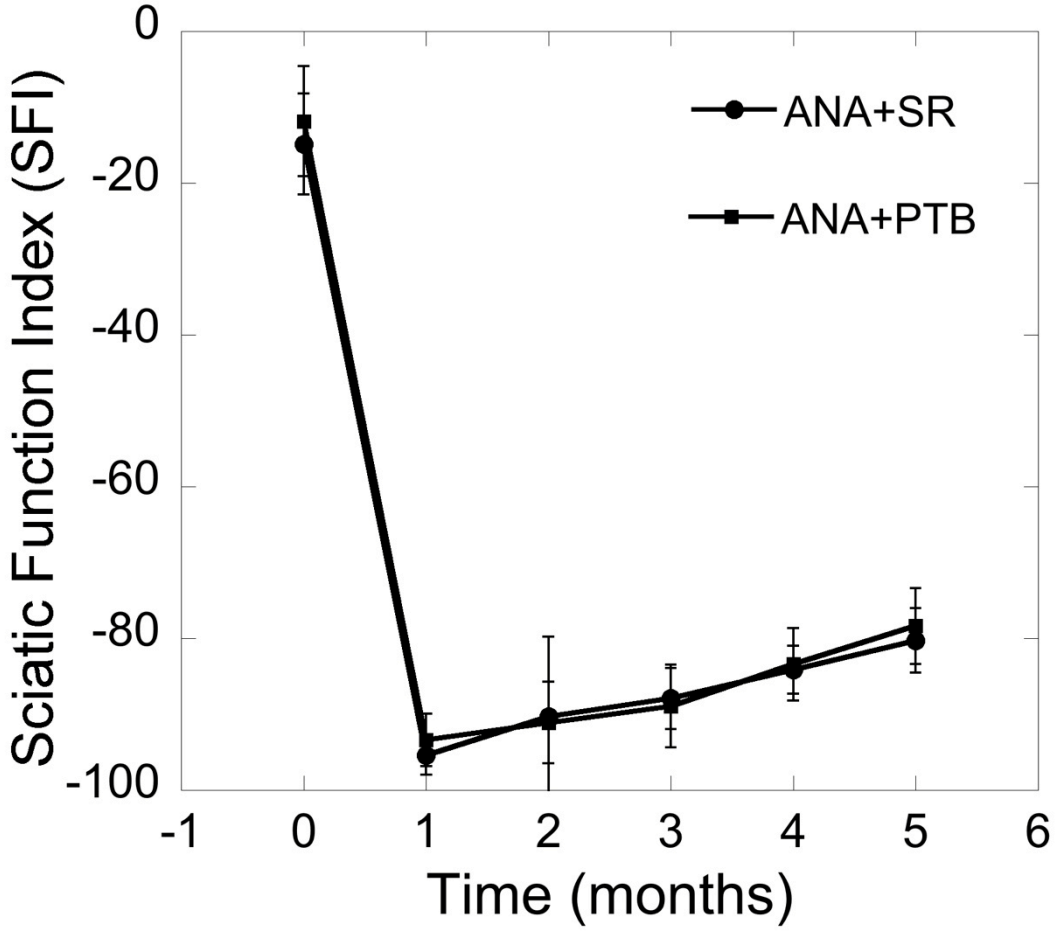

Figure 16: Mean gastrocnemius muscle mass retention. No significant difference in muscle mass retention existed between rat acellular nerve allograft secured with conventional suture vs. rat acellular nerve allograft secured with xHAM+PTB.

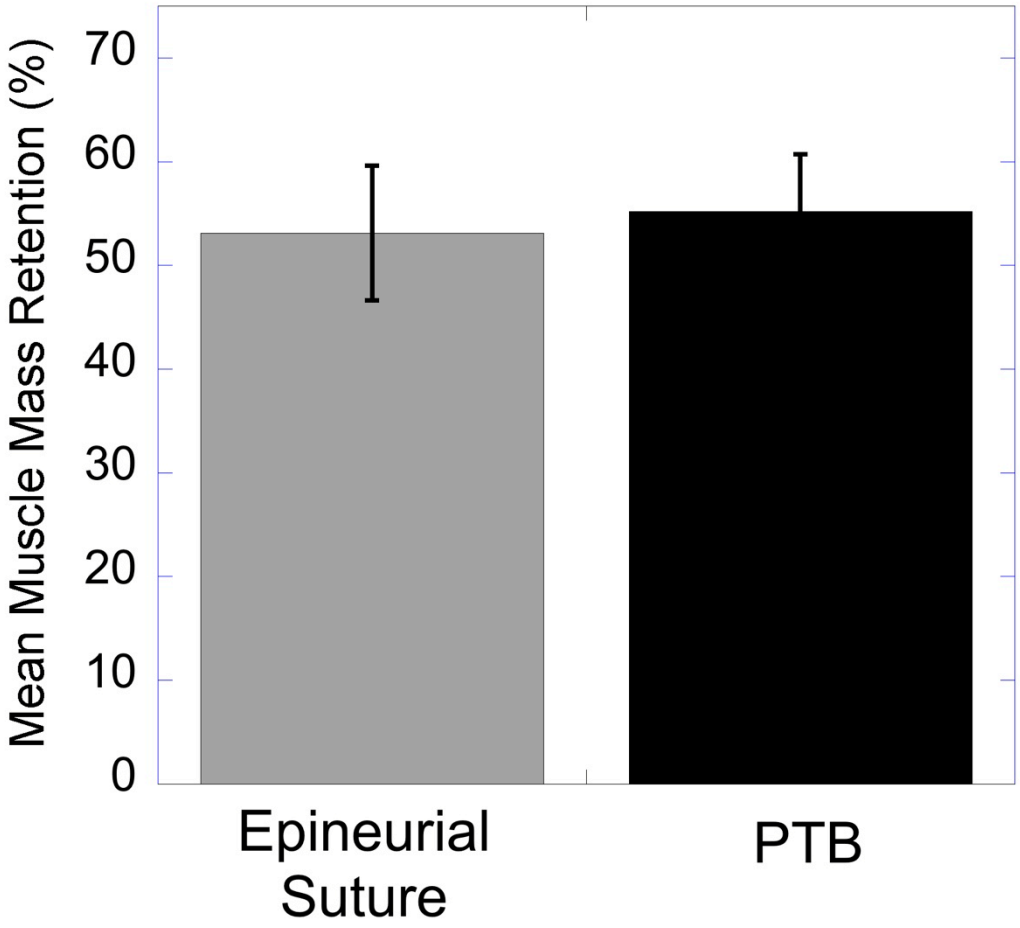

Figure 17. C. Findings following sacrifice in ANA +xHAM+PTB group. Note the relative absence of fibrinous adhesions around proximal and distal neurorrhaphy sites. Photochemically sealed ANA showed remnants of RB stained amnion wraps. D. Findings following sacrifice in ANA/standard repair (positive control) group. Note the extent of fibrinous adhesions around proximal and distal neurorrhaphy sites (arrows).

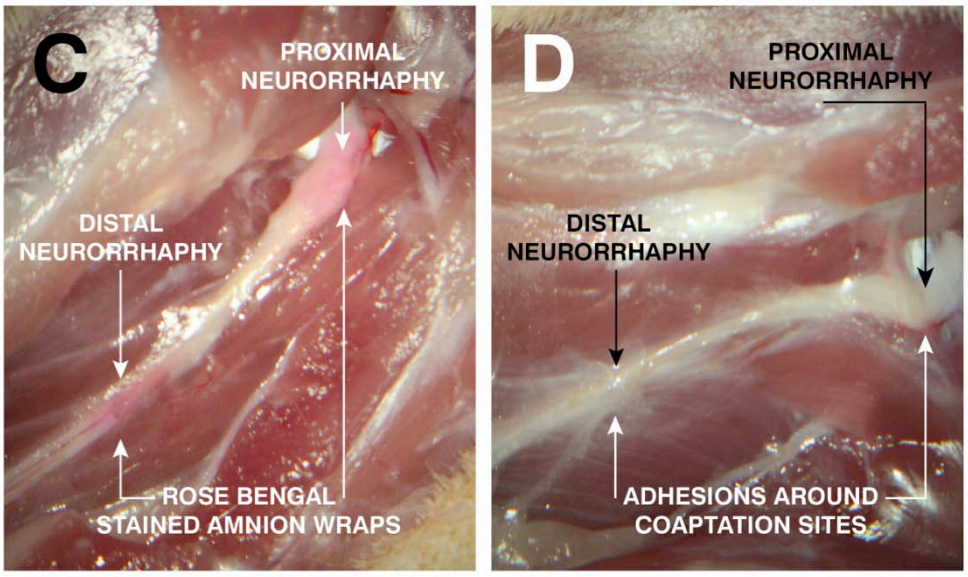

Figure 18. H&E stained midgraft sections of 30 days following repair with (A) Avance + PTB; (B) Avance + microsurgery, and (C) Isograft + microsurgery. All sections show infiltration of nerve with inflammatory cells.

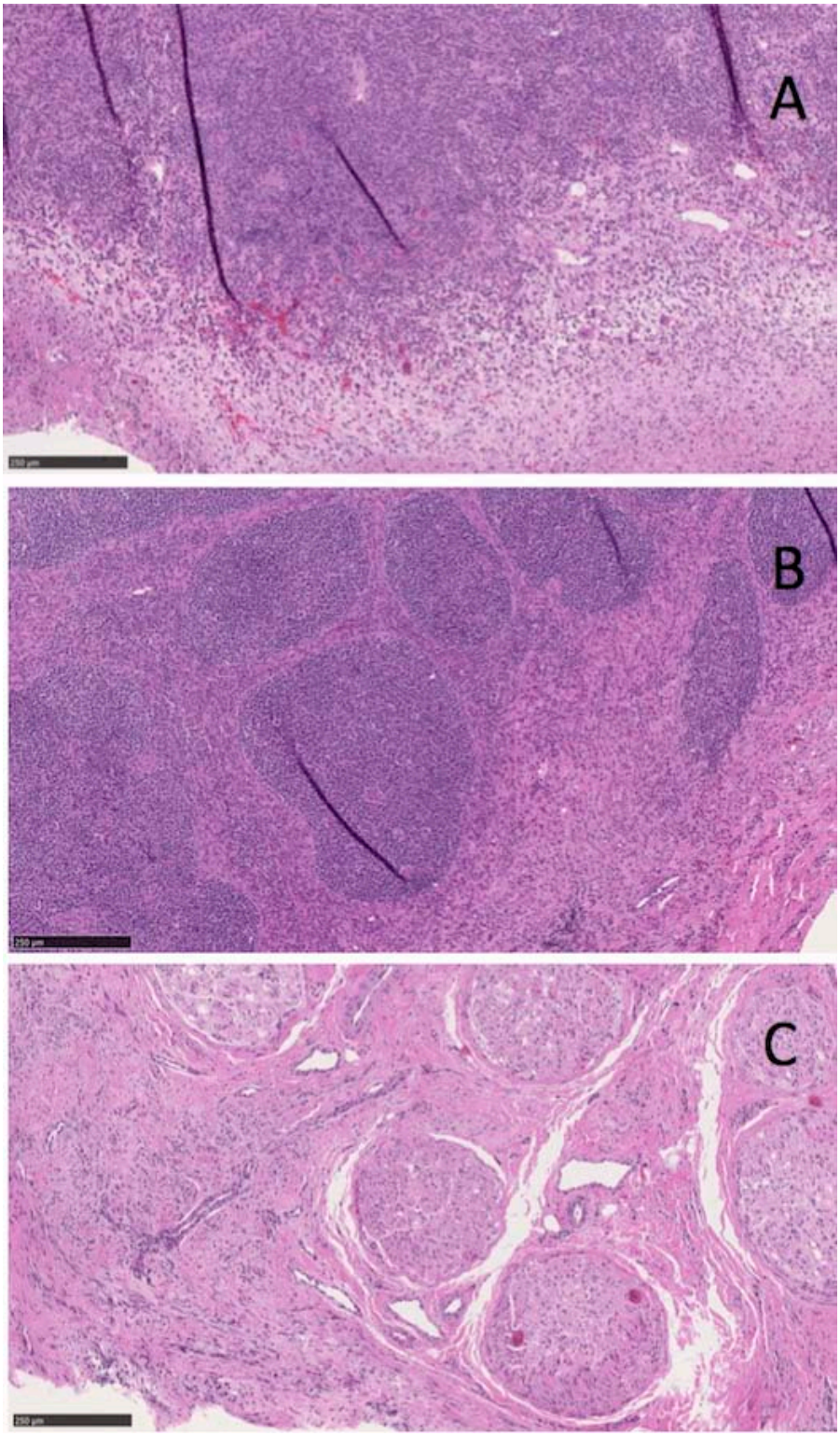

Figure 19: Intraoperative images of autologous nerve graft repair. **A** Dissection of ulnar nerve. **(B)** After resection of 5 cm nerve segment. **(C)** After standard repair with 5 cm saphenous isograft. Intraoperative images of PTB/Avance nerve graft repair. (**D**) Avance graft attached using stay suture. **E**: RB-stained xHAM wrapped around each anastomosis site (pre-PTB). **(F)** Avance graft photosealed across nerve gap.

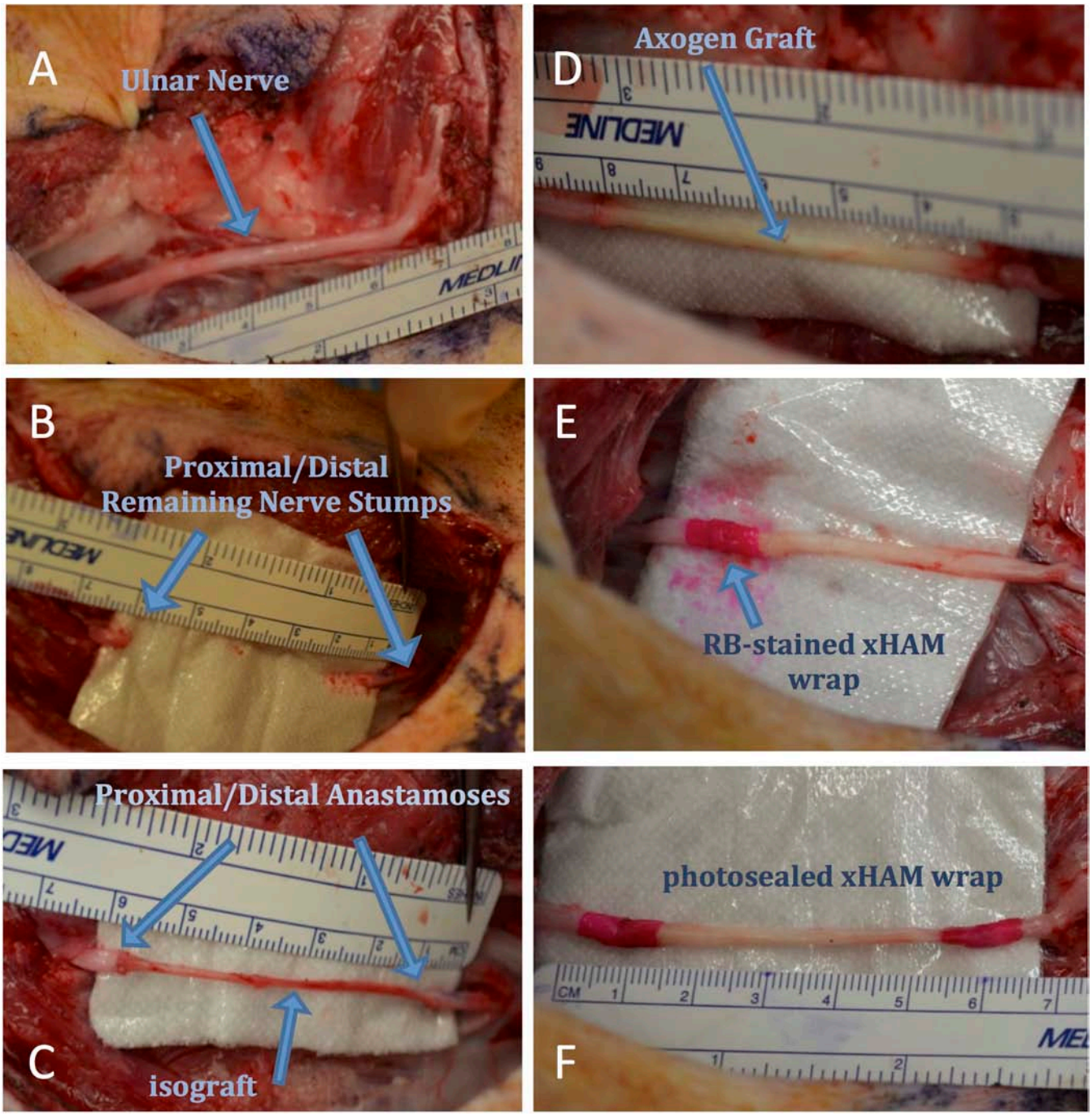

Figure 20: Representative intra-surgical images at Day 0 and Day 150 post repair of control repair (microsurgical repair with autograft) and light-activated repair (Avance nerve graft and photosealing).

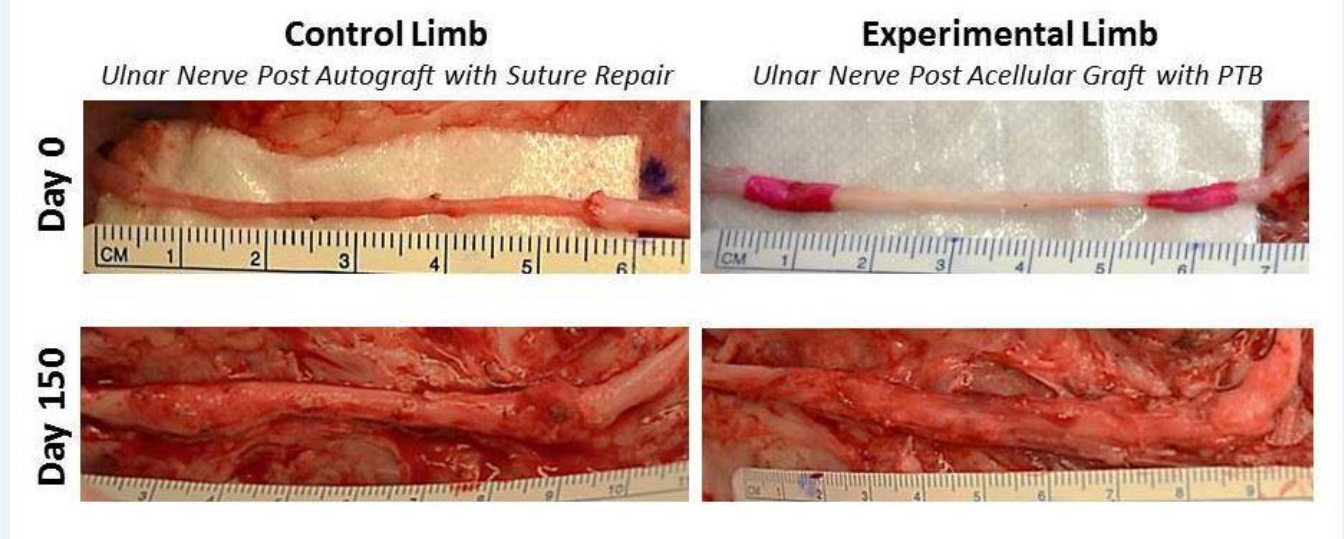

Figure 21: Representative Compound Muscle Action Potential (CMAP) recordings in the same animal at days 0 and 150 after large ulnar nerve gap repair. Ulnar nerve stimulation proximal to nerve graft.

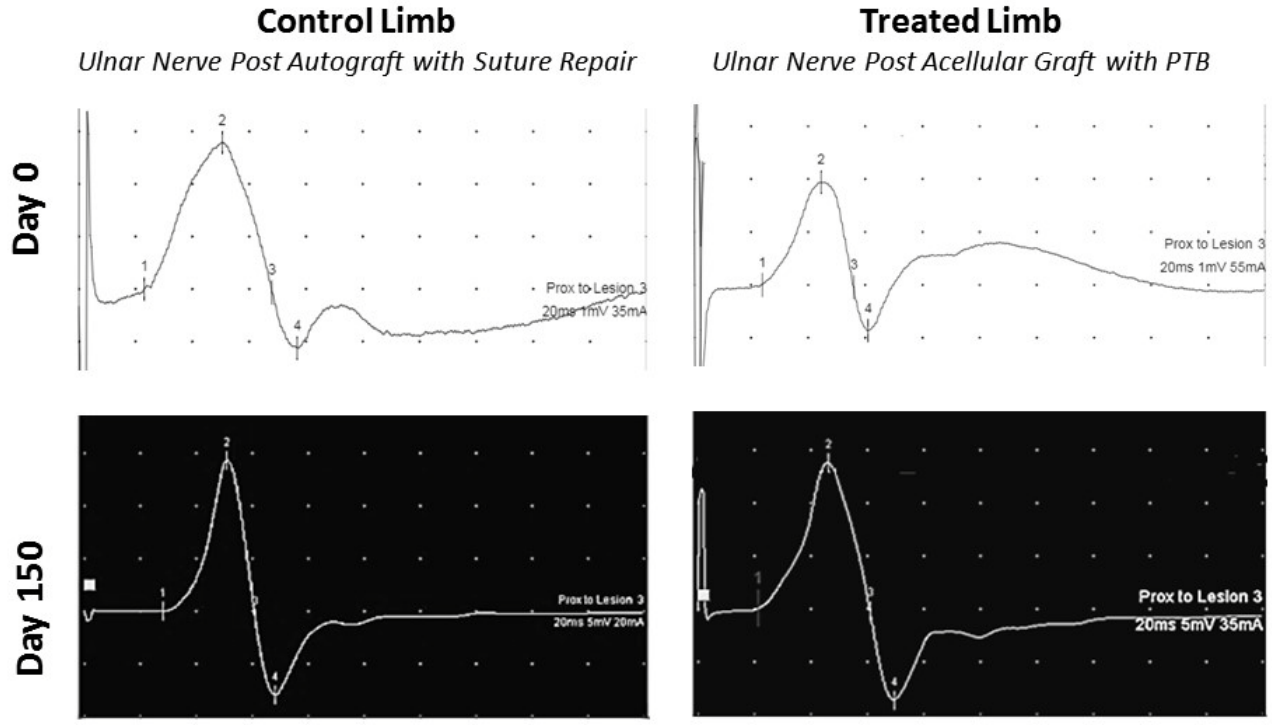

Figure 22: Electrophysiology outcomes at 150 days post repair between control repair (microsurgical repair with autograft) and light-activated repair (Avance nerve graft and photosealing). (A) CMAP amplitude. (B) Conduction velocity. No significant differences in outcomes were observed between repair procedures. (n=5 per group).

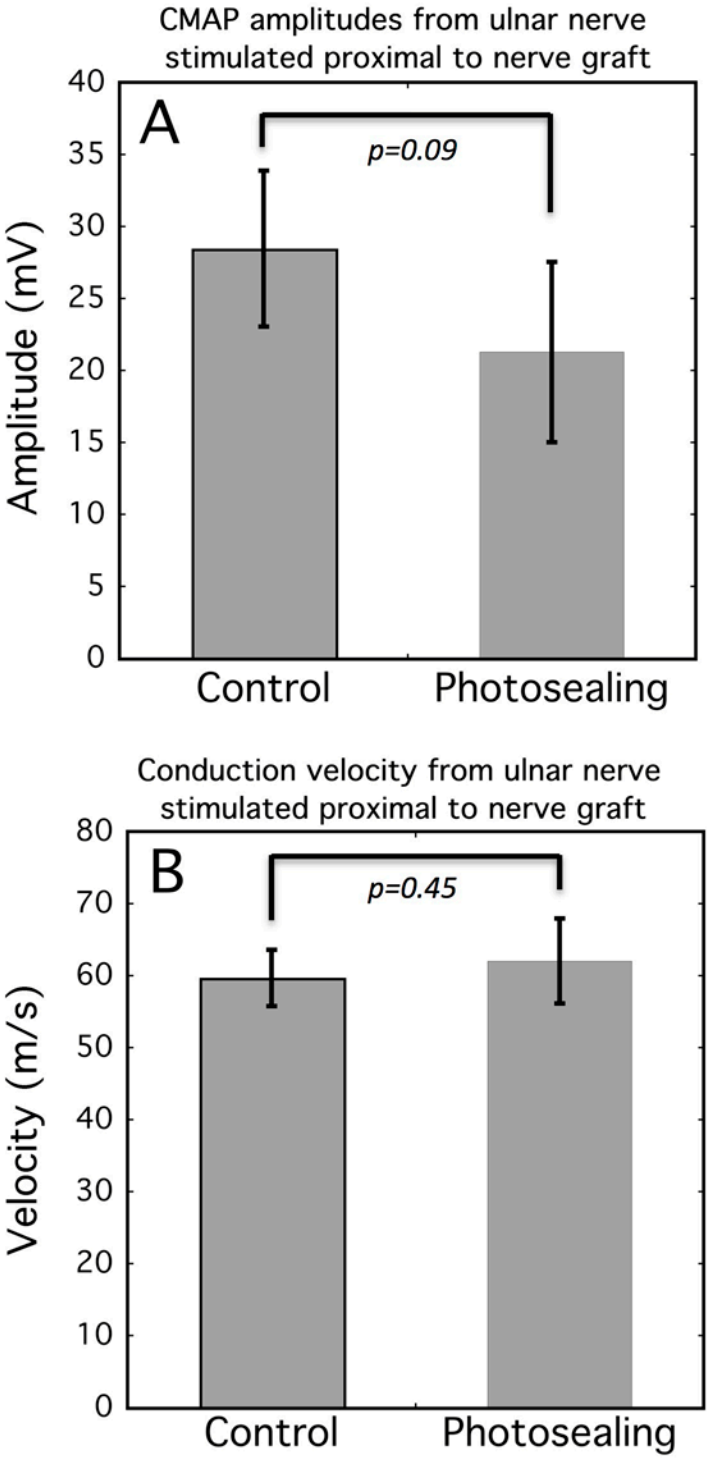

Figure 23: OCT and OFDI images of rat sciatic nerve before surgery and of inter-positional allograft at 6 days following surgical repair of a 1 cm deficit injury.

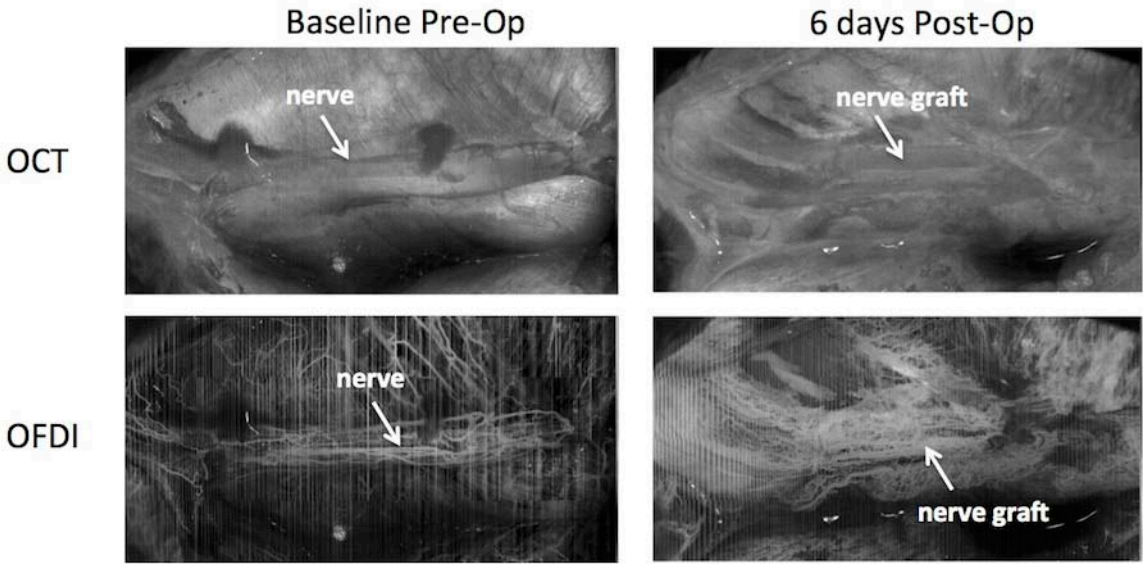

Journal of Plastic, Reconstructive & Aesthetic Surgery (2014) 67, 662–675

JPRAS
An International Journal of Surgical Reconstruction
www.JPRASurg.com

REVIEW

The clinical applications of human amnion in plastic surgery

N.G. Fairbairn*, M.A. Randolph, R.W. Redmond

Division of Plastic Surgery, Massachusetts General Hospital, Harvard Medical School, 15 Parkman Street, WAC 453, Boston, MA 02114, USA

Received 29 May 2013; accepted 23 January 2014

KEYWORDS
Human amnion;
Plastic surgery;
Biological dressing

Summary Since the early 1900s, human amnion has been applied to a wide variety of clinical scenarios including burns, chronic ulcers, dural defects, intra-abdominal adhesions, peritoneal reconstruction, genital reconstruction, hip arthroplasty, tendon repair, nerve repair, microvascular reconstruction, corneal repair, intra-oral reconstruction and reconstruction of the nasal lining and tympanic membrane. Amnion epithelial and mesenchymal cells have been shown to contain a variety of regulatory mediators that result in the promotion of cellular proliferation, differentiation and epithelialisation and the inhibition of fibrosis, immune rejection, inflammation and bacterial invasion. The full repertoire of biological factors that these cells synthesise, store and release and the mechanisms by which these factors exert their beneficial effects are only now being fully appreciated. Although many commercially available biological and synthetic alternatives to amnion exist, ethical, religious, and financial constraints may limit the widespread utilisation of these products. Amnion is widely available, economical and is easy to manipulate, process and store. Although many clinical applications are of historical interest only, amnion offers an alternative source of multi-potent or pluripotent stem cells and therefore may yet have a great deal to offer the plastic surgery and regenerative medicine community. It is the purpose of this article to review the clinical applications of human amnion relevant to plastic surgery.

Introduction and history

Prior to the realisation of its medical and surgical applications, human amnion was the focus of myth and superstition. Being born with the fetal membranes or "caul" intact was considered extremely lucky. Children were gifted with life-long happiness, the ability to see spirits, and protection from death by arms and drowning. The magical powers of

* Corresponding author. Division of Plastic Surgery, Massachusetts General Hospital, Harvard Medical School, 78 Winter Street, Cambridge, Boston, MA 02141, USA. Tel.: +1 617 515 2701.
E-mail address: NGF174@hotmail.com (N.G. Fairbairn).

1748-6815/$ - see front matter © 2014 British Association of Plastic, Reconstructive and Aesthetic Surgeons. Published by Elsevier Ltd. All rights reserved.
http://dx.doi.org/10.1016/j.bjps.2014.01.031

the caul were not confined to the original bearer and could be transferred by inheritance or legitimate sale. As a result, the trade of caul amulets became extremely popular, particularly between seafaring men during the 1800s at the time of the Napoleonic War.[1]

In 1910, Davis reported on early experience with fetal membranes in skin transplantation.[2] Over the last century, the beneficial effects of amnion have been applied to burns, chronic vascular and diabetic ulcers, dural defects, intra-abdominal adhesions, peritoneal reconstruction, genital reconstruction, hip arthroplasty, tendon repair, nerve repair, microvascular grafts, corneal repair, intra-oral reconstruction and reconstruction of the nasal lining and tympanic membrane. More recently amnion has been shown to be a viable source of stem cells with a potentially exciting future in tissue engineering and regenerative medicine. Although many of these roles are of historical interest only, an awareness of this history is an important pre-requisite for future development and innovation. It is the purpose of this article to review past and present applications of human amnion relevant to plastic surgery and how it may contribute to our future.

Anatomy and physiology

Amnion forms during the transition of the morula into the blastocyst at approximately 7-days following fertilisation.[3] Amnion is between 0.02 and 0.05 mm thick and consists of five distinct layers: (1) epithelium, (2) basement membrane, (3) compact layer, (4) fibroblast layer, (5) spongy layer (see Figure 1). The innermost epithelium consists of a single layer of cells in direct contact with amniotic fluid. Microvilli at the apical surface of these cells play an important role in amniotic fluid homeostasis.

The basement membrane border of the cells contains blunt projections that inter-digitate with similar processes in the basement membrane, forming a densely adherent bond. The basement membrane is a thin layer composed of reticular fibers. The compact, fibroblast and spongy layers are referred to as the amniotic mesenchyme and originate from the primary extra-embryonic mesoderm of the blastocyst. The mesenchyme contains collagen I—VII and non-collagenous proteins such as elastin, laminin, fibronectin and vitronectin. The compact layer is composed of a dense network of fibers and is almost entirely free from cells. Abundant type I, II and III collagen and elastin within this layer endow amnion with tensile strength and elasticity.[4] These properties help protect the fetus from mechanical stress and desiccation. The fibroblast layer is the thickest layer and is composed of a loose fibroblast network within a matrix of reticulin. The outermost spongy layer represents the transitional layer between amnion and chorion and is composed of bundles of reticulin within a background of mucin. The two layers are loosely adherent, allowing a degree of gliding during gestation and easy separation by blunt dissection during harvest.[5]

In spite of being devoid of vascularity, nerves, muscles and lymphatics, amnion is highly metabolically active.[5] Oxygen and nutrients are obtained by diffusion from amniotic fluid and chorionic vasculature. The epithelial layer is a source of prostaglandins, particularly prostaglandin-E2, and is thought to play an important role in the initiation and maintenance of uterine contractions.[6] The epithelium also contains human chorionic gonadotrophin receptors that regulate prostaglandin production and activity. Epithelial cells manufacture multiple vasoactive peptides, growth factors, cytokines and extracellular matrix (ECM) proteins.[5] These biological factors may reside in the epithelium or may be transported and accumulated in the mesenchyme where they act as a reservoir from which the amnion exerts its therapeutic effects following transplantation.

Mechanism of therapeutic effect

As a barrier and analgesic

The application of amnion to a wound bed prevents desiccation and excessive fluid loss and provides an analgesic effect by protecting exposed nerve ends from the environment.

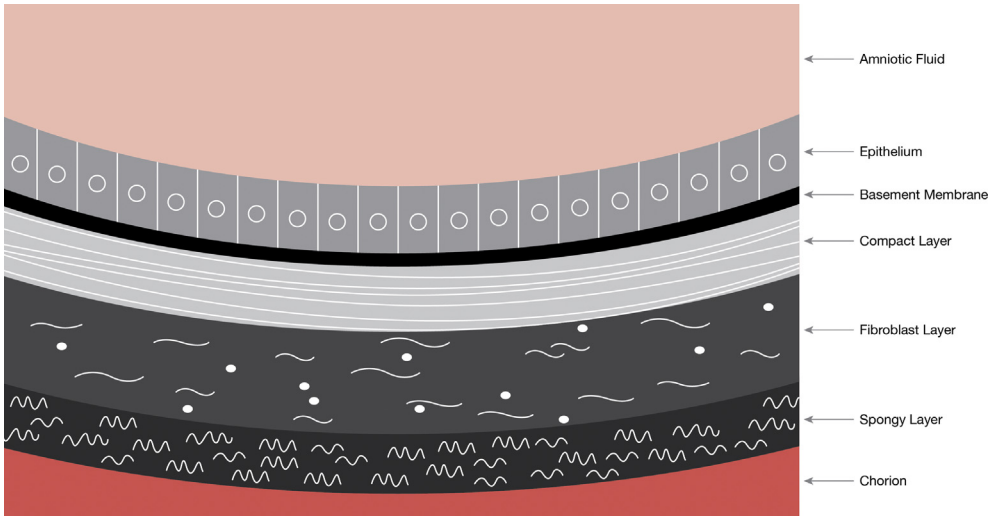

Figure 1 Schematic of amnion structure.

As a non-immunogenic material

Several investigators have concluded that amniotic epithelial and mesenchymal cells lack HLA class A, B, DR and co-stimulatory molecules CD-40, CD-80 and CD-86.[7] In contrast, others have shown the presence of class-1 and class-1b antigens in epithelial cells, mesenchymal cells and fibroblasts.[8] Radiobiological studies suggest that although amnion cells retain the ability to synthesise HLA, they do not express HLA-A, B, C or DR antigens of β-2 microglobulin on the cell surface.[9] Mesenchymal stromal cells may inhibit the maturation of peripheral blood monocytes into antigen-presenting dendritic cells.

As a promoter of epithelialisation and an inhibitor of fibrosis and scar

Amniotic epithelial and mesenchymal cells contain epidermal growth factor (EGF), keratinocyte growth factor (KGF), keratinocyte growth factor receptor (KGFR), hepatocyte growth factor (HGF), and hepatocyte growth factor receptor (HGFR). These growth factors are responsible for proliferation, migration and differentiation of epithelial cells and the promotion of epithelialisation.[10] Basic fibroblast growth factor (bFGF), and transforming growth factor (TGF) -β1, β2, β3 have also been demonstrated in amnion cells. bFGF is a pro-angiogenic factor and plays a role in the formation of granulation tissue through the proliferation of fibroblasts. The TGF-β family is responsible for the synthesis and deposition of ECM proteins and the regulation and transformation of fibroblasts into myofibroblasts.[11] Mesenchymal hyaluronic acid may inhibit TGF-β and the generation of excessive fibrosis and scar.[10] This may explain the beneficial effect amnion has on scar formation and why fetal wound healing is essentially scarless.

As an anti-inflammatory and anti-bacterial

Amniotic epithelial cells contain interleukin 10 (IL-10) that down-regulates the expression of Th1 cytokines, major histocompatibility complex (MHC) class II antigens and co-stimulatory molecules on macrophages.[12] IL-10 also enhances B-cell survival, proliferation and antibody production and has been shown to inhibit the production of pro-inflammatory cytokines such as interferon-γ, IL-2, IL-3, tumour necrosis factor-α (TNF-α), and granulocyte macrophage colony stimulating factor (GM-CSF). Other anti-inflammatory mediators such as IL-1 receptor antagonist and tissue inhibitors of metalloproteinase-1, 2, 3, 4 (TIMPs) have also been found in amniotic cells.

Amniotic fluid contains lysozymes and immunoglobulins.[13] In vitro experiments confirm reduced viability of group-A and group-B Streptococcus, *Staphylococcus aureus and Staphylococcus saprophyticus* in the presence of amnion.[14] Amnion has also been shown to produce human-beta-3-defensin. These antimicrobial peptides are implicated in the resistance of epithelial surfaces to microbial colonisation and have been shown to be upregulated in inflamed amnion.[15] Amnion epithelial cells can be induced to express intercellular adhesion molecule-1 (ICAM-1) by pro-inflammatory cytokines such as tumour necrosis factor-α (TNF-α) and IL-1β.[16] ICAM-1 has a role in the attraction and adhesion of leukocytes and may also have a role in signal transduction in pro-inflammatory pathways resulting in the recruitment of inflammatory mediators such as macrophages and granulocytes.[17]

As a regulator of angiogenesis

The angiogenic influence of amnion is uncertain. The presence of platelet derived growth factor (PDGF) and vascular endothelial derived growth factor (VEGF) are suggestive of a pro-angiogenic role.[18] bFGF may have an even greater pro-angiogenic influence than PDGF and VEGF. However, a large amount of ophthalmological research contends that it is the ability of amnion to suppress angiogenesis that renders it useful in corneal healing. The expression of tissue inhibitors of metalloproteinase (TIMP-1, 2, 3, 4), thromboplastin-1 and endostatin in amniotic cells supports these claims.[12]

Amnion collection and processing

Elective cesarean section donors undergo rigorous serological screening for human immunodeficiency virus-1/2, Hepatitis B, Hepatitis C, human T-cell lymphotrophic virus, syphilis, cytomegalovirus, and tuberculosis.[19] Following delivery, amnion is separated from the placenta by blunt dissection (see Figure 2). Once gross contaminants are removed, amnion is usually de-epithelialised to limit immunogenicity, sterilised to reduce risks of disease transmission, and preserved to improve longevity and convenience for storage. Improvements in processing have focused on preserving membrane architecture and growth factor content in order to optimise therapeutic effect.

De-epithelialisation can be performed by mechanical scraping or exposure to chemicals.[19] It is uncertain how these protocols affect the levels of growth factors and ECM proteins. Koizumi et al. showed that, although amnion denuded of its epithelium contained EGF, TGF-α, KGF, HGF, bFGF, TGF-β1, and TGF-β2, protein levels were reduced in comparison to samples with intact epithelium.[10] Whether this is clinically significant is uncertain. Neurotransmitters, neurotrophic factors and neuropeptides are concentrated in the epithelium and therefore amnion with intact epithelium may be

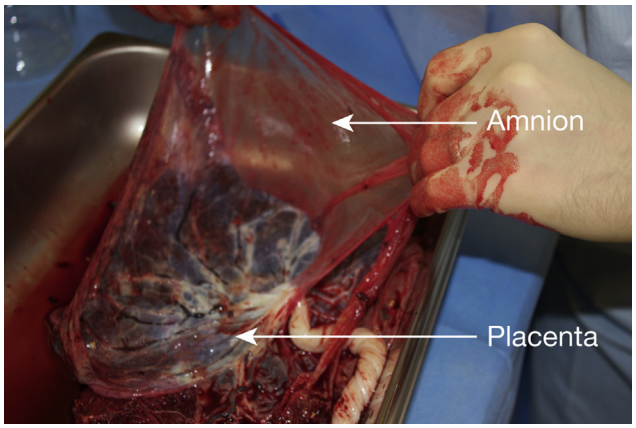

Figure 2 Amnion being bluntly dissected from human placenta.

superior when applied to neural injury.[20] In contrast, denuded amnion results in superior cell adhesion, migration and proliferation and therefore may be preferable when applied to acute and chronic wounds.[21] As the majority of clinical applications concern wound healing, the use of denuded amnion has greater representation in the literature.

Developed in the late 1980s, cryopreservation in glycerol is the most widely used preservation technique. Antibacterials and anti-fungals are often added before freezing at −80 °C. Cells are devitalised although not sterilised.[23] Viable bacteria and viruses can be present following several months of storage.[24] The effect on biological properties is uncertain. Thomasen et al. reported no detrimental impact on sterility, histological integrity or the availability of biological mediators. Amnion cryopreserved in 50% glycerol/DMEM at −80° for 1-month contained EGF, TGF-α, KGF, HGF, bFGF, TGF-β1, -β2, β3, KGFR and HGFR.[22] Cryopreservation requires expensive equipment that may be unavailable for some institutions, particularly in developing nations.

Lyophilisation is an alternative technique allowing storage of amnion at room temperature, obviating the requirement for deep freeze facilities and increasing surgeon convenience. Lyophilised membranes are commonly sterilised with gamma irradiation. Concerns exist regarding detrimental changes to membrane architecture and growth factor levels. Nakamura et al. reported no significant difference in tensile properties, tissue structure or ECM composition between lyophilised, gamma-irradiated and cryopreserved membrane.[25] Lim et al. showed that lyophilisation reduced the levels of several growth factors and ECM proteins although there was no appreciable difference in clinical performance when compared with cryopreserved samples.[26] Other methods of preservation and sterilisation exist although these are less well accepted.

The variation in processing within the literature makes it difficult to draw definitive conclusions on the optimal method. Variation also exists amongst commercially available products (Table 1). Independent of processing technique, several donor specific factors can influence the biochemical composition of amniotic membrane. Lopez-Valladares et al. showed that in fresh, cryopreserved and lyophilised amnion, levels of bFGF, HGF, KGF and TGF-β1 were significantly lower in those membranes of greater chronological and gestational age.[27] Velez et al. found significant differences in cytokine profiles between African Americans and Caucasians.[28] Membrane architecture and growth factor profile can also vary depending on what area of amnion a specimen originates from.[29] As a result, standardisation of collection and processing may be essential if consistent therapeutic results are to be achieved. If consistent relationships between donor variables and biochemical profile exist, it may become possible to select certain varieties of amnion for specific clinical situations.

Applications relevant to plastic surgery

Broadly speaking, amnion has been applied as an alternative biological dressing or has in some way augmented reconstruction. Table 2 provides examples of

Table 1 Commercially available human amnion products.

Manufacturer	Product	Membrane thickness	Indications for use	Processing technique
MiMedx (Marietta, Georgia)	AmnioFix membrane	50—100 microns	Dural reconstruction, spinal surgical barrier	Proprietary Purion process (dehydration and sterilization)
	AmnioFix Wrap	50—100 microns	Tendon and soft tissue inflammatory conditions	As above
	AmnioFix Injectable	N/A	Nerve and tendon repair	As above
	EpiFix	50—100 microns	Chronic and acute partial and full thickness wounds	As above
Bio-Tissue Inc (Miami, Florida)	Prokera corneal bandage	50—100 microns	Corneal erosion, infectious and inflammatory keratitis, herpes, superficial epithelial defects	Proprietary CryoTek process (cryopreservation)
	AmnioGraft	50—100 microns	Chemical burns, Pterygium, corneal defects, leaking glaucoma blebs, Stevens-Johnson syndrome, Strabismus	As above
	AmnioGuard	300—400 microns	Coverage of glaucoma drainage devices	As above
AcelaGraft Cellular Therapeutics (Cedar Knolls, New Jersey)	AcelaGraft	50—100 microns	General wound dressing and ophthalmic wounds	Deoxycholic acid, gel drying, electron beam irradiation

Table 2 Summary of evidence on the applications of human amnion relevant to plastic surgery.

Clinical Scenario	Author	Study design	Application	Amnion Prep	Summary of outcomes
Biological dressing					
Burns	Lin et al., 1985[30]	OCC ($n = 11$)	Overlay on autograft	Fresh	Amnion compared to conventional dressings. Good adherence, not rejected by patient, reduced pain, infection, bleeding, number of dressing changes and time to healing in amnion group
	Subrahmanyan, 1995[31]	CS ($n = 22$)	Overlay on micro-skin grafts	Fresh	Epithelialisation within 7—10 days in 16 patients. Superior wound healing due to occlusive, growth promoting effect of amnion
	Sawhney, 1989[32]	OCC ($n = 90$)	PT burns	Processed	Amnion vs conventional silver dressings. Superficial, mid-dermal and full thickness burns. Amnion reduced wound exudate, expedited epithelialisation and reduced granulation tissue and scar formation in all groups. In mid-dermal burns, amnion degraded and required regular replacement. Amnion applied to FT burns once eschar separated
	Ramakrishnan et al., 1997[33]	OCC ($n = 350$)	PT burns	Processed	Amnion compared to conventional dressings. Amnion had superior adherence, porosity allowing egress of exudate, transparency allowing wound monitoring, reduction in pain, healing times demands on nursing staff and cost
	Branski et al., 2007[34]	P-RCT ($n = 102$)	PT burns	Processed	Amnion vs topical antimicrobials. Significantly less dressing changes with amnion. Time to healing, length of stay and incidence of hypertrophic scarring were not significantly different between groups
	Singh et al., 2007[35]	OCC ($n = 50$)	PT burns	Processed	Gamma irradiated amnion compared with glycerol preserved amnion. Radiation sterilised amnion easier to apply that glycerol sterilized. No significant difference in time to healing, infection, scarring
	Fraser et al., 2009[36]	Animal ($n = 21$)	PT burns	Processed	Symmetrical lower limb deep dermal burns. Amnion vs paraffin gauze. Histopathological and immunohistochemical analysis showed significantly reduced scar tissue formation in amnion group.
	Mostaque et al., 2011[37]	P-RCT ($n = 102$)	PT burns	Processed	Paediatric burns. Amnion vs silver sulfadiazine dressings. Amnion resulted in: significantly reduced mean hospital stay, dressings changes, mean time to epithelialisation, reduced pain, increased mobility. Patient and surgeon

					satisfaction high.
	Adly et al., 2010[38]	P-RCT (n = 46)	PT + FT burns	Processed	Amniotic membrane group compared to Tegaderm dressings. Amnion resulted in significantly faster healing, lower rates of infection, lower pain scores and lower levels of electrolyte and albumin loss.
	Mohammadi et al., 2013[39]	P-RCT (n = 38)	Symmetric upper and lower limb burns	Fresh	Right limb autograft + amnion overlay vs left limb autograft + conventional dressing. Graft success assessed after 21 days. Mean graft take in right limbs was significantly higher than left (90% vs 67%)
Acute wounds	Seashore et al., 1975[40]	CS (n = 16)	Omphalocele and gastroschiasis	Fresh	Fresh amnion compared to porcine xenograft and silastic sheeting; mean time to healing 55 days; amnion superior due to ready availability, reduced bacterial counts, rapid epithelialisation
	Tekin et al., 2007[41]	CS (n = UNK)	Coverage of exposed viscera	Fresh	Amnion applied as a cover in place of Bogota bag every 48 h; reduction in serosal erosions and adhesions between bowel loops; visceral and abdominal wall oedema reduced
Chronic wounds	Troensegaard-Hansen et al., 1950[42]	CS (n = 7)	Chronic leg ulcers	Processed	Amnion used in case patients compared with 1 control treated with conventional dressings. Chronic ulceration duration 4—15 years. All amnion patients healed within 10 weeks. No healing in control patient. No wound breakdown during follow-up
	Faulk et al., 1980[18]	CS (n = 15)	Chronic leg ulcers	Fresh	Amnion vs regular dressings. Samples for histology + immunohistochemistry before and after 5-days amnion. New vessel formation + granulation tissue superior in amnion group.
	Ward et al., 1984[43]	CS (n = 28)	Chronic leg ulcers	Fresh	Amnion applied for 5-days after which ulcer was autografted. 50% recurrence at 1-year (defined as ulceration >1 cm)
	Ward et al. 1989[44]	CS (n = 27)	Chronic leg ulcers	Various	Healing compared amongst groups treated with fresh, frozen, tissue cultured maintained or lyophilized amnion. No statistically significant difference between groups. Lyophilised judged to be easiest to use and store
	Singh et al., 2004[45]	CS (n = 50)	Chronic leg ulcers	Processed	Successful pain relief and healing of ulcers of varying aetiologies
	Gajiwala et al., 2003[46]	CS (n = 8)	Pressure sore	Processed	Superficial sores treated with lyophilized, irradiated human amnion. Easy to handle and apply, analgesic, reduction in exudate, accelerated epithelialisation. Complete healing with single application

(*continued on next page*)

Table 2 (*continued*)

Clinical Scenario	Author	Study design	Application	Amnion Prep	Summary of outcomes
	Insausti et al. 2010[47]	CS ($n = 2$)	Large post-traumatic wounds	Processed	Amnion applied to large, deep wounds. Accelerated epithelialisation. Up-regulation of c-Jun expression and modification of keratinocyte migration
Reconstruction					
Dura	Tomita et al., 2012[48]	CS ($n = 10$)	Skull base	Processed	No CSF leakage or adverse outcome directly related to amnion were observed
	Hasegawa et al., 2004[49]	CR ($n = 1$)	Myelomeningocele	Fresh autograft	Autologous onlay graft; no rejection; prevention of infection following wound dehiscence; graft epithelialised; absence of excessive scar tissue formation; rapid, water-tight solution; neurotrophic factors from amnion promoted neural healing
	De Weerd et al., 2013[50]	CR ($n = 1$)	Myelomeningocele	Fresh, autograft	No rejection; absence of excessive scar tissue formation; graft epithelialised; rapid, water-tight solution; neurotrophic factors from amnion promoted neural healing
Oral cavity	Lawson, 1985[52]	CS ($n = 12$)	Pectoralis major flap oral mucosal lining	Fresh	Amnion provided scaffolding function. Flaps formed granulation tissue and epithelialised twice as fast untreated flaps. Wound contracture reduced.
	Samandari et al., 2004[55]	CS ($n = 7$)	Mandibular vestibuloplasty	Fresh	No infection or graft rejection. Amnion present for 3 weeks and led to rapid granulation tissue formation, mucosalisation and maintenance of post-operative buccal vestibular height. Prosthodontic surgery possible at 1-month
	Kothari et al., 2012[56]	CS ($n = 10$)	Mandibular vestibuloplasty	Processed	No infection or graft rejection. Amnion present for 3 weeks and led to rapid granulation tissue formation, mucosalisation and maintenance of post-operative buccal vestibular height. Prosthodontic surgery possible at 1-month
Genitalia	Tancer et al., 1979[53]	CS ($n = 4$)	Vaginal reconstruction	Fresh	Amnion applied over obturator; no rejection or infective complications; epithelialisation complete in all 4 cases by 8 weeks
	Ashworth et al., 1986[54]	CS ($n = 15$)	Vaginal reconstruction	Fresh	No rejection; purulent discharge between obturator changes although no overt infection; excellent results in partial or complete vaginal agenesis reconstruction; improvement in vaginal strictures; epithelialisation by 4 weeks
Flap and microvascular	Ozkaya et al., 2012[57]	Animal ($n = 32$)	Random pattern skin flaps	Fresh	Amnion applied to undersurface of flaps; greater survival of treated flaps. Significant reduction in polymorphonuclear leukocyte number; significant increase in capillary

					proliferation and density
	Gray et al., 1987[58]	Animal (n = 120)	Vascular interpositional grafts	Processed	Grafts soft, pliable; no collapse of graft walls; transparent wall helped to prevent back wall suturing; easier to suture than alternative synthetic (PTFE) grafts; No rejection. Patency after 3 months comparable to other synthetic grafts but inferior to control autogenous vein grafts
Tendon and nerve	Ozboluk et al., 2010[59]	Animal (n = 42)	Flexor tendon repair	Fresh	Adhesion formation reduced in amnion treated group compared with untreated control group after 6 weeks follow-up
	Meng et al.[60]	Animal (n = 36)	Nerve wrap	Processed	Significant improvements in functional recovery and nerve histomorphometric outcomes at early time points; no significant difference after 12 weeks; significantly less perineural scar tissue formation in amnion group
	Henry et al., 2009[61]	Animal (n = 24)	Nerve wrap	Processed	Photochemical sealing of amnion wrap to neurorrhaphy site resulted in significant improvement of electrophysiological and histomorphometric outcomes and reduction in axonal escape
	O'Neill et al., 2009[62]	Animal (n = 48)	Nerve wrap	Processed	Photochemical sealing of amnion wrap to neurorrhaphy site showed significantly improved functional and histomorphometric outcomes and reduction in extraneural adhesions
	Mohammad et al., 2000[63]	Animal (n = 66)	Nerve conduit	Processed	Amnion conduits vs silicone conduits vs standard autograft over 1 cm defect. Regeneration through amnion conduit comparable to autograft and superior to silicone conduit. Functional recovery statistically better at early time points in amnion group. Amnion degraded by 4-months.
	O'Neill et al., 2009[64]	Animal (n = 24)	Nerve conduit	Processed	Amnion conduits secured with either photochemical tissue bonding (PTB) or suture and compared to autograft. Functional outcomes, muscle mass retention and histomorphometry in amnion conduit + PTB comparable to autograft

PT = partial thickness; FT = full thickness; OCC = observational case controlled trial; CS = case series; CR = case report; P-RCT = prospective randomised controlled trial; UNK = unknown.

experimental and clinical evidence supporting therapeutic benefit according to these categories. In spite of the large evidence base, there is a paucity of well-designed, randomised controlled trials testing amnion performance against gold standard alternatives. A list of ongoing human clinical trials, as listed by ClinicalTrials.gov, is provided in Table 3. The following discussion makes reference to this evidence and aims to provide a more cohesive understanding. A summary of the advantages and disadvantages of amnion according to application are listed in Table 4. The applications amnion has for tissue engineering and regenerative medicine is also discussed.

Biological wound dressing

Burns

The history of amnion use for the management of burns is extensive. The use of amnion for corneal burns and other ophthalmological epithelial defects is commonplace and has led to the development of several commercially available products (Table 1). Membranes have been used as overlay following standard autografting and microskin grafting and also in place of conventional dressings following superficial and mid-dermal burns, including cadaveric allograft and porcine xenograft.[30–39]

Acute wounds

Amnion has been used as an alternative temporary biological dressing to protect exposed viscera in cases of congenital abdominal wall defects such as omphalocele and gastroschiasis and also full thickness defects secondary to major trauma, infection or oncological resection.[40] Amnion provides an alternative to the Bogota bag and can form part of a staged abdominal wall reconstruction with or without negative pressure therapy (NPT).[41]

Chronic wounds

Chronic wounds represent a major financial burden on healthcare services worldwide. Multiple studies have reported superior wound healing following the application of amnion to chronic leg ulcers of varying aetiology[18,42–45] Areas of pressure necrosis have also been treated although the suitability of amnion in these complex and often extensive wounds is most likely limited to only the most early and superficial cases.[46] Amnion has also been applied to areas of stalled healing following large traumatic soft tissue loss in patients unfit for complex reconstruction.[47] In each of these situations, amnion can be applied in conjunction with NPT.

Reconstruction

Dural repair

Amnion has been used to reconstruct dural defects in the skull base and in cases of myelomeningocele.[48–50] Water tight closure in these situations is essential in order to prevent CSF leak and potentially life threatening infection. Although synthetic materials are available in these situations, autologous solutions are preferred. In congenital anomalies such as myelomeningocele, amnion can be applied as an autograft immediately or as a delayed procedure following storage. When soft tissue defects are large, amnion can form part of a layered closure under loco-regional or free tissue transfer.[49,50] Amnion may

Table 3 Summary of registered clinical trials using human amnion.

Description	Design	Trial identifier	Institution	Status
The treatment of partial thickness burns: treated amnion versus currently in use topical medication	Phase 2/3 RCT	NCT00674999	University of Texas, Galveston	Recruiting
Evaluation of the cryopreserved amniotic membranes in the care of resistant vascular ulcers	Phase 2 single group interventional	NCT00820274	University Hospital, Limoges Etablissement Français du Sang	Recruiting
An Evaluation of the Effect of the AmnioFix™ Amniotic Membrane Allograft on Scar Tissue and Adhesions in Patients Undergoing Posterior Instrumentation Removal	Phase 2/3 Observational case controlled	NCT01357187	UNKNOWN	Not yet recruiting
The role of AMT (amniotic membrane transplantation) in treating epithelial defects and symbelpharon, preventing corneal opacification, decreasing pain, improving visual acuity and treating acute chemical burns	Phase 2/3 RCT	NCT00370812	Shaheed Beheshti Medical University	Recruiting

RCT = Randomised controlled trial.

Table 4 Advantages and disadvantages of human amnion for different clinical application.

Amniotic membrane for clinical application		
Application	Advantages	Disadvantages
General		
	Abundant supply; no donor morbidity; inexpensive; easy processing and storage; off-the-shelf availability; high tensile strength; non-immunogenic; anti-bacterial, anti-inflammatory, anti-fibrotic, regulator of angiogenesis; reduced social, cultural, religious obstacles compared with allograft and xenograft products	Donor screening; risk of disease transmission; optimal processing method uncertain; problematic handling and suturing; variable biological properties depending on sample location, donor and gestational age and race; proteolytic degradation
Biological dressing		
Burns	Readily adherent; transparent allowing wound monitoring; reduction in exudate and infection; accelerated epithelialisation; analgesic; reduction in dressing changes, analgesia requirements, demand on nursing staff; reduced cost; reduced scarring	Handling and suturing may be difficult; Membrane architecture and growth factor content varies with location, gestational age, donor age and race; Degradation may require reapplication; no adherence in full thickness burns
Acute wounds	As above; allows temporary coverage of exposed abdominal viscera; autograft possible in omphalocele and gastroschiasis;	As above
Chronic wounds	Conformable to deep, irregular wounds; permeable allowing egress of exudates; reduced requirement for autografting, time to autografting and graft failure; reduced scarring; use with NPT	As above
Reconstructive		
Dural repair	Water tight barrier; neurotrophic factors support neural tissue; autografting possible (myelomeningocele)	As above
Oral cavity and vaginal vault	Rapid epithelialisation removing need for autograft; bone coverage possible	As above
Flap and microvascular	Angiogenic effect; inhibits neutrophils and free radicals; allows manufacture of vascular grafts; amnion scaffold permits growth factor and stem cell seeding	As above; degradation may interfere with vascular graft success
Nerve and tendon	Wrap reduces scar tissue/adhesions; prevents leakage of growth factors; provides neurotrophic support; allows manufacture of conduits; amnion scaffold permits growth factor and stem cell seeding	As above; empty nerve conduits limited to short distances; degradation may interfere with conduit support

support underlying neurological tissue through the production of neurotrophic factors such as nerve growth factor (NGF), brain derived neurotrophic factor (BDNF) and brain natriuretic peptide (BNP).[14,51]

Mucosal lining

Amnion has been used to expedite epithelialisation of muscle flaps following intra-oral and vaginal vault reconstruction.[52–54] In the absence of a cutaneous paddle, these surfaces can be reconstructed with split and full thickness skin grafts, buccal mucosa grafts, intestinal mucosa, peritoneum or commercially available collagen based products. Skin grafts are perhaps the most widely practiced technique although they are associated with complications such as donor site wound, colour and texture mismatches, dryness, desquamation, hair growth, poor mobility and contracture. Commercial products are expensive and require complex processing that can reduce their clinical efficacy. Amnion has also been used to successfully cover bone following excision of gingival leukoplakia and vestibuloplasty.[55,56]

Flap and microvascular

Partial or complete flap necrosis is a dreaded complication when performing tissue transfer. Amnion applied to the undersurface of random pattern skin flaps has been shown to significantly increase capillary proliferation, reduce infiltrating neutrophils and improve flap survival.[57] Local factors liberated by amnion may reduce leukocyte activation and free radical formation, limiting endothelial injury, thrombosis and flap necrosis.

The survival of free tissue transfer relies on successful microvascular anastomosis. In major trauma or complex elective reconstruction, this can require interpositional grafting. Autogenous vein remains the gold standard graft material although the associated donor morbidity is unsavoury. Alternative biological or synthetic materials with equivalent patency and functional outcomes are desirable. Amnion has been rolled into interpositional grafts and, in a rat model, resulted in re-endothelialisation at equal time points compared with vein autografts.[58]

Tendon and nerve

Successful functional recovery, particularly in the hand and upper limb, is dependent on accurate reconstruction of tendons and nerves. Wrapping tenorrhaphy and neurorrhaphy sites with amnion can reduce adhesions and improve functional recovery.[59,60] Reducing suture burden at the repair site can also reduce scar tissue formation. Amnion wraps have been sealed around neurorrhaphy sites with a novel, sutureless, photochemical tissue bonding technique, resulting in improved functional and histological outcomes.[61,62] Amnion scaffolds may act as a reservoir of neurotrophic factors. Sealing the regenerative milieu may prevent the elution of these and other endogenous neuroregenerative factors into the surrounding tissue.

As with vessel injury, loss of nerve tissue may require bridging techniques. Autogenous nerve grafts remain the gold standard technique although in situations of major trauma, demand for autogenous material can exceed supply. Processed allografts and biological and synthetic nerve conduits are options although all are associated with limitations. Amnion provides an alternative material for the construction of nerve conduits.[63,64] As with any hollow conduit, applications remain limited to short deficits.

Tissue engineering and regenerative medicine

Amnion as a scaffold

Biological scaffolds require the presence of extracellular matrix proteins such as collagen, laminin and fibronectin. Adhesion molecules specific to these proteins facilitate cell adhesion, transmembrane receptor activation and intracellular signalling cascades that regulate cell migration, proliferation, differentiation and apoptosis.[65] Ideal scaffolds are biocompatible, mechanically stable, flexible, resorbable at a rate consistent with repair and allow the incorporation of growth factors and genetic materials.[66] Amnion basement membrane contains collagen III, IV and other glycoproteins such as laminin and fibronectin. Amnion scaffolds have been used to cultivate epithelial cells in vitro before in vivo transplantation. This has been used to reconstruct corneal surfaces following chemical burns, limbal stem cell deficiency and other related pathology.[67] Amnion scaffolds seeded with human keratinocytes have generated living skin equivalents and have been successfully transplanted into an animal model.[68] Denuded amnion has been used as a carrier matrix for chondrocytes and cartilage regeneration.[69] Amnion seeded with human umbilical vein endothelial cells and human vascular smooth muscle cells has been rolled into a cell dense, mechanically stable, multi-layered blood vessel conduit.[70] Although growth factor levels in denuded amnion may be reduced, several studies have suggested scaffolding function is more effective in the absence of epithelium. Due to the interference of hemidesmosome formation, amniotic epithelium may hinder uniform cell expansion.[71]

Amnion as an alternative source of stem cells

The use of pluripotent embryonic stem cells (ESCs) is hindered by ethical controversy. Mesenchymal stem cells (MSCs) are a less controversial, non-embryonic source of multipotent cells. Bone marrow mesenchymal stem cells (BM-MSCs) are perhaps the gold standard adult multipotent cell. However, due to the invasive and painful nature of harvest, alternatives such as adipose derived mesenchymal stem cells (AD-MSCs) have become popular. Adipose tissue is abundant, readily accessible with low morbidity, provides cell numbers and stem cell fractions that greatly exceed that of BM-MSCs, and have superior proliferation capacity and differentiation potential in vitro.[72] Adipose derived stem cells can also be induced into pluripotent cells. These cells are reprogrammed into pluripotency by inducing the expression of transcription factors characteristic of undifferentiated embryonic stem cells.[73]

Several limitations of AD-MSCs exist. Cell populations are not homogenous. Considerable variations in phenotype, proliferative capacity and differentiation potential exist between and within individuals. Proliferative capacity and differentiation potential may decrease with donor age, a characteristic shared by all adult derived MSCs.[74] The secretion of tumour promoting factors such as IL-6 and the pro-angiogenic effect of these cells have also raised concerns regarding malignant transformation.[75] With regards to induced pluripotency, the persistence of source cell epigenetic memory may render these cells unstable and unpredictable.[76]

Amnion has advantages over all adult derived MSCs. Amnion supply is unlimited and is arguably more convenient to obtain than adipose tissue. Total cell number and stem cell fraction from amnion is thought to greatly exceed both BM-MSCs and AD-MSCs.[72] In addition to amnion, placental tissue provides chorionic membrane, chorionic villi, maternal decidua, umbilical cord, umbilical cord blood and Whartons jelly. These provide additional MSCs and also embryonic populations such as endothelial and haematopoietic stem cells.[77] Proliferative capacity and differentiation potential of amnion derived cells is thought to exceed that of adipose tissue. Derivatives from all three germ layers such as adipogenic, osteogenic, chondrogenic, hepatic, pancreatic, cardiac, vascular and neural cells have been cultured and shown to possess reparative and functional capabilities. Placental cells of fetal origin (amnion, chorion, chrionic villi) may have greater differentiation potential than those of maternal origin (decidua).[78] Fetal origins may also prevent age related reductions in proliferative and differentiation potential characteristic of adult cells. Due to a maximum gestational age of 9—10 months, it is also likely that amnion provides a population of cells that have accumulated less genetic damage than adult sources.

It is currently uncertain whether amnion cells are truly pluripotent or whether multiple sub-populations of mutlipotent stem cells exist. The existence of multiple subpopulations is potentially problematic. Not unlike growth factor level, the proliferative and differentiation characteristics of these cells may vary according to membrane location, gestational and donor age, race and processing technique. In addition, different methods of culture, isolation and expansion may artificially select certain subpopulations and obscure true biological activity. Pluripotency is supported by the identification in amniotic cells of multiple molecular markers typically found on embryonic stem cells, such as octamer-4 (OCT-4), NANOG, sex-determining Y-box-2 (SOX-2), Lefty-A, FGF-4, REX-1 and

Table 5 Comparison between amnion, adipose tissue and bone marrow as alternative sources of mesenchymal stem cells.

Variable	Tissue		
	Amnion	Adipose	Bone marrow
Invasiveness of procurement	−	+	+ +
Ethical issues	−	−	−
Availability of tissue	+ + +	+ +	+
Stem cell fraction (% of total cells)	5–50	1–5	0.01–0.05
Proliferation capacity in vitro	+ + +	+ +	+
Senescence with passage	+	+ +	+ + +
Differentiation potential	+ + +	+ +	+
Reduction in differentiation potential with donor age	−	+	+
Age and environmental acquired DNA damage	−	+	+
Cryogenic storage of cells for future use following birth	+	−	−

teratocarcinoma derived growth factor-1 (TDGF-1).[79] OCT-4 is responsible for the maintenance of pluripotency and it has been shown that the level of this marker decreases with increasing cellular differentiation. Embryonic stem cells are derived from the inner cell mass of the blastocyst, which in turn gives rise to the epiblast. The epiblast, from which the amnion is derived, gives rise to all 3 germ cell layers. It is therefore possible that amniotic cells retain epiblastic pluripotency. In addition, gastrulation plays an important role in the differentiation and determination of cell fate. Amnion forms prior to this phase and it is therefore possible that these cells are pluripotent.[80] Table 5 provides a comparison of the salient characteristics of bone marrow, adipose tissue and amnion as sources of stem cells.

Conclusion

Human amnion provides the plastic surgeon with an incredibly versatile material. It is economical, widely available, easy to harvest and store and has no ethical constraints. Amnion contains a plethora of biological mediators and is a well-established alternative wound dressing. It is biocompatible, highly conformable, thin, and yet retains considerable tensile strength. Amnion can mechanically support and improve survival of transferred tissue and, through the manufacture of vessel and nerve conduits, may also directly contribute to neurovascular reconstruction. Amnion has provided a vehicle for the development of a novel photochemical tissue bonding technique that has proved efficacious for the sutureless repair of skin, tendon, nerve and vessel. Amnion may prove useful as a biological scaffold for tissue engineering and is emerging as an alternative source of multipotent and even pluripotent stem cells. After more than a century of clinical use, the application of human amnion in plastic and reconstructive surgery continues to evolve.

Conflict of interest

None.

Funding

None.

References

1. Richardson R. Copperfields caul. *Lancet* 2002;**359**:2209.
2. Davis JW. Skin transplantation with a review of 550 cases at the Johns Hopkins Hospital. *Johns Hopkins Med J* 1910;**15**:307–96.
3. Trelford JD, Anderson DG, Hanson FW, Mendel V, Sawyer RH. Amnion autografts and allografts as a cover for skin defects in sheep. A preliminary report. *J Med* 1972;**3**:81–7.
4. Mamaede AC, Carvalho MJ, Abrantes AM, Laranjo M, Maia CJ, Botelho MF. Amniotic membrane: from structure and functions to clinical applications. *Cell Tissue Res* 2012;**349**:447–58.
5. Bourne GL. The microscopic anatomy of the human amnion and chorion. *Am J Obstet Gynecol* 1960;**79**:1070–3.
6. Okazaki T, Casey ML, Okita JR, MacDonald PC, Johnston JM. Initiation of human parturition. XII. Biosynthesis and metabolism of prostaglandins in human fetal membranes and uterine decidua. *Am J Obstet Gynecol* 1981;**139**:373–81.
7. Bilic G, Zeisberger SM, Mallik AS, Zimmermann R, Zisch AH. Comparative characterization of cultured human term amnion epithelial and mesenchymal stromal cells for application in cell therapy. *Cell Transpl* 2008;**17**:955–68.
8. Hammer A, Hutter H, Blaschitz A, et al. Amnion epithelial cells, in contrast to trophoblast cells, express all classical HLA class I molecules together with HLA-G. *Am J Reprod Immunol* 1997;**37**:161–71.
9. Adinolfi M, Akle CA, McColl I, et al. Expression of HLA antigens, beta 2-microglobulin and enzymes by human amniotic epithelial cells. *Nature* 1982;**295**:325–7.
10. Koizumi NJ, Inatomi TJ, Sotozono CJ, Fullwood NJ, Quantock AJ, Kinoshita S. Growth factor mRNA and protein in preserved human amniotic membrane. *Curr Eye Res* 2000;**20**:173–7.
11. Sporn MB, Roberts AB, Wakersfield LM, de Crombrugghe B. Some recent advances in the chemistry and biology of transforming growth factor-beta. *J Cell Biol* 1987;**105**:1039–45.
12. Hao Y, Ma DH, Hwang DG, Hwang DG, Kim WS, Zhang F. Identification of antiangiogenic and antiinflammatory proteins in human amniotic membrane. *Cornea* 2000;**19**:348–52.
13. Thadepalli H, Bach VT, Davidson EC. Antimicrobial effect of amniotic fluid. *Obstet Gynecol* 1978;**52**:198–204.
14. Kjaergaard N, Hein M, Hyttel L, et al. Antibacterial properties of human amnion and chorion in vitro. *Eur J Obstet Gynecol Reprod Biol* 2001;**94**:224–9.
15. Buhimschi IA, Jabr M, Buhimschi CS, et al. The novel antimicrobial peptide beta3-defensin is produced by the amnion: a possible role of the fetal membranes in innate immunity of the amniotic cavity. *Am J Obstet Gynecol* 2004;**191**:1678–87.
16. Marvin KW, Hansen WR, Miller HC, Eykholt RL, Mitchell MD. Amnion-derived cell express intercellular adhesion molecule-1: regulation by cytokines. *J Mol Endocrinol* 1999;**22**:193–205.

17. Etienne-Manneville S, Chaverot N, Strosberg AD, Couraud PO. ICAM-1-coupled signaling pathways in astrocytes converge to cyclic AMP response element-binding protein phosphorylation and TNF-alpha secretion. *J Immunol* 1999;**163**:668—74.
18. Faulk WP, Matthews R, Stevens PJ, Bennett JP, Burgos H, Hsi BL. Human amnion as an adjunct in wound healing. *Lancet* 1980;**1**:1156—8.
19. Riau AK, Beurman RW, Lim LS, Mehta JS. Preservation, sterilization and de-epithelialisation of human amniotic membrane for use in ocular surface reconstruction. *Biomaterials* 2010;**31**:216—25.
20. Sakuragawa N, Elwan MA, Uchida S, Fujii T, Kawashima K. Non-neuronal neurotransmitters and neurotrophic factors in amniotic epithelial cells: expression and function in humans and monkey. *Jpn J Pharmacol* 2001;**85**:20—3.
21. Koizumi N, Rigby H, Fullwood NJ, et al. Comparison of intact and denuded amniotic membrane as a substrate for cell-suspension culture of human limbal epithelial cells. *Graefes Arch Clin Exp Ophthalmol* 2007;**245**:123—34.
22. Hennerbichler S, Reichi B, Pleiner D, Gabriel C, Eibl J, Redi H. The influence of various storage conditions on cell viability in amniotic membrane. *Cell Tissue Bank*; 2007:81—8.
23. Van Baare J, Cameron PU, Vardaxis N, et al. Comparison of glycerol preservation with cryopreservation methods on HIV-1 inactivation. *J Burn Care Rehabil* 1998;**19**:494—500.
24. Thomasen H, Pauklin M, Noelle B, et al. The effect of long term storage on the biological and histological properties of cryopreserved amniotic membrane. *Curr Eye Res* 2001;**36**: 247—55.
25. Nakamura T, Yoshitani M, Rigby H, et al. Sterilized, freeze-dried amniotic membrane: a useful substrate for ocular surface reconstruction. *Invest Ophthalmol Vis Sci* 2004;**45**:93—9.
26. Lim LS, Poh RW, Riau AK, Beuerman RW, Tan D, Mehta JS. Biological and ultrastructural properties of acelagraft, a freeze dried γ-irradiated human amniotic membrane. *Arch Ophthalmol* 2010;**128**:1303—10.
27. Lopez-Valladares MJ, Teresa Rodriguez-Ares M, Tourino R, Gude F, Teresa Silva M, Couceiro J. Donor age and gestational age influence on growth factor levels in human amniotic membrane. *Acta Ophthalmol* 2010;**88**:e211—6.
28. Velez DR, Fortunato SJ, Morgan N, et al. Patterns of cytokine profiles differ with pregnancy outcome and ethnicity. *Hum Reprod* 2008;**23**:1902—9.
29. Gicquel JJ, Dua HS, Brodie A, et al. Epidermal growth factor variations in human amniotic membrane used for ex vivo tissue constructs. *Tissue Eng Part A* 2009;**15**:1919—27.
30. Lin SD, Lai CS, Hou MF, Yang CC. Amnion overlay meshed autograft. *Burns Incl Therm Inj* 1985;**11**:374—8.
31. Subrahmanyam M. Amniotic membrane as a cover for micro-skin grafts. *Br J Plast Surg* 1995;**48**:477—8.
32. Sawhney CP. Amniotic membrane as a biological dressing in the management of burns. *Burns* 1989;**15**:339—42.
33. Ramakrishnan KM, Jayaraman V. Management of partial thickness burn wounds by amniotic membrane: a cost-effective treatment in developing countries. *Burns* 1997;**23**: S33—6.
34. Branski LK, Herndon DN, Celis MM, et al. Amnion in the treatment of pediatric partial-thickness facial burns. *Burns* 2008;**34**:393—9.
35. Singh R, Purohit S, Chacharkar, et al. Microbiological safety and clinical efficacy of radiation sterilized amniotic membranes for treatment of second degree burns. *Burns* 2007;**33**: 505—10.
36. Fraser JF, Cuttle L, Kempf M, et al. A randomised controlled trial of amniotic membrane in the treatment of standardised burn injury in the merino lamb. *Burns* 2009;**35**:998—1003.
37. Mostaque AK, Rahman KB. Comparisons of the effects of biological membrane (amnion) and silver sulfadiazine in the management of burn wounds in children. *J Burn Care Res* 2011;**32**:200—9.
38. Adly OA, Moghazy AM, Abbas AH, et al. Assessment of amniotic and polyurethane membrane dressings in the treatment of burns. *Burns* 2010;**36**:703—10.
39. Mohammadi AA, Seyed Jafari SM, Kiasat M, et al. Effect of fresh human amniotic membrane dressing on graft take in patients with chronic burn wounds compared with conventional methods. *Burns* 2013;**39**:349—53.
40. Seashore JH, MacNaughton RJ, Talbert JL. Treatment of gastroschisis and omphalocele with biological dressings. *J Pediatr Surg* 1975;**10**:9—17.
41. Tekin S, Tekin A, Kucukkartallar T, Cakir M, Kartal A. Use of chorioamniotic membrane instead of bogota bag in open abdomen: how i do it? *World J Gastroenterol* 2008;**14**:815—6.
42. Troensegaard-Hansen E. Amniotic grafts in chronic skin ulceration. *Lancet* 1950;**1**:859—60.
43. Ward DJ, Bennett JP. The long-term results of the use of human amnion in the treatment of leg ulcers. *Br J Plast Surg* 1984;**37**:191—3.
44. Ward DJ, Bennett JP, Burgos H, et al. The healing of chronic venous leg ulcers with prepared human amnion. *Br J Plast Surg* 1989;**42**:463—7.
45. Singh R, Chouhan US, Purohit S, et al. Radiation processed amniotic membranes in the treatment of non-healing ulcers of different aetiologies. *Cell Tissue Bank* 2004;**5**:129—34.
46. Gajiwala K, Lobo Gajiwala A. Use of banked tissue in plastic surgery. *Cell Tissue Bank* 2003;**4**:141—6.
47. Insausti CL, Alcaraz A, Garcia-Vizcaino, et al. Amniotic membrane induces epithelialization in massive posttraumatic wounds. *Wound Repair Regen* 2010;**18**:368—77.
48. Tomita T, Hayashi N, Okabe M, et al. New dried human amniotic membrane is useful as a substitute for dural repair after skull base surgery. *J Neurol Surg* 2012;**73**:302—7.
49. Hasegawa M, Fujisawa H, Hayashi Y, Yamashita J. Autologous amnion graft for repair of myelomeningocele: technical note and clinical implication. *J Clin Neurosci* 2004;**11**:408—11.
50. de Weerd L, Weum S, Sjavik K, Acharya G, Hennig RO. A new approach in the repair of a myelomeningocele using amnion and a sensate perforator flap. *J Plast Reconstr Aesthet Surg* 2013;**66**:860—3.
51. Itoh H, Sagawa N, Hasegawa M, et al. Brain natriuretic peptide is present in the human amniotic fluid and is secreted from amnion cells. *J Clin Endocrinol Metab* 1993;**76**:907—11.
52. Lawson VG. Oral cavity reconstruction using pectoralis major muscle and amnion. *Arch Otolaryngol* 1985;**111**:230—3.
53. Tancer ML, Katz M, Veridiano NP. Vaginal epithelialization with human amnion. *Obstet Gynecol* 1979;**54**:345—9.
54. Ashworth MF, Morton KE, Dewhurst J, Lilford RJ, Bates RG. Vaginoplasty using amnion. *Obstet Gynecol* 1986;**67**:443—6.
55. Samandari MH, Yaghmaei M, Ejlali M, Moshref M, Saffar AS. Use of amnion as a graft material in vestibuloplasty: a preliminary report. *Oral Surg Oral Med Oral Pathol Oral Radiol Endod* 2004;**97**:574—8.
56. Kothari CR, Goudar G, Hallur N, Sikkerimath B, Gudi S, Kothari MC. Use of amnion as a graft material in vestibuloplasty: a clinical study. *Br J Oral Maxillofac Surg* 2012;**50**:545—9.
57. Ozkaya O, Egemen O, Yesilada A, Sakiz D, Ugurlu K. The effect of non-preserved human amniotic membrane on the survival of ischaemic skin flaps in rats. *J Plast Reconstr Aesthet Surg* 2012;**65**:1700—5.
58. Gray KJ, Shenaq SM, Engelmann UH, Fishman IJ, Jeraj K, Spira M. Use of human amnion for microvascular interpositional grafts. *Plast Reconstr Surg* 1987;**79**:778—85.
59. Ozboluk S, Ozkan Y, Ozturk A, Gul N, Ozdemir RM, Yanik K. The effects of human amnion membrane and periosteal autograft on tendon healing: experimental study in rabbits. *J Hand Surg Eur Vol* 2010;**35**:262—8.

60. Meng H, Li M, You F, Du J, Luo Z. Assessment of processed human amniotic membrane as a protective barrier in rat model of sciatic nerve injury. *Neurosci Lett* 2011;**496**:48—53.
61. Henry FP, Goyal NA, David WS, et al. Improving electrophysiologic and histologic outcomes by photochemically sealing amnion to the peripheral nerve repair site. *Surgery* 2009;**145**:313—21.
62. O'Neill AC, Randolph MA, Bujold KE, Kochevar IE, Redmond RW, Winograd JM. Photochemical sealing improves outcome following peripheral neurorraphy. *J Surg Res* 2009;**151**:33—9.
63. Mohammad J, Shenaq J, Rabinovsky E, Shenaq S. Modulation of peripheral nerve regeneration: a tissue engineering approach. The role of amnion tube nerve conduit across a 1 cm nerve gap. *Plast Reconstr Surg* 2000;**105**:660—6.
64. O'Neill AC, Randolph MA, Bujold KE, Kochevar IE, Redmond RW, Winograd JM. Preparation and integration of human amnion nerve conduits using a light activated technique. *Plast Reconstr Surg* 2009;**124**:428—37.
65. Alpin AE. Cell adhesion molecule regulation of nucleocytoplasmic trafficking. *FEBS Lett* 2003;**534**:11—4.
66. Yang S, Leong KF, Du Z, Chua CK. The design of scaffolds for use in tissue engineering. Part 1. Traditional factors. *Tissue Eng* 2001;**7**:679—89.
67. Koizumi N, Inatomi T, Suzuki T, Sotozono C, Kinoshita S. Cultivated corneal epithelial stem cell transplantation in ocular surface disorders. *Ophthalmology* 2001;**108**:1569—74.
68. Yang L, Shirikata Y, Shudou M, et al. New skin equivalent model from de-epithelialised amnion membrane. *Cell Tissue Res* 2006;**326**:69—77.
69. Jin CZ, Park SR, Choi BH, Lee KY, Kang CK, Min BH. Human amniotic membrane as a delivery matrix for articular cartilage repair. *Tissue Eng* 2007;**13**:693—702.
70. Amensag S, McFetridge PS. Rolling the human amnion to engineer laminated vascular tissues. *Tiss Eng Part C Methods* 2012;**18**:903—12.
71. Burman S, Tejwani S, Vemuganti GK. Ophthalmic applications of preserved human amniotic membrane: a review of current indications. *Cell Tissue Bank* 2004;**5**:161—75.
72. Miki T, Lehmann T, Cai H, Stolz DB, Strom SC. Stem cell characteristics of amniotic epithelial cells. *Stem Cells* 2005;**23**:1549—59.
73. Park IH, Zhao R, West JA. Reprogramming of human somatic cells to pluripotency with defined factors. *Nature* 2008;**451**:141—6.
74. Witkowska-Zimny M, Walenko K. Stem cells from adipose tissue. *Cell Mol Biol Lett* 2011;**16**:236—57.
75. Walter M, Liang S, Ghosh S, Hornsby PJ, Li R. Interleukin 6 secreted from adipose stromal cells promotes migration and invasion of breast cancer cells. *Oncogene* 2009;**28**:2745—55.
76. Blasco MA, Serrano M, Fernandez-Capetillo O. Genomic instability in iPS: time for a break. *EMBO J* 2011;**30**:991—3.
77. Hass R, Kasper C, Bohm S, Jacobs R. Different populations and sources of human mesenchymal stem cells (MSC): a comparison of adult and neonatal tissue derived MSC. *Cell Commun Signal* 2011;**9**:12.
78. De Coppi P, Bartsch G, Siddiqui MM, et al. Isolation of amniotic stem cell lines with potential for therapy. *Nat Biotechnol* 2007;**25**:100—6.
79. Miki T. Amnion-derived stem cells: in quest of clinical applications. *Stem Cell Res Ther* 2011;**2**:25.
80. Enders AC, King BF. Formation and differentiation of extraembryonic mesoderm in the rhesus monkey. *Am J Anat* 1988;**181**:327—40.

Light-Activated Sealing of Nerve Graft Coaptation Sites Improves Outcome following Large Gap Peripheral Nerve Injury

Neil G. Fairbairn, M.D.
Joanna Ng-Glazier, M.D.
Amanda M. Meppelink, B.S.
Mark A. Randolph, M.A.S.
Ian L. Valerio, M.D.
Mark E. Fleming, M.D.
Jonathan M. Winograd, M.D.
Robert W. Redmond, Ph.D.

Boston, Mass.; and Bethesda, Md.

Background: Nerve repair using photochemically bonded human amnion nerve wraps can result in superior outcomes in comparison with standard suture. When applied to nerve grafts, efficacy has been limited by proteolytic degradation of bonded amnion during extended periods of recovery. Chemical cross-linking of amnion before bonding may improve wrap durability and efficacy.
Methods: Three nerve wraps (amnion, cross-linked amnion, and cross-linked swine intestinal submucosa) and three fixation methods (suture, fibrin glue, and photochemical bonding) were investigated. One hundred ten Lewis rats had 15-mm left sciatic nerve gaps repaired with isografts. Nine groups ($n = 10$) had isografts secured by one of the aforementioned wrap/fixation combinations. Positive and negative control groups ($n = 10$) were repaired with graft and suture and no repair, respectively. Outcomes were assessed using sciatic function index, muscle mass retention, and histomorphometry. Statistical analysis was performed using analysis of variance and the post hoc Bonferroni test ($p < 0.05$).
Results: Cross-linking improved amnion durability. Photochemically bonded cross-linked amnion recovered the greatest sciatic function index, although this was not significant in comparison with graft and suture. Photochemically bonded cross-linked amnion recovered significantly greater muscle mass (67.3 ± 4.4 percent versus 60.0 ± 5.2 percent; $p = 0.02$), fiber diameter, axon diameter, and myelin thickness (6.87 ± 2.23 μm versus 5.47 ± 1.70 μm; 4.51 ± 1.83 μm versus 3.50 ± 1.44 μm; and 2.35 ± 0.64 μm versus 1.96 ± 0.47 μm, respectively) in comparison with graft and suture.
Conclusion: Light-activated sealing of cross-linked human amnion results in superior outcomes when compared with conventional suture. (*Plast. Reconstr. Surg.* 136: 739, 2015.)

Outcomes following peripheral nerve repair are poor, particularly when tissue loss results in large gaps between nerve ends. Gold standard repair involves sutured autografting. However, even with meticulous microsurgical technique, needle trauma and suture material result in scar tissue formation.[1] This presents an obstacle for regenerating axons and can result in tethering, compression, and traction neuritis. These effects are amplified in the context of nerve grafting when axons must traverse two coaptation sites. Reducing manipulation of injured nerve ends and suture burden at the repair site is a logical solution to this problem.

Several sutureless repair techniques have been investigated such as fibrin glue and laser welding. Fibrin glue relies on the combination of fibrinogen and thrombin to form a fibrin clot. Although originally designed for hemostasis, off-label application for peripheral nerve repair dates back to the 1940s.[2,3] Proponents claim that fibrin

From the Division of Plastic Surgery and the Wellman Center for Photomedicine, Massachusetts General Hospital; and the Plastic Surgery Service and the Department of Orthopedics, Walter Reed National Military Medical Center.
Received for publication August 19, 2014; accepted March 26, 2015.
The last two authors are joint senior authors on this article.
Presented at the 12th Quadrennial Congress of the European Society for Plastic, Reconstructive and Aesthetic Surgeons, in Edinburgh, Scotland, July 6 through 11, 2014; the 55th Annual Meeting of the New England Society of Plastic and Reconstructive Surgeons, in Sebasco Harbor, Maine, June 6 through 8, 2014; and the 2014 American Society for Peripheral Nerve Meeting, in Kauai, Hawaii, January 8 through 14, 2014.

DOI: 10.1097/PRS.0000000000001617

Disclosure: *The authors have no financial interest to declare in relation to the content of this article.*

glue can be applied rapidly, results in less scar tissue formation, and can improve outcomes.[4–9] In contrast, others report excessive fibrosis, poor bond strength, and high rates of dehiscence.[10–13] Laser welding relies on a photothermal reaction to create coagulative bonds of denatured protein. Proposed advantages include shorter repair times and reduced inflammation, scarring, and neuroma. In some rodent models, laser welding was comparable to fibrin glue and epineurial suture.[14,15] However, because of thermal damage, poor bond strength, and high rates of dehiscence, the technique has not been adopted clinically.[16–21] Although the use of biological solder such as fascia and bovine albumin promised to enhance bond strength and limit thermal damage, interest in its potential has largely been abandoned.

Photochemical tissue bonding uses visible light to create covalent bonds between apposed tissue proteins that have been prestained with a nontoxic, photoactive dye. Dye photoactivation creates reactive species, cross-linking between amino acid residues, and the formation of nonthermal, watertight bonds.[22–25] The absence of thermal damage is a distinct advantage over laser welding. In recent years, light-activated sealing of nerve repair sites with amnion nerve wraps (Fig. 1) has emerged as an alternative to standard suture, resulting in superior functional and histologic outcomes.[26–29] These observations are likely attributable to a reduction in scar tissue formation, reduced axonal escape, and reduced leakage of neuroregenerative factors. It is possible that growth-promoting and antifibrotic factors within amniotic membrane may also be involved.

Amnion is susceptible to proteolytic degradation. When applied to corneal ulcers, untreated amnion degrades within 7 days.[30] When used to photochemically seal nerve grafts in a rabbit model, distal coaptation sites dehisced because of proteolytic degradation of amnion wraps and bonds before the arrival of regenerating axons (unpublished). Cross-linking of biomaterials reduces enzymatic degradation. Glutaraldehyde and irradiation are common cross-linking methods but are limited by toxicity and inconsistent cross-linking.[31–35] Water-soluble 1-ethyl-3-(3-dimethylamionopropyl) carbodiimide hydrochloride (EDC) is an alternative nontoxic agent resulting in carboxyl-to-amine cross-linking

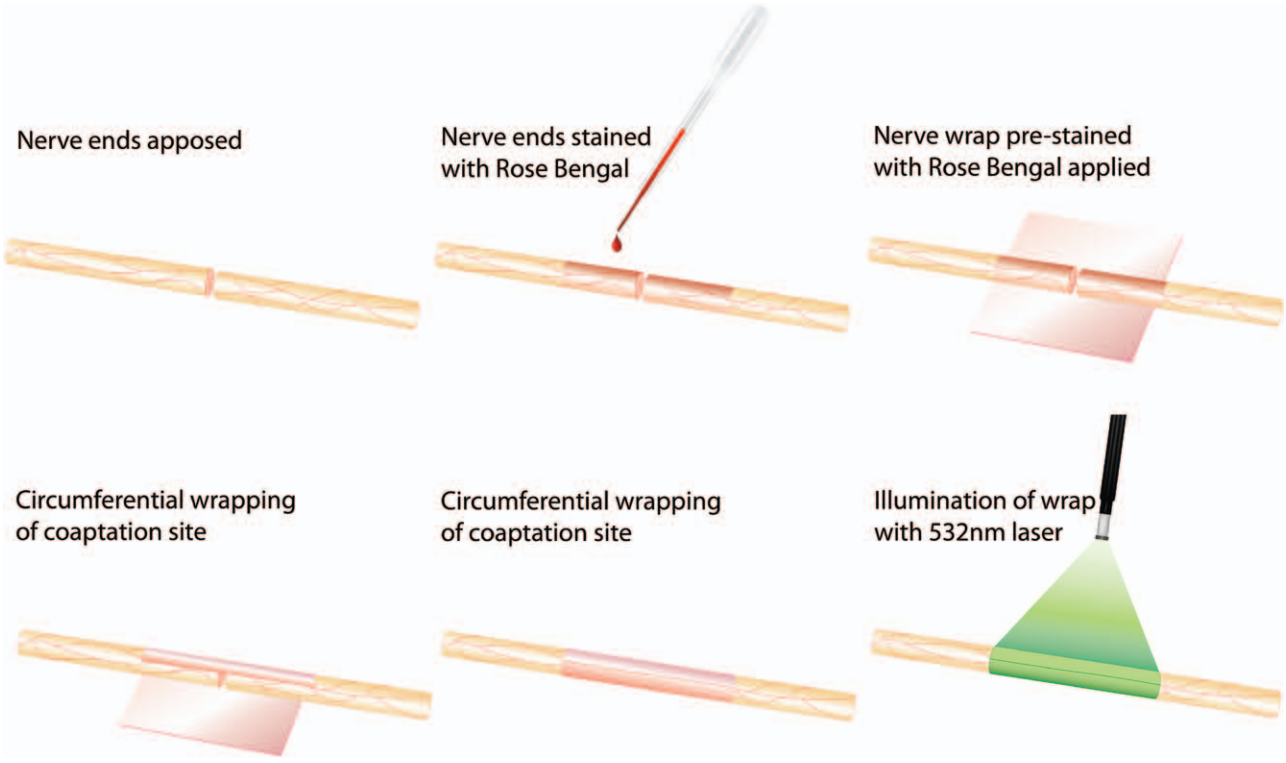

Fig. 1. Technique of nerve repair using photochemical tissue bonding. Divided nerve ends are brought into close apposition. If retraction of nerve ends prevents this, two epineurial tacking sutures may be placed 180 degrees apart to facilitate apposition. Nerve ends and nerve wrap are stained with Rose Bengal for 60 seconds. Nerve wrap is wrapped circumferentially around nerve ends and is illuminated with 532-nm laser for 60 seconds. Nerve is rotated 180 degrees and the back wall is illuminated for an additional 60 seconds.

between proteins. Used in combination with *N*-hydroxysuccinimide (NHS), EDC has been used to improve biomechanical strength and resistance to degradation of several collagen-based biomaterials, including amnion.[36–40]

Recent ex vivo work has confirmed that EDC/NHS treated amnion is stronger and more resistant to proteolytic degradation (manuscript in preparation). This work identified that a concentration of 4 mM EDC/NHS optimized biomechanical properties without jeopardizing photochemical bonding. Cross-linking and bonding was also effective when applied to a single-layer swine intestinal submucosa. This validates swine intestinal submucosa as a commercially available biomaterial approved for human use that could facilitate the clinical translation of light-activated sealing. Cross-linking nerve wraps before sealing may prevent premature degradation of photochemical bonds in vivo, improving outcomes when applied to nerve grafting of large gap injuries. By testing the efficacy of three different nerve wraps (i.e., amnion, cross-linked amnion, and cross-linked swine intestinal submucosa) and three different fixation methods (i.e., suture, fibrin glue, and photochemical tissue bonding) against gold standard isograft and suture, this study seeks to ascertain the optimal repair strategy for these challenging injuries. In light of the proposed benefits of light-activated sealing and nerve wrap cross-linking, this study aims to disprove the null hypothesis that light-activated sealing of nerve graft coaptation sites with cross-linked nerve wraps offers no advantage over conventional, gold standard suture.

MATERIALS AND METHODS

Nerve Wrap Biomaterials

Human Amnion Harvest and Processing

Amnion was obtained from elective cesarean section patients who had been screened serologically for transmissible disease. Following delivery, amnion was bluntly removed from the placenta and washed with phosphate-buffered saline (Sigma-Aldrich Co., St. Louis, Mo.). Membranes were deepithelialized using a cell scraper, cut into strips, wrapped around nitrocellulose paper, and placed in a storage solution containing a 1:1 mix of 100% sterile glycerol and Dulbecco's Modified Eagle Medium (Gibco, Grand Island, N.Y.), penicillin-streptomycin-neomycin (Gibco), and amphotericin B. Human amnion was stored at −80°C until needed. Following thawing, the amnion was mounted onto nitrocellulose paper before being dried and cut into 1 × 1-cm sections.

Swine Intestinal Submucosa

Single-layer swine intestinal submucosa material was obtained from HealthPoint Biotherapeutics (Fort Worth, Texas). Dehydrated submucosa was removed from packaging and cut into 1 × 1-cm sections before use.

Nerve Wrap Cross-Linking

Cross-linking solution was made by adding EDC/NHS (Sigma-Aldrich) to 2-(N-morpholino) ethanesulfonic acid buffer (Sigma-Aldrich). Nerve wraps were immersed in EDC/NHS for 1 hour on a platform shaker. Based on ex vivo experiments, optimal cross-linker concentration was 4 mM EDC/NHS.

Sciatic Nerve Injury and Reconstruction

The Institutional Subcommittee on Research Animal Care at the Massachusetts General Hospital approved all animal procedures during this study. One hundred ten male, inbred Lewis rats weighing 250 to 300 g were randomized to one of 11 experimental groups. This breed permitted immunotolerant isograft exchange between rodents. Induction and maintenance anesthesia was achieved using isoflurane (5% induction/2 to 3% maintenance) (Baxter Healthcare Corp., Deerfield, Ill.). Two surgeons performed all procedures together. The lead surgeon (N.G.F.) was a senior plastic surgery trainee experienced in microsurgical technique. The second surgeon (J.N.G.) was a general surgical trainee who received microsurgical training before rodent operations. A dorsolateral, muscle-splitting incision was made on the left hindquarter of each animal. Under the operating microscope, the sciatic nerve was mobilized along its length and marked 5 mm proximal to the trifurcation. Using digital calipers, nerve grafts measuring 15 mm proximal to this mark were excised, reversed, and exchanged between two simultaneously anesthetized animals. Two groups (n = 10) served as positive (six epineurial sutures) and negative (no repair) controls. The remaining nine groups (n = 10) had nerves reconstructed using different combinations of the three different nerve wraps and three different fixation methods (Table 1 and Fig. 2). Wounds were closed with 4-0 Vicryl (Ethicon, Inc., Somerville, N.J.) (muscle and deep dermal) and 4-0 Monocryl (Ethicon) (subcuticular). Topical antibacterial ointment and bitter apple were applied to wounds. Rodents were returned to the animal facility and had access to food and water as required.

Group 1: Negative Control ($n = 10$)

After the creation of nerve defects, a small incision was made in adjacent muscle. Proximal nerve ends were sutured into muscle pockets using two 10-0 Ethilon sutures (Ethicon). Distal nerve ends were left free.

Group 2: Positive Control ($n = 10$)

Following nerve exchange, grafts were secured with six 10-0 epineurial sutures at each neurorrhaphy site. After repair, any axons protruding from the repair site were trimmed.

Suture Fixation ($n = 10$): Groups 3, 4, and 5

Candidate nerve wraps were prepared as described. Nerve grafts were secured using two 10-0 nylon sutures at each end. Nerve wraps were rehydrated for 60 seconds in phosphate-buffered saline before being wrapped circumferentially around coaptation sites. Wraps were secured with one proximal and one distal 10-0 suture. Care was taken to include only the wrap and the underlying epineurium in each bite.

Fibrin Glue Fixation ($n = 10$): Groups 6, 7, and 8

Wraps were prepared and nerve grafts tacked into place as described. Following wrap application, Tisseel glue (Baxter) was applied to each nerve wrap interface, ensuring that the entire wrap was covered in glue.

Photochemical Tissue Bonding Fixation ($n = 10$): Groups 9, 10, and 11

Wraps were prepared and nerve grafts tacked into place as described. Wraps and nerve repair sites were stained with 0.1% (weight/volume) Rose Bengal (Sigma-Aldrich) for 60 seconds. After 60 seconds, excess dye was removed. Rose Bengal–stained wraps were wrapped circumferentially around repair sites, ensuring that a minimum of

Table 1. Experimental Groups*

	Nerve Wrap Material		
	HAM	**xHAM**	**xSIS**
Suture	Group 3 (HAM + suture)	Group 4 (xHAM + suture)	Group 5 (xSIS + suture)
Fibrin glue	Group 6 (HAM + fibrin)	Group 7 (xHAM + fibrin)	Group 8 (xSIS + fibrin)
PTB	Group 9 (HAM + PTB)	Group 10 (xHAM + PTB)	Group 11 (xSIS + PTB)

HAM, human amnion; xHAM, cross-linked human amnion; xSIS, cross-linked swine intestinal submucosa; PTB, photochemical tissue bonding.
*Nine treatment groups composed of different combinations of three different nerve wraps and three different fixation methods. Two control groups consisted of no repair (negative control) and nerve graft and standard epineurial suture (positive control).

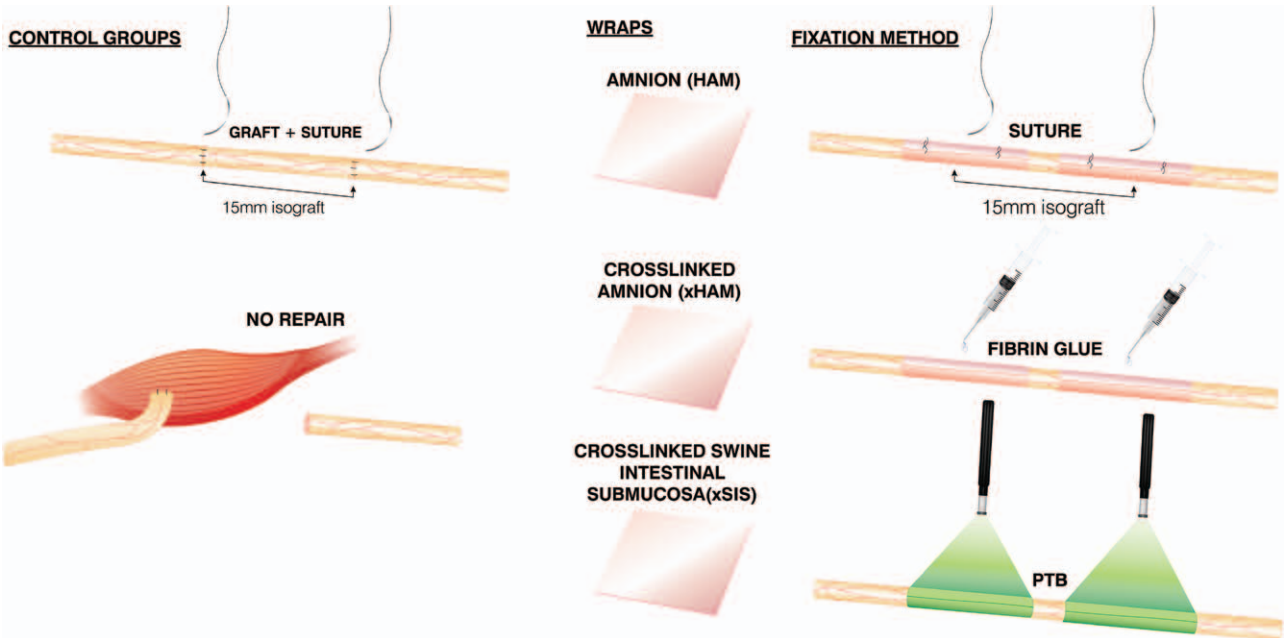

Fig. 2. Methods of nerve repair for control and experimental groups. Positive controls had nerves repaired using isografts secured with standard epineurial suture. Negative controls had 15-mm sections of nerve excised and no repair. Proximal nerve ends were buried into adjacent muscle and secured with two 10-0 nylon sutures. Nine experimental groups were composed of different combinations of the three different nerve wraps and three different fixation methods illustrated.

5 mm of overlap existed. The area of overlap was irradiated for 60 seconds using a 532-nm potassium-titanyl-phosphate laser (Laserscope, San Jose, Calif.) at an irradiance of 0.5 W/cm^2. The nerve/wrap was then rotated 180 degrees to irradiate the back wall for an additional 60 seconds (Fig. 1).

Outcome Assessment

Walking Track Analysis

Walking track analysis was performed immediately before surgery for baseline sciatic function index (SFI) and at 30-day intervals following surgery. Hind paws were dipped in ink and rats encouraged to walk up a partially enclosed ramp lined with white paper, set at an incline of 30 degrees to horizontal. Print length, toe spread, and intermediary toe spread were measured from footprints using digital calipers. Mean values from three normal and three experimental prints were entered into the sciatic function index formula described by Bain and colleagues.[41]

Muscle Weight Retention

Rodents were killed 150 days postoperatively by carbon dioxide inhalation. Left and right gastrocnemius muscles were harvested and wet weights recorded immediately for calculation of percentage muscle mass retention.

Histomorphometry

After the animals were killed, nerves were harvested 5 mm proximal and distal to the graft and immediately fixed in a mixture of 2% glutaraldehyde/2% paraformaldehyde (Electron Microscopy Sciences, Hatfield, Pa.). After 48 hours, fixed nerves were washed in sodium cacodylate buffer (0.1 M; pH 7.4) and postfixed in 2% osmium tetroxide (Electron Microscopy Sciences) for 2 hours. After further washing in buffer, specimens were dehydrated in increasing concentrations of ethanol (25%, 50%, 75%, 95%, and 100%). After dehydration, specimens were washed with propylene oxide (Electron Microscopy Sciences); embedded in epoxy resin consisting of dodecyl succinic anhydrides 98 percent plus free acid 2 percent/tEPON-812 (epoxy resin)/NMA Ultrapure (methyl-5-norbornene-2,3-dicarboxylic anhydride)/DMP-30 [2,4,6-tri (dimethylaminomethyl)phenol] (Tousimis Research Corp., Rockville, Md.); and then baked overnight in a 60°C oven. Using a diamond blade, 1-μm sections were cut 5 mm proximal and 5 mm distal to the graft.

Histologic slides were digitized using a Hamamatsu NanoZoomer 2.0-HT slide scanner (Meyer Instruments, Houston, Texas) and read using NDP.com software (Hamamatsu Corp., Bridgewater, N.J.). Images were numbered and their identity concealed during analysis. A blinded technician randomly selected five 400× images from each 40× slide. All 40× and 400× images were converted into JPEG images and imported into Adobe Photoshop (Adobe Systems, Inc., San Jose, Calif.). Two blinded researchers manually measured nerve cross-sectional area from 40× images and counted axons from each 400× image. Total counts were entered into a randomization Web site (https://www.randomizer.org) to obtain 50 random numbers. Numbered axons were then identified on each 400× image, from which fiber and axon diameters were measured. This provided measurements for 250 axons per distal nerve section.

Statistical Analysis

Statistical analysis was performed using KaleidaGraph for Windows v4.1 (Synergy Software, Reading, Pa.). Repeated measures analysis of variance (ANOVA) and the post hoc Bonferroni test were applied to monthly SFI data. Mean values across all time points in each group were compared to test for the existence of significant differences over time. Separate ANOVA was also performed on final 5-month SFI data. ANOVA and the post hoc Bonferroni test were also used to analyze muscle mass retention and histomorphometric variables. Statistical significance was set at $p < 0.05$.

RESULTS

Sciatic Nerve Graft Reconstruction

Gross Observations

All rodents survived to the end of the study. Two rodents from the cross-linked swine intestinal submucosa and photochemical tissue bonding group experienced nerve dehiscence. All other nerve repairs were intact. Cross-linked amnion and swine intestinal submucosa wraps that had been stained with Rose Bengal were identifiable (Fig. 3, *right*). In contrast, no evidence of untreated wraps could be found. Although not formally assessed by a blinded observer, the surgeons noticed that nerves repaired photochemically tended to have less extraneural scar tissue formation compared with standard graft and suture (Fig. 3).

Sciatic Function Index

All repairs experienced some degree of functional recovery. Nerves repaired with cross-linked

human amnion and photochemical tissue bonding showed the greatest functional recovery after 5 months. This was not significant compared with graft and suture (−67.9 ± 5.1 versus −71.7 ± 4.8) (Table 2 and Fig. 4). Isolated analysis at the 5-month time point identified significantly poorer SFI in the no-repair group ($p < 0.0001$), cross-linked swine intestinal submucosa and suture group ($p = 0.008$), and submucosa and photochemical tissue bonding group ($p < 0.0001$) compared with graft and suture. Mean SFI values over the entire 5-month follow-up period were significantly poorer in comparison with graft and suture for no repairs ($p < 0.001$), human amnion and suture ($p = 0.007$), cross-linked human amnion and suture ($p = 0.005$), cross-linked human amnion and fibrin ($p = 0.010$), cross-linked swine intestinal submucosa and suture, cross-linked swine intestinal submucosa and fibrin, and cross-linked swine intestinal submucosa and photochemical tissue bonding ($p < 0.001$ for all) (Table 2). There were no other significant differences in time-adjusted SFI between the remaining groups and graft and suture.

Gastrocnemius Muscle Mass Retention

Cross-linked human amnion and photochemical tissue bonding repairs experienced significantly greater muscle mass retention compared with graft and suture (67.3 ± 4.4 percent versus 60.0 ± 5.2 percent; $p = 0.02$). There were no other significant differences between remaining groups and graft and suture controls (Table 3 and Fig. 5). Although not significant, those wraps secured with fibrin glue and photochemical tissue bonding displayed a trend toward superior recovery compared with suture fixation.

Histomorphometry

All distal nerve sections were populated with axons (Fig. 6). Axon counts in the no-repair group were significantly lower than in all other groups. Distal axon counts in all remaining treatment groups did not differ significantly compared with graft and suture (Table 4). However, nerve fiber diameter, axon diameter, and myelin thickness were all significantly increased in the cross-linked human amnion and photochemical tissue bonding group compared with graft and suture repair (Table 4).

DISCUSSION

Photochemical sealing of nerve graft coaptation sites with cross-linked human amnion results in significant improvements in muscle mass retention and nerve histomorphometry compared with standard graft and suture. With the exception of cross-linked swine intestinal submucosa, all cross-linked nerve wraps displayed a trend toward

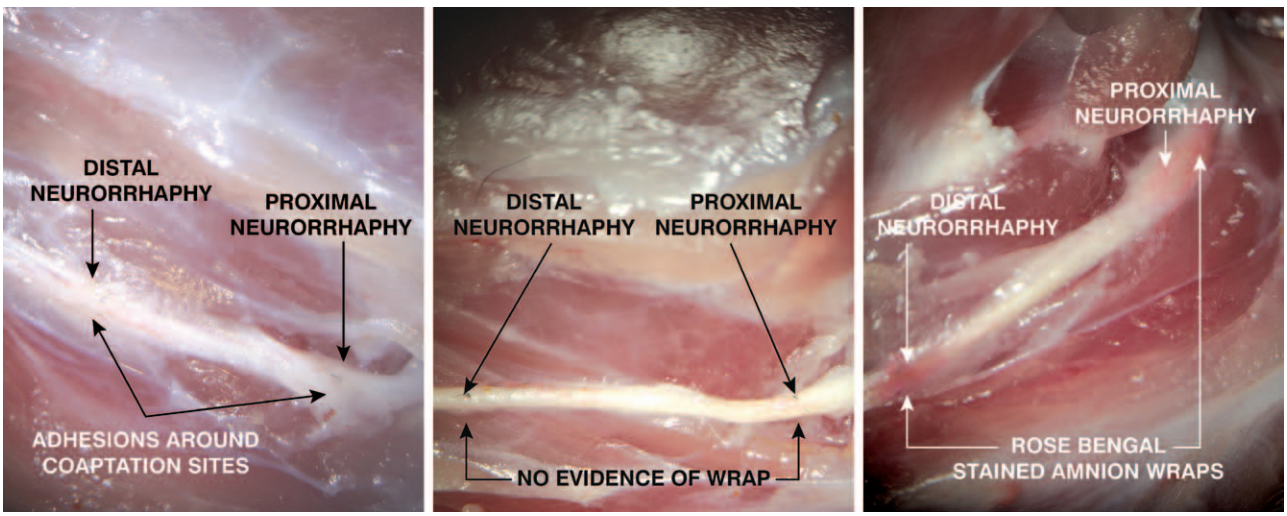

Fig. 3. (*Left*) Graft and suture after the animal was euthanized. All nerves were found to be in continuity. Note the pronounced adhesion formation surrounding each nerve graft coaptation site. (*Center*) Human amnion and photochemical tissue bonding after the animal was euthanized. All nerves were found to be in continuity. No evidence of non–cross-linked nerve wraps could be found at repair sites. Note the relative reduction in adhesion formation surrounding repair sites compared with graft and suture. (*Right*) Cross-linked human amnion and photochemical tissue bonding after the animal was euthanized. All nerves were found to be in continuity. Cross-linked nerve wraps were still identifiable after 5 months, as evidence by the pink staining from Rose Bengal. As observed in the human amnion and photochemical tissue bonding group (*center*), note the relative reduction in adhesion formation surrounding repair sites compared with graft and suture.

Table 2. Monthly Mean Sciatic Function Indexes*

Experimental Group	Mean SFI				
	1 Mo	2 Mo	3 Mo	4 Mo	5 Mo
No repair	−89.0 ± 3.9	−94.2 ± 4.7†	−89.8 ± 5.1†	−89.3 ± 4.8†	−96.2 ± 3.7†‡
Standard graft and suture	−87.6 ± 5.0	−81.1 ± 4.5	−71.8 ± 7.3	−74.7 ± 6.3	−71.7 ± 4.8
HAM + suture	−90.3 ± 5.2	−85.7 ± 9.8	−80.6 ± 3.5†	−79.7 ± 5.7	−77.9 ± 6.3‡
HAM + fibrin	−89.2 ± 4.0	−81.6 ± 4.1	−80.4 ± 7.2†	−79.4 ± 4.3	−75.2 ± 4.6
HAM + PTB	−90.0 ± 5.2	−81.2 ± 2.4	−72.8 ± 4.6	−75.6 ± 3.3	−74.5 ± 4.5
xHAM + suture	−96.6 ± 7.5	−82.4 ± 4.8	−80.0 ± 4.0†	−81.4 ± 4.8	−76.8 ± 2.7‡
xHAM + fibrin	−90.9 ± 3.2	−84.1 ± 3.6	−79.8 ± 3.3†	−81.2 ± 3.1	−75.0 ± 4.0‡
xHAM + PTB	−88.2 ± 3.9	−80.3 ± 3.5	−67.2 ± 3.3	−71.6 ± 5.5	−67.9 ± 5.1
xSIS + suture	−94.7 ± 3.9	−85.6 ± 4.4	−82.5 ± 4.4†	−81.4 ± 4.4	−80.3 ± 3.2†‡
xSIS + fibrin	−93.2 ± 4.6	−84.7 ± 4.9	−82.0 ± 3.7†	−81.5 ± 3.9	−78.8 ± 3.9‡
xSIS + PTB	−92.5 ± 2.0	−84.7 ± 5.0	−84.3 ± 4.6†	−85.3 ± 6.3†	−85.0 ± 6.0†‡

HAM, human amnion; xHAM, cross-linked human amnion; xSIS, cross-linked swine intestinal submucosa; PTB, photochemical tissue bonding; SFI, sciatic function index.
*After 5-month follow-up, xHAM and PTB recovered the greatest degree of SFI, although this was not statistically significant compared with graft and suture. No-repair, xSIS and suture, and xSIS and PTB groups had performed significantly worse than standard graft and suture, with no significant differences existing between the remaining groups. When adjusting for time and compared with standard graft and suture, mean SFI values across the entire 5-month follow-up period were significantly worse in the no-repair, HAM and suture, xHAM and suture, xHAM and fibrin, xSIS and suture, xSIS and fibrin, and xSIS and PTB groups. No other significant differences in time-adjusted SFI existed for the remaining groups.
†Statistically significant at 5-mo time point in comparison with standard graft and suture ($p < 0.05$).
‡Statistically significant mean SFI over entire 5 mo in comparison with standard graft and suture ($p < 0.05$).

greater recovery. Although in vivo nerve wrap degradation was not formally assessed during follow-up, there was visible evidence of cross-linked Rose Bengal–stained wraps after the animals were euthanized (Fig. 3, *right*). In contrast, untreated wraps were completely degraded (Fig. 3, *center*). The prevention of premature wrap degradation, before the arrival of regenerating axons, appears to maintain a protective, growth permissive seal that lasts longer. Partial degradation of cross-linked wraps did occur. Although EDC successfully protects against collagenase degradation, it may be unable to offer protection against other proteolytic enzymes.

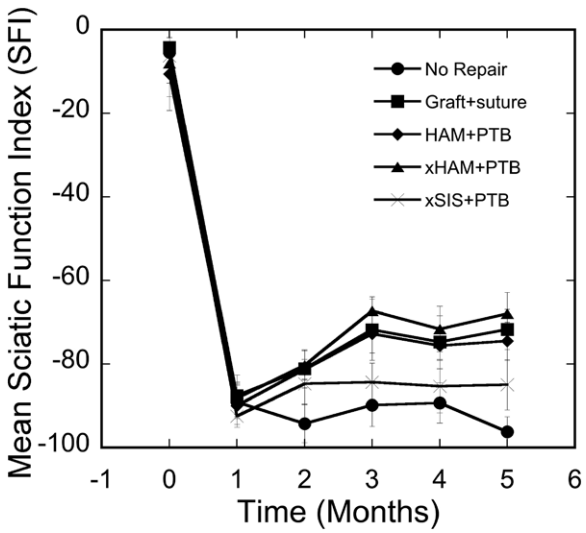

Fig. 4. SFI for select groups. Nerves repaired using cross-linked human amnion and photochemical tissue bonding (*xHAM+PTB*) recovered the greatest level of SFI, although this was not statistically significant compared with standard graft and suture at the 5-month endpoint (67.9 ± 5.1 versus −71.7 ± 4.8). Mean time-adjusted SFI over the entire follow-up period were also not significantly different between these groups. Photochemical repairs using non–cross-linked amnion (human amnion and photochemical tissue bonding; *HAM+PTB*) performed less well than cross-linked human amnion and photochemical tissue bonding and standard graft and suture, although this was not statistically significant (see Table 2). Cross-linked swine intestinal submucosa and photochemical tissue bonding (*xSIS+PTB*) performed least well out of all treatment groups.

Fixation methods associated with reduced suture burden (fibrin glue and photochemical tissue bonding) trended toward greater recovery. These observations are consistent with accepted tenets regarding the detrimental, inflammatory effect of suture. Outcomes following photochemical sealing surpassed those achieved using fibrin glue, and only those nerves repaired with photochemically sealed cross-linked amnion resulted in significant improvements in muscle mass retention and histomorphometry compared with standard graft and suture. This suggests that the benefits of reduced suture burden and photochemical sealing are additive. Axoplasmic fluid, rich in neuroregenerative factors, is released from nerve stumps following injury.[42–44] The containment of this fluid by watertight sealing may be beneficial. The benefits of photochemically sealed untreated amnion for standard neurorrhaphy have been previously demonstrated.[27] The lack of improvement of untreated amnion when applied to isografts suggests that watertight sealing of grafts is efficacious only if amnion can resist proteolytic degradation.

Table 3. Left Gastrocnemius Muscle Mass Retention*

Experimental Group	Mean Left Gastrocnemius Muscle Mass Retention (%)	SD	*p*†
No repair	9.2	0.9	<0.0001
Standard graft and suture	60.0	5.2	1
HAM + suture	56.0	5.6	1
HAM + fibrin	59.8	5.4	1
HAM + PTB	62.5	4.0	1
xHAM + suture	57.7	5.1	1
xHAM + fibrin	62.7	4.3	1
xHAM + PTB	67.3*	4.4	0.02
xSIS + suture	54.9	4.5	0.68
xSIS + fibrin	58.5	5.4	1
xSIS + PTB	54.1	3.2	0.37

HAM, human amnion; xHAM, cross-linked human amnion; xSIS, cross-linked swine intestinal submucosa; PTB, photochemical tissue bonding.
*Those nerves repaired using xHAM and PTB recovered the most gastrocnemius muscle mass retention. This result was statistically significant. Those nerves repaired using xSIS and suture and with xSIS and PTB recovered the least gastrocnemius muscle mass.
†Statistically significant improvement compared with standard graft and suture ($p < 0.05$).

It may be that the added burden of revascularization, which the graft must undergo to survive, compromises its ability to support axonal regrowth, or it may be that benefits manifest themselves only if photochemical seals are preserved long enough for axons to cross through distal coaptation sites.

In isolation, fibrin glue provides insufficient bond strength for nerve repair, although favorable outcomes have been reported when used to augment suture.[4–9] Fibrin bonds have been shown to degrade within 3 weeks[45]; as a result, the suitability of fibrin glue for wrap fixation was questionable. In spite of these concerns, no dehiscence occurred in this group, and recovery was comparable to that with standard graft and suture. This verifies that fibrin glue, in combination with epineurial tacking sutures, provides sufficient strength for repair.

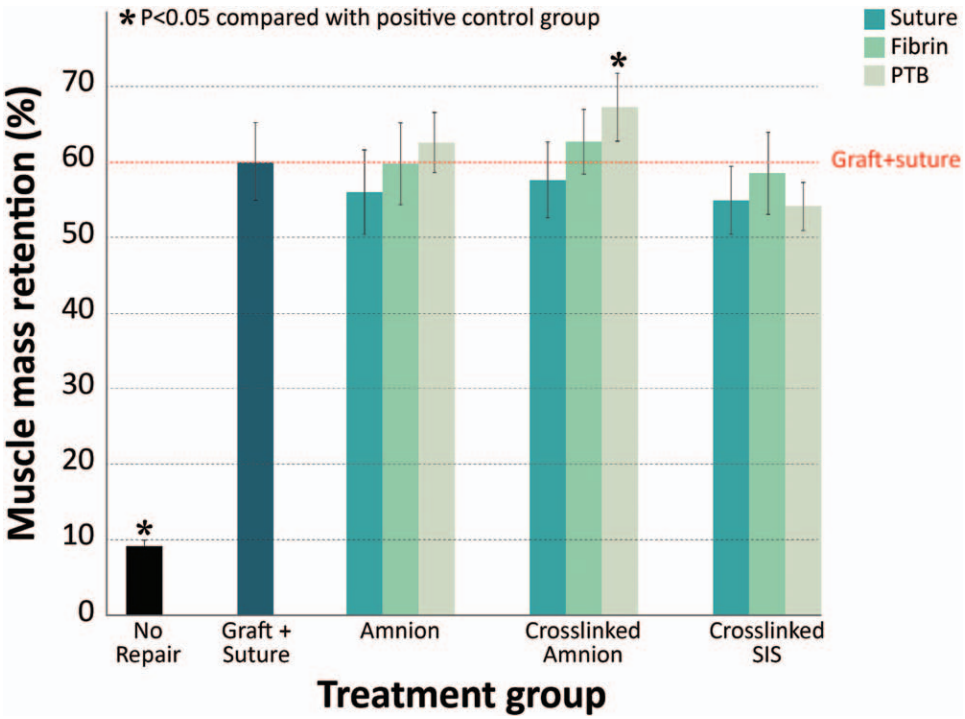

Fig. 5. Gastrocnemius muscle mass retention. Nerves repaired using cross-linked human amnion and photochemical tissue bonding (*PTB*) recovered the most gastrocnemius muscle mass, and this was statistically significant compared with graft and suture (67.3 ± 4.4 versus 60.0 ± 5.2; $p = 0.02$). Photochemical sealing of amnion wraps tended to outperform fibrin and suture fixation. This trend was not observed with cross-linked swine intestinal submucosa (*SIS*), which performed least well out of all treatment groups. *Red line* represents graft and suture.

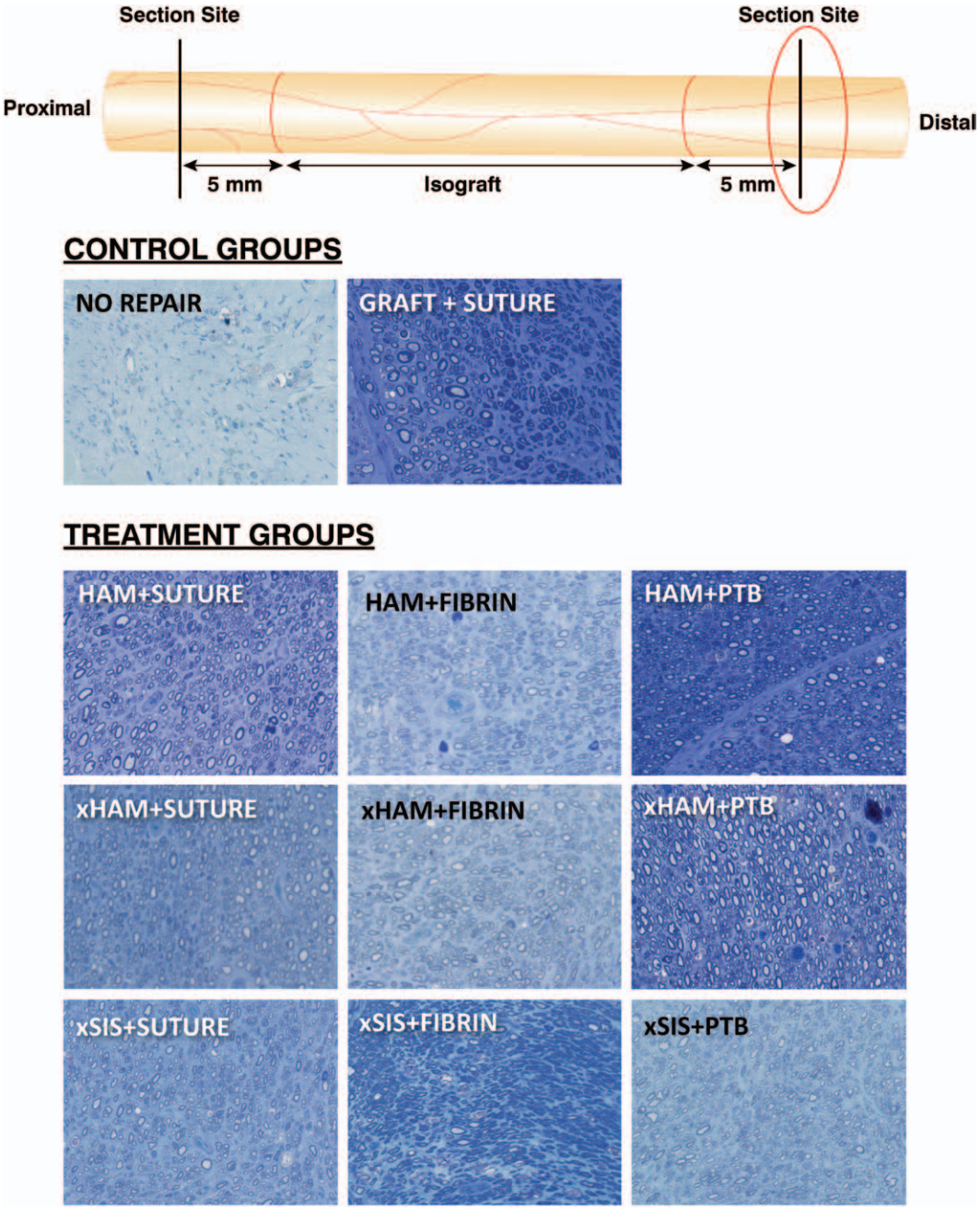

Fig. 6. Histologic slides from distal section sites. Those nerves that were not repaired lacked axons. All treatment groups regenerated axons distal to isografts, with the exception of those nerves that dehisced in the cross-linked swine intestinal submucosa (*xSIS*) and photochemical tissue bonding (*PTB*) group. Axons in the cross-linked human amnion (*xHAM*) and photochemical tissue bonding group had statistically larger fiber diameter, axon diameter, and myelin thickness compared with graft and suture (see Table 4).

Nerves repaired photochemically tended to have fewer extraneural adhesions compared with standard graft and suture (Fig. 3). Although insufficient data were collected to allow robust assessment of this observation, this is a finding consistent with previous studies.[27] The scar-reducing properties of this technique may be related to reduced suture burden, a photoinhibitory effect on tissue fibroblasts, and an antifibrotic effect of amniotic membrane.[46,47]

Two cases of nerve dehiscence occurred in the cross-linked swine intestinal submucosa and photochemical tissue bonding group. Despite superior strength and durability, in vivo use of swine intestinal submucosa was problematic. Increased thickness of swine intestinal submucosa (100 μm

Table 4. Histomorphometric Analysis of Distal Nerve Sections*

Experimental Group	Total Axon Count (× 0.001)	Axon Density (mm^2 × 0.001)	Nerve Fiber Diameter (μm)	Axon Diameter (μm)	Myelin Thickness (μm)	G Ratio
No repair	0.04 ± 0.05	0.48 ± 0.49	4.14 ± 1.15	3.13 ± 1.17	1.01 ± 0.48	0.74 ± 0.12
Standard graft and suture	7.61 ± 3.42	29.36 ± 18.10	5.47 ± 1.70	3.50 ± 1.44	1.96 ± 0.47	0.62 ± 0.08
HAM + suture	10.41 ± 3.99	28.85 ± 18.61	5.07 ± 1.58	3.44 ± 1.39	1.63 ± 0.50	0.67 ± 0.17
HAM + fibrin	10.42 ± 1.54	29.95 ± 14.00	5.22 ± 1.67	3.44 ± 1.45	1.78 ± 0.45	0.64 ± 0.09
HAM + PTB	9.31 ± 4.19	30.70 ± 8.94	5.19 ± 1.76	3.47 ± 1.53	1.72 ± 0.41	0.65 ± 0.09
xHAM + suture	9.79 ± 3.35	27.12 ± 9.22	5.14 ± 1.66	3.54 ± 1.47	1.59 ± 0.36	0.67 ± 0.08
xHAM + fibrin	10.87 ± 4.32	32.12 ± 20.28	5.24 ± 1.68	3.52 ± 1.49	1.72 ± 0.42	0.65 ± 0.09
xHAM + PTB	9.66 ± 3.08	30.73 ± 14.73	6.87 ± 2.23†	4.51 ± 1.83†	2.35 ± 0.64†	0.64 ± 0.08
xSIS + suture	9.36 ± 2.41	30.30 ± 16.46	4.83 ± 1.42	3.31 ± 1.29	1.52 ± 0.38	0.67 ± 0.08
xSIS + fibrin	6.91 ± 2.62	31.55 ± 13.37	5.18 ± 1.50	3.58 ± 1.30	1.59 ± 0.52	0.68 ± 0.11
xSIS + PTB	7.84 ± 2.04	30.06 ± 13.38	4.81 ± 1.49	3.35 ± 1.33	1.45 ± 0.34	0.68 ± 0.08

HAM, human amnion; xHAM, cross-linked human amnion; xSIS, cross-linked swine intestinal submucosa; PTB, photochemical tissue bonding.
*Histomorphometric parameters 5 mm distal to distal isograft coaptation site (mean ± SD). Axon number did not differ significantly between treatment groups. Fiber diameter, axon diameter, and myelin thickness were all significantly greater in those nerves repaired using xHAM and PTB compared with graft and suture.
†Statistically significant improvement compared with standard graft and suture ($p < 0.05$).

versus 20 to 50 μm) prevented satisfactory wrapping and adherence to small-diameter rodent sciatic nerves. As a result, bonding was suboptimal and visibly not watertight. Although ineffective for very small nerves, we are optimistic that this material may still be suitable for larger caliber nerves.

The limitations of outcome assessment in rodent models of peripheral nerve repair are well reported.[48–51] Additional limitations of our model warrant discussion. Photochemical bonding required clear access 5 mm proximal and distal to coaptation sites. As a result, the maximum achievable nerve gap before sciatic trifurcation was 15 mm. The limited "large" gap, coupled with the large regenerative capacity of rodents, may have interfered with the detection of differences between treatment groups. The performance of light-activated sealing was assessed against accepted standard isograft and suture. Outcomes in this positive control group were comparable to those of other studies.[52,53] However, some have reported more successful outcomes with sutured isografts. Methodologic discrepancies between studies commonly exist, making meaningful comparisons difficult. Nonetheless, poorer outcomes may be attributable to technical aspects of repair and microsurgical experience. The lead surgeon in this study was a senior plastic surgery trainee with experience in microsurgical nerve repair. It is possible that if repairs had been performed by an "expert" microsurgeon, outcomes following isograft and suture might have been improved. However, the technical demands of microsurgical repair are a fundamental limitation. Expertise and equipment may not be available clinically. An advantage of light-activated sealing is that surgeons without microsurgery training can readily adopt the technique.

Because of the exchange of isografts between rodents, tensionless repair was impossible. The insertion of two tacking sutures at coaptation sites was necessary to permit photochemical sealing. As a result, repairs were not truly "sutureless." However, in the clinical arena, nerve autografts and allografts can be oversized to eliminate tension, obviating the requirement for sutures. Although tacking sutures may still be necessary for group fascicular repair and cable grafting, subsequent wrapping and sealing of the entire nerve gap still offers the benefit of watertight sealing and containment of neurotrophic-rich fluid.

CONCLUSIONS

Photochemical sealing of nerve graft coaptation sites using cross-linked human amnion nerve wraps results in a significant improvement in muscle mass retention and histomorphometry in comparison with conventional graft and suture. This observation may be related to the creation of watertight seals at nerve graft coaptation sites and the improved longevity of this seal secondary to nerve wrap cross-linking. It is possible that a reduction in scar tissue formation may also contribute. Although unsuitable for small-caliber nerves, swine intestinal submucosa represents a commercially available nerve wrap that may facilitate rapid clinical translation of light-activated sealing for larger caliber nerves.

Neil G. Fairbairn, M.D.
Department of Plastic Surgery
Massachusetts General Hospital
55 Fruit Street
Boston, Mass. 02114
ngf174@hotmail.com

ACKNOWLEDGMENT

This article was funded by the Department of Defense (USMRAA W81XWH-12-1-0511). The content of this article does not necessarily reflect the position or the policy of the U.S. government, and no official endorsement should be inferred.

REFERENCES

1. DeLee JC, Smith MT, Green DP. The reaction of nerve tissue to various suture materials: A study in rabbits. *J Hand Surg Am.* 1977;2:38–43.
2. Tarlov IM, Denslow C, Swarz S, Pineless D. Plasma clot suture of nerves. *Arch Surg.* 1943;47:44–58
3. Young JZ, Medawar PB. Fibrin suture of peripheral nerves. *Lancet* 1940;239:126–128
4. Narakas A. The use of fibrin glue in repair of peripheral nerves. *Orthop Clin North Am.* 1988;19:187–199.
5. Bento RF, Miniti A. Anastomosis of the intratemporal facial nerve using fibrin tissue adhesive. *Ear Nose Throat J.* 1993;72:663.
6. Martins RS, Siqueira MG, Da Silva CF, Plese JP. Overall assessment of regeneration in peripheral nerve lesion repair using fibrin glue, suture, or a combination of the 2 techniques in a rat model: Which is the ideal choice? *Surg Neurol.* 2005;64(Suppl 1):S1:10–S1:16; discussion S1:16.
7. Menovsky T, Beek JF. Laser, fibrin glue, or suture repair of peripheral nerves: A comparative functional, histological, and morphometric study in the rat sciatic nerve. *J Neurosurg.* 2001;95:694–699.
8. Feldman MD, Sataloff RT, Epstein G, Ballas SK. Autologous fibrin tissue adhesive for peripheral nerve anastomosis. *Arch Otolaryngol Head Neck Surg.* 1987;113:963–967.
9. Smahel J, Meyer VE, Bachem U. Glueing of peripheral nerves with fibrin: Experimental studies. *J Reconstr Microsurg.* 1987;3:211–220.
10. Cruz NI, Debs N, Fiol RE. Evaluation of fibrin glue in rat sciatic nerve repairs. *Plast Reconstr Surg.* 1986;78:369–373.
11. Maragh H, Meyer BS, Davenport D, Gould JD, Terzis JK. Morphofunctional evaluation of fibrin glue versus microsuture nerve repairs. *J Reconstr Microsurg.* 1990;6:331–337.
12. Sames M, Blahos J Jr, Rokyta R, Benes V Jr. Comparison of microsurgical suture with fibrin glue connection of the sciatic nerve in rabbits. *Physiol Res.* 1997;46:303–306.
13. Herter T. Problems of fibrin adhesion of the nerves. *Neurosurg Rev.* 1988;11:249–258.
14. Menovsky T, Beek JF, Thomsen SL. Laser(-assisted) nerve repair: A review. *Neurosurg Rev.* 1995;18:225–235.
15. Fischer DW, Beggs JL, Kenshalo DL Jr, Shetter AG. Comparative study of microepineurial anastomoses with the use of CO2 laser and suture techniques in rat sciatic nerves: Part 1. Surgical technique, nerve action potentials, and morphological studies. *Neurosurgery* 1985;17:300–308.
16. Eppley BL, Kalenderian E, Winkelmann T, Delfino JJ. Facial nerve graft repair: Suture versus laser-assisted anastomosis. *Int J Oral Maxillofac Surg.* 1989;18:50–54.
17. Bass LS, Moazami N, Pocsidio J, Oz MC, LoGerfo P, Treat MR. Changes in type I collagen following laser welding. *Lasers Surg Med.* 1992;12:500–505.
18. Dort JC, Wolfensberger M, Felix H. CO2 laser repair of the facial nerve: An experimental study in the rat. *J Laryngol Otol.* 1994;108:466–469.
19. Korff M, Bent SW, Havig MT, Schwaber MK, Ossoff RH, Zealear DL. An investigation of the potential for laser nerve welding. *Otolaryngol Head Neck Surg.* 1992;106:345–350.
20. Huang TC, Blanks RH, Berns MW, Crumley RL. Laser vs. suture nerve anastomosis. *Otolaryngol Head Neck Surg.* 1992;107:14–20.
21. Menovsky T, Beek JF. Carbon dioxide laser-assisted nerve repair: Effect of solder and suture material on nerve regeneration in rat sciatic nerve. *Microsurgery* 2003;23:109–116.
22. Chan BP, Hui TY, Chan OC, et al. Photochemical crosslinking for collagen-based scaffolds: A study on optical properties, mechanical properties, stability, and hematocompatibility. *Tissue Eng.* 2007;13:73–85.
23. Kochevar IE, Redmond RW. Photosensitized production of singlet oxygen. *Methods Enzymol.* 2000;319:20–28.
24. Balasubramanian D, Du X, Zigler JS Jr. The reaction of singlet oxygen with proteins, with special reference to crystallins. *Photochem Photobiol.* 1990;52:761–768.
25. Webster A, Britton D, Apap-Bologna A, Kemp G. A dye-photosensitized reaction that generates stable protein-protein crosslinks. *Anal Biochem.* 1989;179:154–157.
26. Johnson TS, O'Neill AC, Motarjem PM, et al. Photochemical tissue bonding: A promising technique for peripheral nerve repair. *J Surg Res.* 2007;143:224–229.
27. O'Neill AC, Randolph MA, Bujold KE, Kochevar IE, Redmond RW, Winograd JM. Photochemical sealing improves outcome following peripheral neurorrhaphy. *J Surg Res.* 2009;151:33–39.
28. Henry FP, Goyal NA, David WS, et al. Improving electrophysiologic and histologic outcomes by photochemically sealing amnion to the peripheral nerve repair site. *Surgery* 2009;145:313–321.
29. O'Neill AC, Randolph MA, Bujold KE, Kochevar IE, Redmond RW, Winograd JM. Preparation and integration of human amnion nerve conduits using a light-activated technique. *Plast Reconstr Surg.* 2009;124:428–437.
30. Spoerl E, Wollensak G, Reber F, Pillunat L. Cross-linking of human amniotic membrane by glutaraldehyde. *Ophthalmic Res.* 2004;36:71–77.
31. Fujisato T, Tomihata K, Tabata Y, Iwamoto Y, Burczak K, Ikada Y. Cross-linking of amniotic membranes. *J Biomater Sci Polym Ed.* 1999;10:1171–1181.
32. Spira M, Liu B, Xu Z, Harrell R, Chahadeh H. Human amnion collagen for soft tissue augmentation: Biochemical characterizations and animal observations. *J Biomed Mater Res.* 1994;28:91–96.
33. Bigi A, Cojazzi G, Panzavolta S, Rubini K, Roveri N. Mechanical and thermal properties of gelatin films at different degrees of glutaraldehyde crosslinking. *Biomaterials* 2001;22:763–768.
34. Isenburg JC, Simionescu DT, Vyavahare NR. Tannic acid treatment enhances biostability and reduces calcification of glutaraldehyde fixed aortic wall. *Biomaterials* 2005;26:1237–1245.
35. Guldner NW, Jasmund I, Zimmermann H, et al. Detoxification and endothelialization of glutaraldehyde-fixed bovine pericardium with titanium coating: A new technology for cardiovascular tissue engineering. *Circulation* 2009;119:1653–1660.
36. Liu Y, Griffith M, Watsky MA, et al. Properties of porcine and recombinant human collagen matrices for optically clear tissue engineering applications. *Biomacromolecules* 2006;7:1819–1828.
37. Duan X, Sheardown H. Dendrimer crosslinked collagen as a corneal tissue engineering scaffold: Mechanical properties and corneal epithelial cell interactions. *Biomaterials* 2006;27:4608–4617.
38. Rafat M, Li F, Fagerholm P, et al. PEG-stabilized carbodiimide crosslinked collagen-chitosan hydrogels for corneal tissue engineering. *Biomaterials* 2008;29:3960–3972.

39. Liu W, Deng C, McLaughlin CR, et al. Collagen-phosphorylcholine interpenetrating network hydrogels as corneal substitutes. *Biomaterials* 2009;30:1551–1559.
40. Ma DH, Lai JY, Cheng HY, Tsai CC, Yeh LK. Carbodiimide cross-linked amniotic membranes for cultivation of limbal epithelial cells. *Biomaterials* 2010;31:6647–6658.
41. Bain JR, Mackinnon SE, Hunter DA. Functional evaluation of complete sciatic, peroneal, and posterior tibial nerve lesions in the rat. *Plast Reconstr Surg.* 1989;83:129–138.
42. Demirkan F, Snyder CC, Latifoglu O, Siemionow M. A method of enhancing regeneration of conventionally repaired peripheral nerves. *Ann Plast Surg.* 1995;34:67–72.
43. Lundborg G, Longo FM, Varon S. Nerve regeneration model and trophic factors in vivo. *Brain Res.* 1982;232:157–161.
44. Longo FM, Manthorpe M, Skaper SD, Lundborg G, Varon S. Neuronotrophic activities accumulate in vivo within silicone nerve regeneration chambers. *Brain Res.* 1983;261:109–116.
45. Dunn CJ, Goa KL. Fibrin sealant: A review of its use in surgery and endoscopy. *Drugs* 1999;58:863–886.
46. Fairbairn N, Randolph MA, Redmond RW. The clinical applications of human amnion in plastic surgery. *J Plast Reconstr Aesthet Surg.* 2014;67:662–675.
47. Mamede AC, Carvalho MJ, Abrantes AM, Laranjo M, Maia CJ, Botelho MF. Amniotic membrane: From structure and functions to clinical applications. *Cell Tissue Res.* 2012; 349:447–458.
48. Redett R, Jari R, Crawford T, Chen YG, Rohde C, Brushart TM. Peripheral pathways regulate motoneuron collateral dynamics. *J Neurosci.* 2005;25:9406–9412.
49. Streppel M, Azzolin N, Dohm S, et al. Focal application of neutralizing antibodies to soluble neurotrophic factors reduces collateral axonal branching after peripheral nerve lesion. *Eur J Neurosci.* 2002;15:1327–1342.
50. Boyd JG, Gordon T. Glial cell line-derived neurotrophic factor and brain-derived neurotrophic factor sustain the axonal regeneration of chronically axotomized motoneurons in vivo. *Exp Neurol.* 2003;183:610–619.
51. Guntinas-Lichius O, Irintchev A, Streppel M, et al. Factors limiting motor recovery after facial nerve transection in the rat: Combined structural and functional analyses. *Eur J Neurosci.* 2005;21:391–402.
52. Whitlock EL, Tuffaha SH, Luciano JP, et al. Processed allografts and type I collagen conduits for repair of peripheral nerve gaps. *Muscle Nerve* 2009;39:787–799.
53. Fox IK, Brenner MJ, Johnson PJ, Hunter DA, Mackinnon SE. Axonal regeneration and motor neuron survival after microsurgical nerve reconstruction. *Microsurgery* 2012;32:552–562.

Improving Outcomes in Immediate and Delayed Nerve Grafting of Peripheral Nerve Gaps Using Light-Activated Sealing of Neurorrhaphy Sites with Human Amnion Wraps

Neil G. Fairbairn, M.D.
Joanna Ng-Glazier, M.D.
Amanda M. Meppelink, B.S.
Mark A. Randolph, M.A.S.
Jonathan M. Winograd, M.D.
Robert W. Redmond, Ph.D.

Boston, Mass.

Background: Photochemical tissue bonding uses visible light to create sutureless, watertight bonds between two apposed tissue surfaces stained with photoactive dye. When applied to nerve grafting, photochemical tissue bonding can result in superior outcomes compared with suture fixation. Our previous success has focused on immediate repair. It was the aim of this study to assess the efficacy of photochemical tissue bonding when performed following a clinically relevant delay.

Methods: Forty male Lewis rats had 15-mm left sciatic nerve gaps repaired with reversed isografts immediately (n = 20) or after a 30-day delay (n = 20). Repairs were secured using either suture or photochemical tissue bonding. Rats were killed after 150 days. Outcomes were assessed using monthly Sciatic Function Index evaluation, muscle mass retention, and nerve histomorphometry. Statistical analysis was performed using analysis of variance and the post hoc Bonferroni test.

Results: In both immediate and delayed groups, photochemical tissue bonding showed a trend toward greater recovery of Sciatic Function Index, but these results were not significant. The Sciatic Function Index was significantly greater when performed immediately. Significantly greater muscle mass retention occurred following photochemical tissue bonding in both immediate and delayed repairs. Values did not differ significantly between immediate and delayed groups. Histomorphometric recovery was greatest in the immediate photochemical tissue bonding group and poorest in the delayed suture group. Fiber diameter, axon diameter, myelin thickness, and G-ratio were not significantly different between immediate suture and delayed photochemical tissue bonding.

Conclusions: Light-activated sealing of nerve grafts results in significantly better outcomes in comparison with conventional suture. The technique not only remains efficacious but may also help ameliorate the detrimental impacts of surgical delay. (*Plast. Reconstr. Surg.* 137: 887, 2016.)

Early investigators postulated that delaying nerve repair until cell bodies had been metabolically primed and distal nerves had been sufficiently cleared of debris would translate into optimized regeneration and recovery. Similarly, others theorized that predegeneration of nerve grafts would also result in superior outcomes. Despite early promise, these predictions were not substantiated in animal models.[1] Contemporary studies have highlighted the importance of expeditious nerve repair. Fu and Gordon observed that poor recovery was a result of the combined effects of chronic axotomy and chronic denervation of the distal nerve and muscle and delineated the relative contributions played by each.[2,3] These and other studies have confirmed

From the Division of Plastic and Reconstructive Surgery, Massachusetts General Hospital; and the Wellman Centre for Photomedicine, Massachusetts General Hospital.
Received for publication June 7; accepted October 28, 2015.
Presented at 2015 Annual Meeting of the American Society for Peripheral Nerve, in Paradise Island, Bahamas, January 23 through 25, 2015.
Dr. Winograd and Dr. Redmond are co–senior authors.

DOI: 10.1097/01.prs.0000479996.04255.60

Disclosure: *The authors have no financial disclosures in relation to this article.*

that chronic denervation of the distal nerve and target muscle is the most important contributing factor.[2–5] Denervated Schwann cells are less able to support regenerating axons, and chronically denervated muscle undergoes atrophy, is less able to recover from this atrophy, and has also been shown to impart a retrograde inhibitory influence on regenerating axons, the effects of which worsen with time.[5]

Following trauma, priority is given to patient stabilization and wound decontamination before the onset of definitive reconstruction. As a result, long delays before nerve repair can be unavoidable. Denervation times are further extended following proximal limb injury and when substantial nerve gaps exist. Autologous nerve grafts represent the current gold standard method of nerve gap repair although, following major tissue loss and limb amputation, when demand for autograft often exceeds supply, the use of acellular nerve allografts is an alternative option. Outcomes in these circumstances are notoriously poor. Improving regenerative support within grafts and expediting rates of axonal regeneration aims to reduce the deleterious effects of denervation and is the focus of much research. A limitation of many studies is that the intervention under investigation often occurs immediately following nerve repair, a situation that simply does not exist clinically. As a result, some studies may not readily translate into clinical practice.

Researchers have demonstrated superior rates of regeneration and recovery following electrical stimulation.[6–10] At the cellular level, others have reported success following the supplementation of stem cells and neurotrophic factors.[11–14] We propose a novel method that may enhance outcomes following delayed nerve gap repair by sealing the neurorrhaphy site, capturing endogenous regenerative factors within, and excluding unwanted mediators of scarring and inflammation. Light-activated sealing of human amnion nerve wraps around coaptation sites is an alternative fixation method to conventional suture. A photochemical reaction between amnion and epineurium, both of which have been stained with a photoactive dye, results in the formation of watertight bonds. In recent studies, this technique, known as photochemical tissue bonding, has been found to result in superior outcomes in comparison with conventional suture when tested in rodent models of end-to-end[15–17] and immediate isograft repair.[18] The technique has also remained efficacious when used with acellular nerve allografts.[19] Crosslinking of amnion before sealing offers protection from proteolytic degradation over prolonged periods of recovery associated with nerve grafting. The technique has also been applied successfully to peripheral nerve repair using photochemically sealed chitosan adhesive films.[20] This study assesses whether photochemical sealing of nerve grafts remains efficacious following a clinically relevant surgical delay and, indeed, whether outcomes can be enhanced in comparison with conventional suture repair.

METHODS

Amnion Nerve Wrap Preparation

Human amniotic membrane was obtained from elective cesarean section patients who had been screened for human immunodeficiency virus types 1 and 2, hepatitis B, hepatitis C, human T-cell lymphotrophic virus, syphilis, cytomegalovirus, and tuberculosis. Once removed from the placenta, amnion was irrigated with phosphate-buffered saline (Sigma-Aldrich, Co., St. Louis, Mo.). Membranes were mechanically deepithelialized using a cell scraper, cut into strips, wrapped around nitrocellulose paper, and placed in a storage solution containing a 1:1 mix of 100% sterile glycerol and Dulbecco's Modified Eagle Medium (Gibco, Grand Island, N.Y.), penicillin-streptomycin-neomycin (Gibco), and amphotericin B. Human amniotic membrane was stored at −80°C and, when required, thawed, dried onto nitrocellulose paper, and cut into 1 × 1-cm sections. Nerve wraps were cross-linked, as described previously in a recent publication, using water-soluble 1-ethyl-3-(3-dimethylaminopropyl) carbodiimide hydrochloride and *N*-hydroxysuccinimide (Sigma-Aldrich) reconstituted with 2-(*N*-morpholino) ethanesulfonic acid buffer (Sigma-Aldrich).[18]

Sciatic Nerve Injury and Reconstruction

The Institutional Animal Care and Use Committee at the Massachusetts General Hospital approved all procedures. Forty inbred Lewis rats weighing 250 to 300 g were randomized to one of four experimental groups described below. A further 10 Lewis rats were used as isograft donors. This breed was selected to permit immunotolerant isograft exchange between rodents for nerve gap reconstruction. Induction and maintenance anesthesia was achieved using isoflurane (Baxter Healthcare Corp., Deerfield, Ill.), 5% induction and 2% to 3% maintenance. Two surgeons performed all procedures together. The lead surgeon

was a senior plastic surgery trainee with microsurgical experience. The assistant surgeon was a general surgical trainee who received microsurgical training before rodent operations. A dorsolateral, muscle-splitting incision was made on the left hindquarter of each animal and, under the operating microscope, the sciatic nerve was mobilized along its length. To standardize nerve graft location, a site 5 mm proximal to the trifurcation was marked. Using digital calipers, grafts measuring 15 mm proximal to this mark were excised. Groups 1 and 2 had nerve gaps repaired immediately, whereas groups 3 and 4 had nerve gaps repaired following a 30-day delay (Fig. 1). Wounds were closed in three layers with 4-0 Vicryl (Ethicon, Inc., Somerville, N.J.) (muscle and deep dermal) and 4-0 Monocryl (Ethicon) (subcuticular). Topical antibacterial ointment was applied liberally to wounds, and bitter apple sprayed onto the left foot to discourage automutilation. Rodents were housed in the Massachusetts General Hospital small-animal facility and had access to food and water as needed.

Immediate Repair: Groups 1 and 2

Two rodents were anesthetized simultaneously. Following the excision of 15-mm segments of sciatic nerve, nerves were reversed and immediately exchanged as isografts between animals. In group 1, isografts were secured using six 10-0 Ethilon sutures (Ethicon), representing the current standard of care. Following repair, any protruding axons were trimmed and allowed to retract within the coaptation site. In group 2, isografts were secured using photochemical sealing. Amnion nerve wraps were prepared as described

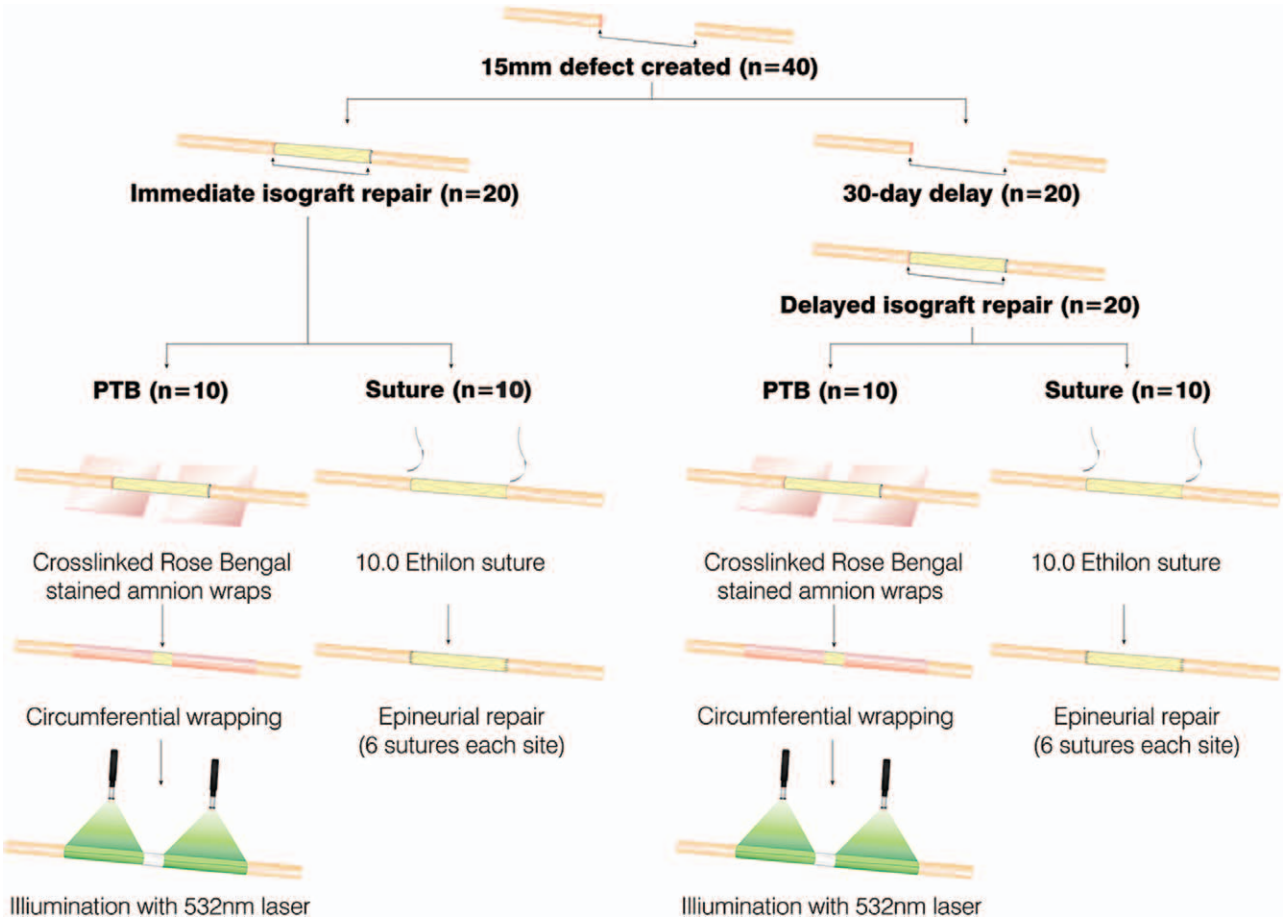

Fig. 1. Methods of immediate and delayed nerve repair. Forty rodents had 15-mm left sciatic nerve gaps created. These were repaired with reversed isografts. In two groups, repair occurred immediately after injury and involved the exchange of isografts between two simultaneously anesthetized rodents. Isografts were secured with either photochemical sealing (n = 10) or conventional epineurial suture (n = 10) using 10-0 Ethilon. In the remaining 20 rodents, repair occurred following a 30-day delay, during which proximal nerve ends were buried into adjacent muscle to prevent regeneration and reinnervation of the distal stump. After this delay, all wounds were reopened and gaps repaired using isografts harvested from 10 donor Lewis rats. As above, these isografts were secured with either photochemical sealing or conventional suture. *PTB*, photochemical tissue bonding.

above. To overcome tension between nerve ends, isografts were tacked into place using two 10-0 Ethilon sutures. Before transfer into the surgical field, wraps and coaptation sites were stained with 0.1% (weight/volume) Rose Bengal (Sigma-Aldrich) for 60 seconds. After 60 seconds, excess dye was removed. Rose Bengal–stained wraps were wrapped circumferentially around sciatic nerves, ensuring that a minimum of 5-mm overlap existed. The area of overlap was irradiated for 60 seconds using a 532-nm potassium titanyl phosphate laser (Laserscope, San Jose, Calif.) at an irradiance of 0.5 W/cm^2. The nerve/wrap was then rotated 180 degrees to irradiate the back wall in the same manner for an additional 60 seconds (Fig. 1).

Delayed Repair: Groups 3 and 4

After the creation of 150-mm sciatic nerve defects, a small incision was made in adjacent muscle, and proximal nerve ends were buried and secured using two 10-0 Ethilon sutures. Distal nerve ends were left free. Wounds were closed as described and the animals were returned to the animal facility. After 30 days, wounds were reopened and nerve ends dissected and mobilized. Simultaneously, fresh isografts were harvested from donor Lewis rats, immediately reversed, and transferred into the nerve gap. In group 3, isografts were secured with 10-0 Ethilon suture, and in group 4, isografts were sealed photochemically as described previously (Fig. 1).

Outcome Assessment

Walking Track Analysis

Walking track analysis was performed immediately before surgery for baseline Sciatic Function Index. In the delayed groups, Sciatic Function Index was also performed following the 30-day delay, immediately before isograft reconstruction. Following isograft repair, walking track analysis was performed at 30-day intervals. After dipping both hind paws in water-soluble ink, rats were encouraged to walk up a 10 × 60-cm, partially enclosed ramp lined with white paper and set at an incline of 30 degrees to horizontal. Print length, toe spread, and intermediary toe spread were measured from footprints using digital calipers. Mean values from three normal and experimental prints were entered into the Sciatic Function Index formula described by Bain and colleagues.[21]

Muscle Weight Retention and Nerve Histomorphometry

After 150 days, animals were killed using carbon dioxide inhalation. Immediately after this, both gastrocnemius muscles were harvested and had wet weights measured for calculation of left-side percentage muscle mass retention. Nerves were harvested 5 mm proximal and distal to isograft coaptation sites. Following fixation, dehydration, and embedding in epoxy resin, nerves had 1-μm sections cut from proximal and distal ends. Once prepared, nerve sections were scanned digitally using a Hamamatsu NanoZoomer 2.0-HT slide scanner (Meyer Instruments, Houston, Texas) and read using NDP.com software (Hamamatsu Corp. Bridgewater, N.J.). The specific details of these methods are available in a recently published article. The identity of digital images was concealed and all histomorphometric analysis (axon count, fiber diameter, axon diameter, myelin thickness, and G-ratio) was conducted by two blinded researchers.

Statistical Analysis

Statistical analysis was performed using KaleidaGraph for Windows v4.1 (Synergy Software, Reading, Pa.). Sciatic Function Index data were analyzed using repeated measures analysis of variance to detect the existence of significant differences over time. All remaining analysis between treatment groups was performed using analysis of variance and the post hoc Bonferroni test. Values of $p < 0.05$ were considered statistically significant.

RESULTS

Gross Observations

Two rodents in the delayed photochemical tissue bonding group had to be killed prematurely because of intractable foot ulcers. Unfortunately, one of these animals was disposed of before necropsy could be performed. In the remaining rodent, the isograft was found to be in continuity but had experienced considerable atrophy at the midportion of the graft (Fig. 2, *above*, *left*). No other episodes of dehiscence occurred in the remaining groups, with all nerves showing evidence of regeneration. Cross-linked amnion nerve wraps were identifiable following sacrifice in all groups, showing that cross-linking protects enzymatic degradation for a minimum of 5 months (Fig. 2, *above*, *right*). Extraneural scarring appeared qualitatively reduced in those nerves repaired photochemically, an observation consistent with previous studies (Fig. 2, *below*).

Sciatic Function Index

After 5 months' follow-up, greatest recovery of Sciatic Function Index occurred in the

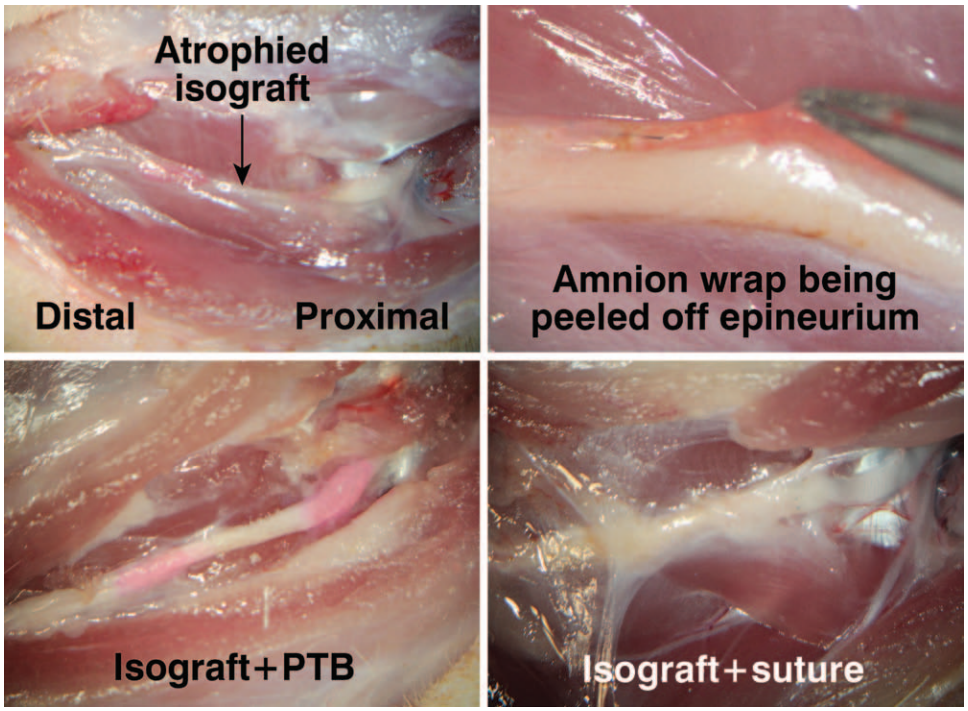

Fig. 2. Gross observations after the animals were killed. Two animals in the isograft plus photochemical tissue bonding (*PTB*) group were killed before the completion of 150 days' follow-up because of intractable foot ulcers. Necropsy of one animal showed intact photochemical bonds but a severely atrophied graft. The remaining animal was disposed of before examination could take place (*above*, *left*). Amnion wraps were found to be present, evidence of successful retardation of proteolytic degradation (*above*, *right*). Qualitatively, isograft plus photochemical tissue bonding nerves had less extraneural scar tissue formation than isograft plus suture groups (*below*).

Table 1. Mean Sciatic Function Index for All Treatment Groups over the 5-Month Follow-Up Period*

	Mean SFI				
Experimental Group	**1 Mo**	**2 Mo**	**3 Mo**	**4 Mo**	**5 Mo**
Immediate suture	−91.4 ± 10.2	−81.4 ± 4.2	−78.2 ± 4.5	−72.4 ± 6.3	−72.3 ± 4.7
Immediate PTB	−91.4 ± 5.2	−81.3 ± 3.6	−74.1 ± 4.7	−71.8 ± 4.2	−68.5 ± 4.7
Delayed suture	−92.9 ± 4.5	−84.9 ± 6.7	−84.9 ± 6.8	−82.8 ± 5.4	−80.1 ± 4.4
Delayed PTB	−92.4 ± 3.3	−84.4 ± 5.6	−80.7 ± 5.2	−79.7 ± 5.4	−77.3 ± 4.1

SFI, Sciatic Function Index; PTB, photochemical tissue bonding.
*Immediate photochemical tissue bonding of isografts recovered greatest Sciatic Function Index after 5 months, although this was not statistically significant in comparison with gold standard immediate suture. Similarly, no significant difference existed between delayed photochemical tissue bonding and delayed suture. Sciatic Function Index in the immediate suture group was significantly better than in the delayed suture group ($p = 0.003$). Likewise, immediate photochemical tissue bonding recovered a significantly greater Sciatic Function Index in comparison with delayed photochemical tissue bonding ($p = 0.002$). Immediate photochemical tissue bonding was significantly better than delayed suture, which performed poorest of all groups ($p < 0.0001$). No significant difference existed between immediate suture and delayed photochemical tissue bonding.

immediate photochemical tissue bonding group. This result was not statistically significant in comparison with gold standard immediate suture, although it was statistically better than that of the delayed photochemical tissue bonding group (−68.5 ± 4.7 versus −72.3 ± 4.7, $p = 0.41$; and −68.5 ± 0.47 versus −77.3 ± 4.1, $p = 0.002$, respectively). Recovery in the immediate suture group was statistically better than delayed suture, which performed poorest of all groups (−72.3 ± 4.7 versus −80.1 ± 4.4). There was no significant difference between immediate suture and delayed photochemical tissue bonding (−72.3 ± 4.7 versus −77.3 ± 4.1) (Tables 1 and 2).

Gastrocnemius Muscle Mass Retention

Muscle mass retention was greatest in the immediate photochemical tissue bonding group,

Table 2. Bonferroni All-Pairs Comparison for Treatment Groups*

Group Comparison	SFI (5-mo)	Muscle Mass	Axon Count	Fiber Diameter	Axon Diameter	Myelin Thickness	G-Ratio
Immediate suture vs. immediate PTB	0.41	0.02	1	<0.0001	<0.0001	<0.0001	<0.0001
Immediate suture vs. delayed suture	0.003	0.10	0.23	<0.0001	<0.0001	<0.0001	1
Immediate suture vs. delayed PTB	0.17	1	1	1	0.35	1	0.06
Immediate PTB vs. delayed suture	<0.0001	<0.0001	0.24	<0.0001	<0.0001	<0.0001	<0.0001
Immediate PTB vs. delayed PTB	0.002	0.16	1	<0.0001	<0.0001	<0.0001	<0.0001
Delayed suture vs. delayed PTB	1	0.03	1	<0.0001	<0.0001	0.001	0.12

SFI, Sciatic Function Index; PTB, photochemical tissue bonding.
*No significant differences in Sciatic Function Index were detected between immediate suture and immediate photochemical tissue bonding or delayed suture and delayed photochemical tissue bonding. Significant differences were detected between immediate and delayed suture and immediate and delayed photochemical tissue bonding, highlighting the detrimental impact of delay. No significant difference existed between immediate suture and delayed photochemical tissue bonding. Muscle mass retention was significantly improved following photochemical tissue bonding repair in both immediate and delayed groups. The effects of delay were not significantly different for suture or photochemical tissue bonding fixation. As with Sciatic Function Index, immediate suture was not significantly different compared with delayed photochemical tissue bonding. No significant differences in axon count or density existed between groups. Fiber diameter, axon diameter, and myelin thickness and G-ratio were not significantly different between immediate suture and delayed photochemical tissue bonding. With the exception of G-ratio, all other histomorphometric parameter comparisons were significantly different between treatment groups, with immediate photochemical tissue bonding achieving greatest recovery and delayed suture being poorest.

Table 3. Gastrocnemius Muscle Mass Retention for All Groups*

Experimental Group	Mean Left Gastrocnemius Muscle Mass Retention (%)	SD (%)	*p*
Immediate suture	59.0	3.6	—
Immediate PTB	64.9†	3.9	0.02
Delayed suture	54.1	5.3	0.10
Delayed PTB	60.2	4.1	1

PTB, photochemical tissue bonding.
*Groups compared statistically to immediate suture. Delayed suture and delayed photochemical tissue bonding did not differ significantly in comparison with the immediate suture group. See Table 2 for Bonferroni all-pairs comparison.
†The immediate photochemical tissue bonding group recovered significantly greater muscle mass than immediate suture.

and this was statistically significant in comparison with the immediate suture group (64.9 ± 3.9 percent versus 59.0 ± 3.6 percent, $p = 0.02$). A similar significant improvement was also observed in the delayed photochemical tissue bonding group in comparison with delayed suture (60.2 ± 4.1 percent versus 54.1 ± 5.3 percent, $p = 0.03$). With regard to the surgical delay, no significant difference existed between immediate suture and delayed suture, or immediate photochemical tissue bonding and delayed photochemical tissue bonding groups. Muscle mass retention was not significantly different between immediate suture and delayed photochemical tissue bonding (59.0 ± 3.6 percent versus 60.2 ± 4.1 percent, $p = 1$) (Tables 2 and 3).

Nerve Counts and Histomorphometry

No significant differences in axon counts existed between any of the treatment groups. The immediate photochemical tissue bonding group recovered greatest fiber diameter, axon diameter, myelin thickness, and G-ratio, and this was statistically significant in comparison with immediate suture and all remaining groups (Fig. 3). With the exception of G-ratio, all measurements were significantly greater in the delayed photochemical tissue bonding group in comparison with the delayed suture group. With regard to surgical delay, fiber diameter, axon diameter and myelin thickness were significantly greater in the immediate suture group compared with the delayed suture group. No significant difference in G-ratio was detected. All measurements in the immediate photochemical tissue bonding group were significantly better compared with the delayed photochemical tissue bonding group. No significant difference in any histomorphometric measurement existed between immediate suture and delayed photochemical tissue bonding (Tables 2 and 4 and Fig. 3).

DISCUSSION

This study verifies that light-activated sealing remains superior to conventional suture when performed both immediately and after a clinically relevant delay. Although this relationship was not significant for Sciatic Function Index, mean values were greater for light-activated sealing. Both muscle mass retention and nerve histomorphometry were significantly improved in immediate and delayed photochemical tissue bonding groups, suggesting that this may be a more sensitive measure than Sciatic Function Index in detecting a difference in regeneration. Sciatic Function Index and histomorphometric outcomes between immediately sutured nerves and delayed, photochemical repairs were not significantly different. This suggests that

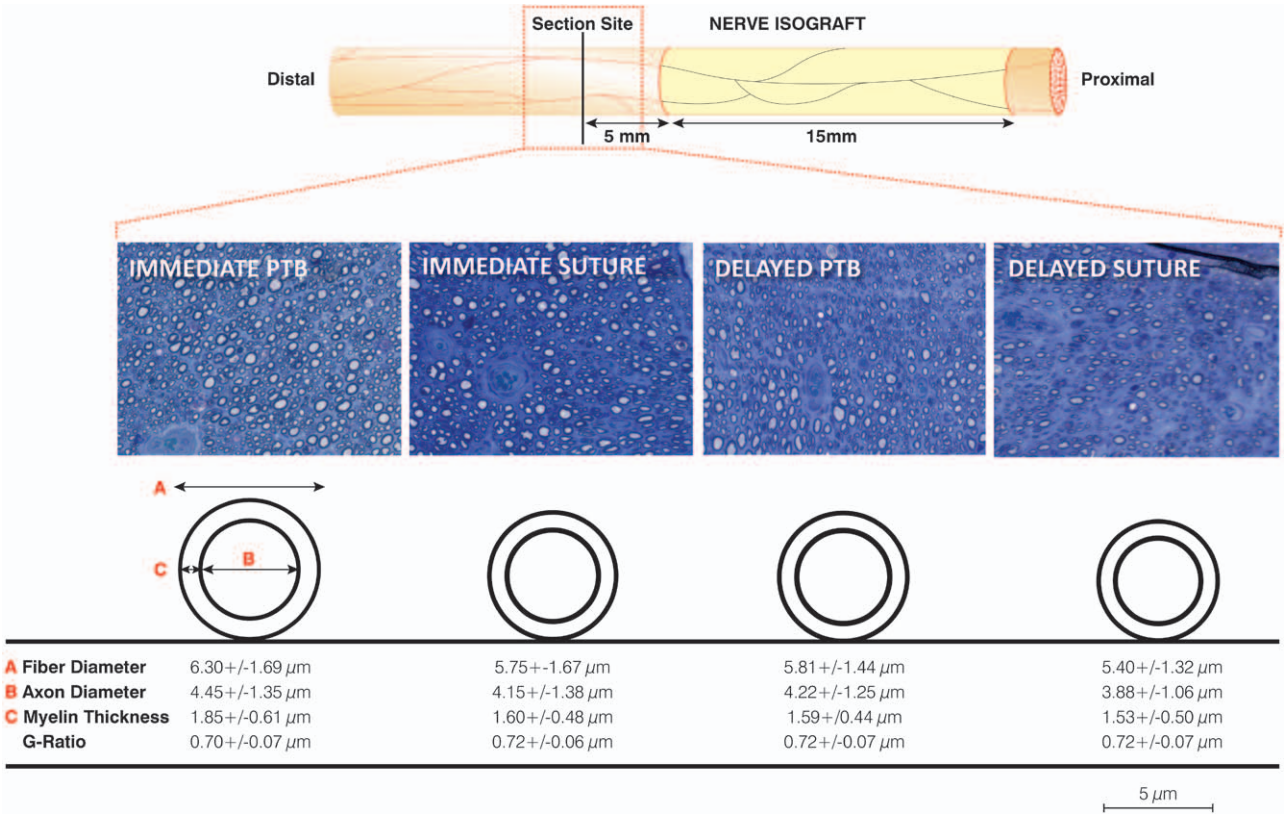

Fig. 3. Histology of distal nerve sections from each group and schematic depiction of nerve fiber and axon diameters. Sections were taken 5 mm distal to the distal isograft coaptation site. With the exception of the two rodents that were killed prematurely, all rodents successfully regenerated axons through isografts into the distal nerve stump after 5 months. Axons in the immediate groups were more abundant, although this was not significant. Histomorphometric measurements were generally greater in immediate repairs versus delayed repairs and in those repairs performed photochemically versus suture. No significant differences existed between the immediate suture and the delayed photochemical tissue bonding (*PTB*) groups.

Table 4. Histomorphometric Analysis 5 mm Distal to the Distal Isograft Coaptation Site for All Treatment Groups*

Experimental Group	Total Axon Count (× 0.001)	Axon Density (mm^2 × 0.001)	Nerve Fiber Diameter (μm)	Axon Diameter (μm)	Myelin Thickness (μm)	G-Ratio
Immediate suture	7.34 ± 4.38	24.83 ± 4.23	5.75 ± 1.67	4.15 ± 1.38	1.60 ± 0.48	0.72 ± 0.06
Immediate PTB	7.29 ± 4.63	23.25 ± 2.25	6.30 ± 1.69†	4.45 ± 1.35†	1.85 ± 0.61†	0.70 ± 0.07†
Delayed suture	4.04 ± 1.42	24.17 ± 2.70	5.40 ± 1.32	3.88 ± 1.06	1.53 ± 0.50	0.72 ± 0.07
Delayed PTB	5.77 ± 1.31	23.00 ± 2.37	5.81 ± 1.44	4.22 ± 1.25	1.59 ± 0.44	0.72 ± 0.07

PTB, photochemical tissue bonding.
*Although mean axon counts were considerably greater in immediate repair groups, because of the large standard deviation, these values were not significantly different. All histomorphometric measurements were greater in the immediate photochemical tissue bonding group compared with immediate suture.
†Statistically significant improvement compared with immediate suture. Table 2 provides detailed cross-pairs comparison.

photochemical sealing may have the ability to ameliorate the poorer outcomes expected following a surgical delay using standard microsurgical repair.

Outcomes following suture repair depend on surgical technique and microsurgical experience. Rodent operations in this study were performed by "nonexpert" microsurgeons. It is possible that the involvement of an "expert" microsurgeon may have improved outcomes following standard suture repair, ameliorating the observed superiority of light-activated sealing. However, the technical demands of microsurgery are its primary limitation. Expertise and equipment may not be available clinically. An advantage of light-activated sealing is that surgeons without microsurgery training can readily adopt the technique.

The delay of 30 days in this study had a deleterious impact on recovery, regardless of whether isografts were secured using conventional suture or photochemical sealing. This is consistent with

the tenet that increasing periods of axotomy and denervation result in a reduction in regenerating axons, reduced regenerative support in the distal fiber, and reduced motor unit reinnervation in muscle targets. Curiously, this effect was not evident from the analysis of muscle mass retention. Gordon et al. showed that freshly axotomized axons were able to recover full muscle mass and force of contraction when periods of distal fiber and muscle denervation were less than 50 days.[5] This was also observed when chronically axotomized nerve regenerated down freshly denervated distal nerve and muscle, reflecting compensatory increases in motor unit size.[5] A lack of significant difference in regenerative outcomes with shorter periods of delay has been reported by others.[22] Although mean muscle mass retention was greater in immediate repair groups in this study, it is possible that the lack of statistical significance reflects an element of compensation through an increased innervation ratio. Significant differences in Sciatic Function Index between immediate and delayed groups suggests that compensatory increases in innervation ratio, although sufficient to maintain muscle mass of the lower limb, may be unable to compensate for poor reinnervation of intrinsic musculature of the foot and sensory loss, both essential components for coordinated motor control.

The beneficial effects of photochemical sealing may be related to watertight isolation of the repair site. The avoidance of suture, prevention of axonal escape, protection from infiltrating scar tissue, and containment of neurotrophic rich fluid that is liberated from transected axons may all play a role. The absence of suture and therefore a reduction in foreign body reaction may lead to a less tumultuous repair environment, expediting the regeneration of axons across nerve graft coaptation sites. In a related set of experiments, the previously demonstrated beneficial effect of photochemical sealing of isografts, in comparison with conventional suture, was abrogated when applied to acellular nerve allografts (unpublished data). This suggests that the mechanism of effect may involve Schwann cells and the neurotrophic factors they release.

Following denervation, Schwann cells in the distal nerve up-regulate regeneration-associated genes and the expression of neurotrophic factors. With increasing denervation time, this expression progressively declines and Schwann cells become dormant, diminishing their ability to support regeneration.[13] The supplementation of exogenous Schwann cells and neurotrophic factors at the repair site has the potential to improve rates of regeneration. However, the delivery of these factors and their temporal and spatial regulation is far from being realized clinically. Inappropriately high concentrations of some neurotrophic factors can be inhibitory to regeneration and can even promote cell death.[11,12] Electrical stimulation of nerve repair sites may up-regulate regeneration-associated gene expression and the production of neurotrophic factors.[6,7] Improved rates of regeneration have been demonstrated in animal models of immediate and delayed repair[9,10] and, most recently, has facilitated full reinnervation of thenar muscles in humans with severe carpal tunnel syndrome.[8] This represents one of the few clinically translatable solutions to date. Light-activated sealing of nerve graft coaptation sites offers an alternative translatable approach that may help maintain neurotrophic levels and also retard Schwann cell dormancy by preventing the loss of mitogenic stimuli released from fresh nerve grafts. The uncertainty surrounding these mechanisms will provide impetus for further study.

The loss of two animals in the delayed plus photochemical tissue bonding group and the unsuccessful regeneration in one of these rodents was a concern. It is uncertain what caused this, although the delivery of excessive energy from the light source is most likely. The light used in this study was delivered by means of a divergent beam. As a result, small, inadvertent reductions in the distance between nerve and light source during bonding may have resulted in the delivery of excessive energy. Although not apparent at the time of bonding, subtle thermal damage to the internal architecture of nerve stumps and grafts may have compromised axonal regeneration and revascularization. Collimation of the beam would be a simple, easily achievable solution that would standardize spot size and energy delivery and improve safety for clinical translation.

A criticism of this study is that the period of delay may have been insufficient. Gordon et al. showed that the deleterious effects of prolonged axotomy and denervation were maximal following considerably longer surgical delays than found in this study. However, the exponential decline of motor unit reinnervation was evident with delays of less than 50 days.[5] In addition to surgical delay, denervation time is further extended by slow rates of regeneration. Although rates are commonly quoted as 1 to 3 mm/day, Brushart et al. explained that this referred to only the fastest growing sensory axons.[7] Large numbers of axons can take many weeks to traverse coaptation sites. This "staggered regeneration" is the result of the physical obstacle

presented by suture repairs, the arborization of daughter axons and the rationing of raw materials from the cell body, and sensory-motor mismatching leading to pruning.[7] These effects are exacerbated following nerve grafting when axons must traverse two coaptation sites. Clinically, denervation time may typically exceed that which has been tested in this study. Nevertheless, the 30-day delay led to a deleterious and detectable impact on regeneration and has allowed significant differences to be detected between treatment groups.

CONCLUSIONS

Importantly, this study confirms that light-activated sealing of isograft coaptation sites remains efficacious following a clinically relevant surgical delay and, as demonstrated in recent studies, results in significant improvements in outcome in comparison with conventional suture fixation. The use of light-activated sealing following delayed repair results in outcomes that are statistically comparable to those achieved with immediate suture. This finding is analogous to a recent study investigating efficacy of technique when applied to acellular nerve allografts[19] and, together, these findings may have potentially important clinical implications for the future repair of nerve gaps following periods of delay, particularly when the nature of the injury precludes the use of autologous tissue.

Neil G. Fairbairn, M.D.
Department of Plastic Surgery
St Johns Hospital
Howden Road West
Livingston, West Lothian EH54 6PP, United Kingdom
ngf174@hotmail.com

ACKNOWLEDGMENT

This article was funded by U.S. Department of Defense (USMRAA W81XWH-12-1-0511).

REFERENCES

1. Ellis JC, McCaffrey TV. Nerve grafting: Functional results after primary vs delayed repair. *Arch Otolaryngol.* 1985;111:781–785.
2. Fu SY, Gordon T. Contributing factors to poor functional recovery after delayed nerve repair: Prolonged denervation. *J Neurosci.* 1995;15:3886–3895.
3. Fu SY, Gordon T. Contributing factors to poor functional recovery after delayed nerve repair: Prolonged axotomy. *J Neurosci.* 1995;15:3876–3885.
4. Furey MJ, Midha R, Xu QG, Belkas J, Gordon T. Prolonged target deprivation reduces the capacity of injured motoneurons to regenerate. *Neurosurgery* 2007;60:723–732; discussion 732.
5. Gordon T, Tyreman N, Raji MA. The basis for diminished functional recovery after delayed peripheral nerve repair. *J Neurosci.* 2011;31:5325–5334.
6. Al-Majed AA, Neumann CM, Brushart TM, Gordon T. Brief electrical stimulation promotes the speed and accuracy of motor axonal regeneration. *J Neurosci.* 2000;20:2602–2608.
7. Brushart TM, Hoffman PN, Royall RM, Murinson BB, Witzel C, Gordon T. Electrical stimulation promotes motoneuron regeneration without increasing its speed or conditioning the neuron. *J Neurosci.* 2002;22:6631–6638.
8. Gordon T, Brushart TM, Chan KM. Augmenting nerve regeneration with electrical stimulation. *Neurol Res.* 2008;30:1012–1022.
9. Huang J, Zhang Y, Lu L, Hu X, Luo Z. Electrical stimulation accelerates nerve regeneration and functional recovery in delayed peripheral nerve injury in rats. *Eur J Neurosci.* 2013;38:3691–3701.
10. Xu C, Kou Y, Zhang P, et al. Electrical stimulation promotes regeneration of defective peripheral nerves after delayed repair intervals lasting under one month. *PloS One* 2014;9:e105045.
11. Boyd JG, Gordon T. The neurotrophin receptors, trkB and p75, differentially regulate motor axonal regeneration. *J Neurobiol.* 2001;49:314–325.
12. Boyd JG, Gordon T. A dose-dependent facilitation and inhibition of peripheral nerve regeneration by brain-derived neurotrophic factor. *Eur J Neurosci.* 2002;15:613–626.
13. Boyd JG, Gordon T. Neurotrophic factors and their receptors in axonal regeneration and functional recovery after peripheral nerve injury. *Mol Neurobiol.* 2003;27:277–324.
14. Gordon T. The role of neurotrophic factors in nerve regeneration. *Neurosurg Focus* 2009;26:E3.
15. Henry FP, Goyal NA, David WS, et al. Improving electrophysiologic and histologic outcomes by photochemically sealing amnion to the peripheral nerve repair site. *Surgery* 2009;145:313–321.
16. Johnson TS, O'Neill AC, Motarjem PM, et al. Photochemical tissue bonding: A promising technique for peripheral nerve repair. *J Surg Res.* 2007;143:224–229.
17. O'Neill AC, Randolph MA, Bujold KE, Kochevar IE, Redmond RW, Winograd JM. Photochemical sealing improves outcome following peripheral neurorrhaphy. *J Surg Res.* 2009;151:33–39.
18. Fairbairn NG, Ng-Glazier J, Meppelink AM, et al. Light-activated sealing of nerve graft coaptation sites improves outcome following large gap peripheral nerve injury. *Plast Reconstr Surg.* 2015;136:739–750.
19. Fairbairn NG, Ng-Glazier J, Meppelink AM, et al. Light-activated sealing of acellular nerve allografts following nerve gap injury. *J Reconstr Microsurg.* (accepted for publication).
20. Barton MJ, Morley JW, Stoodley MA, Shaikh S, Mahns DA, Lauto A. Long term recovery of median nerve repair using laser-activated chitosan adhesive films. *J Biophotonics* 2015;8:196–207.
21. Bain JR, Mackinnon SE, Hunter DA. Functional evaluation of complete sciatic, peroneal, and posterior tibial nerve lesions in the rat. *Plast Reconstr Surg.* 1989;83:129–138.
22. Miyamoto Y, Sugita T, Higaki T, Ikuta Y, Tsuge K. The duration of denervation and regeneration in nerve grafting: Quantitative histological assessment in the rat. *Int Orthop.* 1985;9:271–276.

Light-Activated Sealing of Acellular Nerve Allografts following Nerve Gap Injury

Neil G. Fairbairn, MD[1] Joanna Ng-Glazier, MD[1] Amanda M. Meppelink, BS[1] Mark A. Randolph, MAS[1] Ian L. Valerio, MD[2] Mark E. Fleming, MD[3] Irene E. Kochevar, PhD[4] Jonathan M. Winograd, MD[1] Robert W. Redmond, PhD[4]

[1] Division of Plastic and Reconstructive Surgery, Massachusetts General Hospital, Boston, Massachusetts
[2] Plastic Surgery Service, Walter Reed National Military Medical Center, Bethesda, Maryland
[3] Department of Orthopaedics, Walter Reed National Military Medical Center, Bethesda, Maryland
[4] Wellman Centre for Photomedicine, Massachusetts General Hospital, Boston, Massachusetts

Address for correspondence Robert W. Redmond, PhD, Wellman Center for Photomedicine, Harvard Medical School, Massachusetts General Hospital, Boston, MA 02114, USA (e-mail: redmond@helix.mgh.harvard.edu).

J Reconstr Microsurg

Abstract

Introduction Photochemical tissue bonding (PTB) uses visible light to create sutureless, watertight bonds between two apposed tissue surfaces stained with photoactive dye. In phase 1 of this two-phase study, nerve gaps repaired with bonded isografts were superior to sutured isografts. When autograft demand exceeds supply, acellular nerve allograft (ANA) is an alternative although outcomes are typically inferior. This study assesses the efficacy of PTB when used with ANA.

Methods Overall 20 male Lewis rats had 15-mm left sciatic nerve gaps repaired using ANA. ANAs were secured using epineurial suture (group 1) or PTB (group 2). Outcomes were assessed using sciatic function index (SFI), gastrocnemius muscle mass retention, and nerve histomorphometry. Historical controls from phase 1 were used to compare the performance of ANA with isograft. Statistical analysis was performed using analysis of variance and Bonferroni all-pairs comparison.

Results All ANAs had signs of successful regeneration. Mean values for SFI, muscle mass retention, nerve fiber diameter, axon diameter, and myelin thickness were not significantly different between ANA + suture and ANA + PTB. On comparative analysis, ANA + suture performed significantly worse than isograft + suture from phase 1. However, ANA + PTB was statistically comparable to isograft + suture, the current standard of care.

Conclusion Previously reported advantages of PTB versus suture appear to be reduced when applied to ANA. The lack of Schwann cells and neurotrophic factors may be responsible. PTB may improve ANA performance to an extent, where they are equivalent to autograft. This may have important clinical implications when injuries preclude the use of autograft.

Keywords
- nerve gap
- allograft
- sutureless repair

received
August 10, 2015
accepted after revision
November 15, 2015

DOI http://dx.doi.org/10.1055/s-0035-1571247.
ISSN 0743-684X.

The current standard of care for repairing peripheral nerve gap is the nerve autograft. Autograft harvest requires sacrifice of an "expendable" donor nerve and is associated with prolonged operating time, additional scarring, sensory loss, and increased risk of neuroma. In cases of major trauma associated with tissue loss and amputation, the demand for autograft may exceed that which can be harvested from the patient. In these situations, excluding nerve or tendon transfers, an alternative reconstructive solution is the allograft. Nerve allografts provide the most accurate representation of intraneural architecture and axonal guidance. Initially, allografts were fresh and cellularized, requiring immunosuppression to overcome rejection and preserve donor Schwann cell (SC) viability over the course of recovery. However, due to the risk of infective and neoplastic disease, this approach has fallen out of favor, driving the development of decellularization protocols and the use of acellular nerve allograft (ANA).[1–4] In 2007, human ANA (Avance, AxoGen Inc., Alachua, FL), processed by a detergent-based method, was approved for clinical use.[5]

Although obviating the risks of immunosuppression, decellularization removes SCs and other proregenerative components. The detrimental impact that this has on axonal regeneration has been demonstrated in animal models of nerve gap injury.[1,6] Recent clinical studies have shown that ANAs are safe and can result in motor and sensory outcomes that are superior to hollow conduits and can even match autograft for gaps between 5 and 50 mm.[5,7,8] Nevertheless, leaders in the field reserve ANA for small diameter, noncritical sensory nerve defects of less than 4 cm, for restoring autograft donor-site sensation, for nerve supercharging and for end-to-side nerve transfers in the hand. The use of ANA for the reconstruction of motor nerves, large diameter nerves, critical sensory nerves, and sensory nerves greater than 4 cm in length has been discouraged.[9] Broadening the clinical application of ANAs and ultimately supplanting autograft provides strong impetus to improve regeneration through these grafts. Recent efforts have focused on the supplementation of ANA with neurotrophic factors, SCs, and stem cells.[10] Although conceptually exciting, preclinical experience has, up to now, been disappointing. Although a tissue engineered or cell-based solution is far from being realized, addressing the technical limitations of suture coaptation may offer a more simplistic and rapidly translatable solution.

The use of suture for neurorrhaphy has several limitations. Suture material is inflammatory, resulting in fibrosis and intra- and extraneural scar tissue formation.[11] Scar tissue presents a direct obstacle to regenerating axons and can lead to tethering and external compression, all of which may compromise outcome. Even under high magnification and with meticulous technique, coaptation sites are imperfect. Leakage of growth promoting factors and misguided axons at the repair site may further compromise outcome. These effects are exacerbated in nerve grafts when axons must traverse two coaptation sites.

Sutureless repair can be achieved by a novel light-activated technique known as photochemical tissue bonding (PTB). Opposed nerve ends are wrapped circumferentially with human amnion that has been stained with a nontoxic, photoactive dye. Illumination of the nerve-wrap interface with a visible light source results in dye photoactivation, the formation of reactive species, subsequent cross-linking between amino acid residues and the creation of nonthermal, watertight bonds.[12–15] In rodent models of end-to-end repair, this technique produced superior outcomes in comparison to conventional suture.[16–19] Chemical cross-linking of amnion before light-activated sealing improves ex vivo and in vivo nerve wrap durability and has recently been shown to result in superior muscle weight retention and histomorphometric outcomes in comparison to conventional isograft + suture when applied to nerve gap reconstruction.[20] It is the aim of this study to test the efficacy of this strategy when used in conjunction with ANA. Our overarching goal is to optimize regeneration through ANAs and improve recovery, particularly following injury complicated by tissue loss and amputation, when autograft may be unavailable.

Methods

Allograft Preparation

Entire lengths of sciatic nerve from sciatic notch to distal trifurcation were harvested from Sprague–Dawley rats (Charles River Laboratories, Wilmington, MA). A total of 20 ANAs were required for implantation. An additional two were requested as extra. Graft yield (number of useable ANAs obtained from harvested grafts) can be in the region of 50% and a certain number of nerves must also be reserved for quality control purposes. As a result, 44 donor Sprague–Dawley sciatic nerves were harvested in the hope of obtaining sufficient numbers. Overdissection of the nerve was avoided to prevent inadvertent structural damage. Following harvest, nerves were cleaned of gross contaminants, placed in phosphate buffered saline (PBS; Sigma-Aldrich, Co., St Louis, MO), and stored at −80°C before being shipped to AxoGen Inc. for decellularization and sterilization. Nerves were harvested in batches over the course of 2 weeks and were stored at −80°C until shipping to AxoGen. Once processed ANAs were received back from AxoGen, they were stored at −80°C until the day of surgery. All ANAs were implanted and surgeries completed within 2 weeks of delivery. Due to the sequential nature of donor graft harvesting, cryopreservation and ANA implantation, storage times and elapsed time, between processing and implantation were not standardized.

Human Amniotic Membrane Nerve Wrap Preparation

Human amniotic membrane (HAM) was obtained from elective cesarean section patients who had been screened serologically for human immunodeficiency virus-1/2, hepatitis B, hepatitis C, human T-cell lymphotrophic virus, syphilis, cytomegalovirus, and tuberculosis. Membranes were washed liberally with PBS, mechanically deepithelialized using a cell scraper and placed into a storage solution containing a 1:1 mix of 100% sterile glycerol and Dulbecco-modified Eagles medium (Gibco, Grand Island, NY), penicillin–streptomycin–neomycin (Gibco) and amphotericin B. HAM was stored at −80°C until required. Once thawed, HAM was cross-linked

(×HAM) using 4-mM 1-ethyl-3-(3-dimethylamionopropyl) carbodiimide hydrochloride and 1-mM N-hydroxysuccinimide, reconstituted in 2-(N-morpholino) ethanesulfonic acid buffer (all products obtained from Sigma-Aldrich, Co.). Cross-linked amnion was then dried onto nitrocellulose paper and cut into 1 cm × 1 cm sections.

Sciatic Nerve Injury and Reconstruction

The Institutional Animal Care and Use Committee at the Massachusetts General Hospital and the Animal Care and Use Review Office at the United States Army Medical Research and Command approved all procedures. Under isoflurane anesthesia (Baxter Healthcare Corp., Deerfield, IL; 5% induction/2–3% maintenance), 20 male inbred Lewis rats weighing 250 to 300 g had sciatic nerves exposed through dorsolateral, muscle-splitting incisions on the left hindquarter. Two surgeons performed all procedures. The lead surgeon was a senior plastic surgery trainee (N. G. F.) and the assistant surgeon (J. N. G.) was a senior general surgical trainee. Both surgeons were experienced in microsurgical technique. Using the operating microscope, sciatic nerves were mobilized free from investing tissue. ANAs were thawed in a 37°C water bath and cut into 15-mm sections before being placed into the field adjacent to the sciatic nerve. The nerve was cut at a point 5-mm proximal to the trifurcation. The appropriate length of nerve was excised to permit tension-free interposition, ensuring that the graft was in reverse orientation. In group 1 ($n = 10$), ANAs were secured with six 10–0 epineurial sutures at each site (►**Fig. 1**). Following repair, any protruding axons were trimmed and allowed to retract inside the repair. In group 2 ($n = 10$), nerves were repaired using ANA secured with photochemically sealed ×HAM (►**Fig. 1**). ANAs were

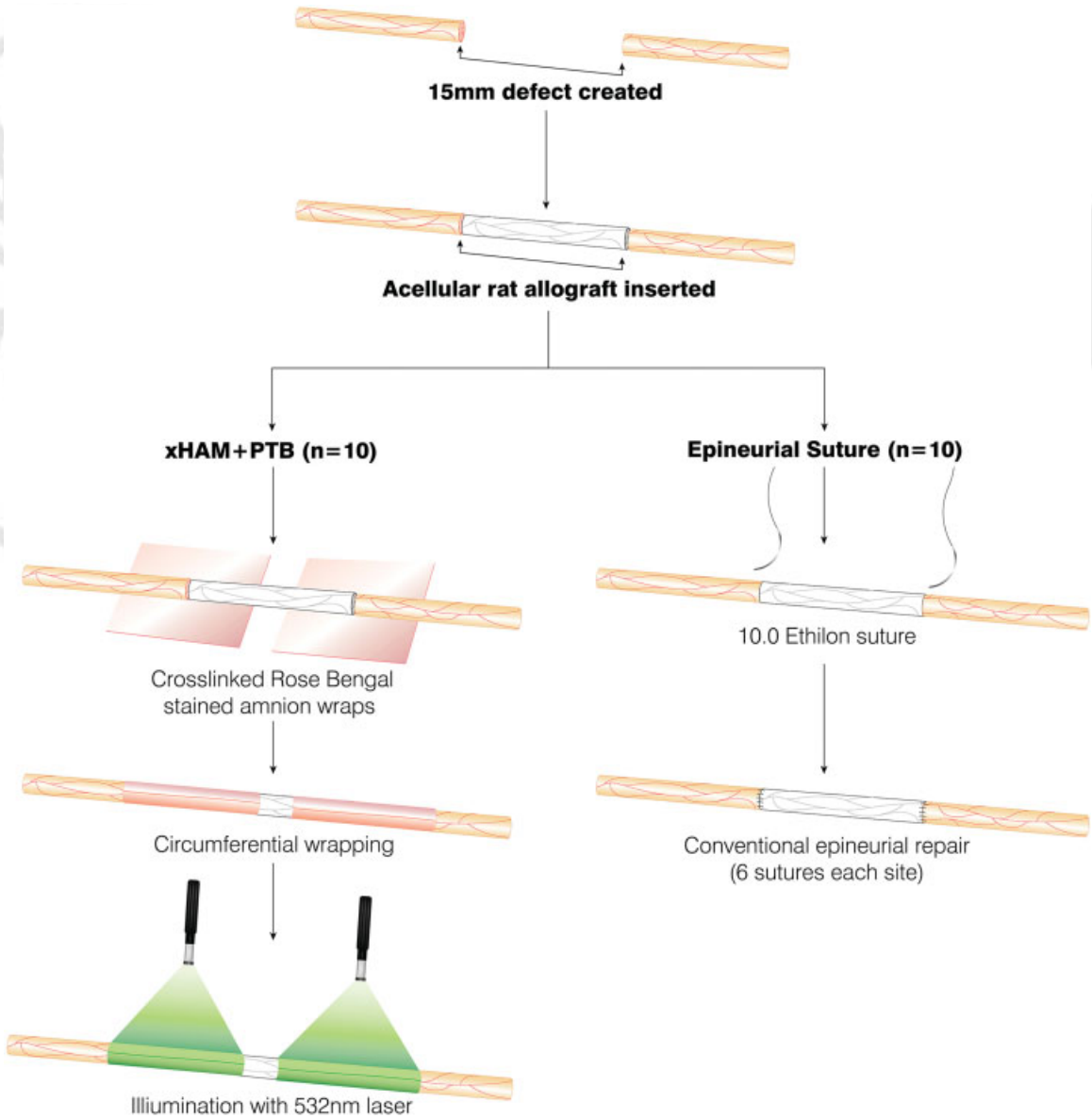

Fig. 1 Methods of rodent sciatic nerve injury and repair with ANA. All left sciatic nerves had 15-mm sections excised. These gaps were reconstructed with sections of processed rat ANA. In group 1 ($n = 10$), ANAs were secured with conventional 10.0 Ethilon suture (Ethicon Inc., Somerville, NJ). In group 2 ($n = 10$), ANAs were secured using photochemically sealed cross-linked amnion nerve wraps. ANA, acellular nerve allograft.

tacked into place using two 10–0 epineurial sutures at each coaptation site. After staining nerve wraps and nerve ends with 0.1% Rose Bengal (RB; Sigma-Aldrich, Co.) for 60 seconds, each ANA coaptation was wrapped circumferentially with ×HAM, ensuring a 5-mm overlap existed at each site. The area of overlap was irradiated for 60 seconds using a 532-nm KTP laser (Laserscope, San Jose, CA) at an irradiance of 0.5 W/cm^2. The nerve/wrap was then rotated 180 degrees to irradiate the back wall in the same manner for an additional 60 seconds (►**Fig. 1**). Wounds were closed using 4–0 Vicryl sutures (muscle and deep dermal; Ethicon Inc., Somerville) and 4–0 Monocryl sutures (subcuticular, Ethicon Inc.). Topical antibacterial ointment and bitter apple were applied to the limb to discourage infection and automutilation. Rodents were housed in the Massachusetts General Hospital small animal facility and had access to food and water as required.

Outcome Assessment

Sciatic Function Index and Muscle Mass Retention

Walking track analysis was performed immediately before surgery and at 30-day intervals. Rats had hind paws dipped in ink and were encouraged to run up a partially enclosed ramp set at an incline of 30 degrees. Measurement of print length, toe spread, and intermediary toe spread from inked footprints allowed the calculation of sciatic function index (SFI) using the formula described by Bain et al.[21] After 150 days, animals were sacrificed using carbon dioxide inhalation. Immediately following this, both gastrocnemius muscles were harvested and had wet weights measured for calculation of left-sided percentage muscle mass retention.

Histomorphometry

Following sacrifice, nerves were harvested 5 mm proximal and distal to ANAs. Nerves were immediately fixed in a mixture of 2% glutaraldehyde/2% paraformaldehyde (Electron Microscopy Sciences, Hatfield, PA). After 48 hours, fixed nerves were washed in sodium cacodylate buffer (0.1 M; pH = 7.4) and postfixed in 2% osmium tetroxide (Electron Microscopy Sciences) for 2 hours. Following further washing in buffer, specimens were dehydrated in increasing concentrations of ethanol. Following dehydration, specimens were washed with propylene oxide (Electron Microscopy Sciences), embedded in Epoxy resin (Tousimis Research Corporation, Rockville, MD), and then baked overnight in a 60°C oven. From each proximal and distal end, 1 µm sections were cut using a diamond blade. Once mounted, nerve sections were digitally scanned using a Hamamatsu NanoZoomer 2.0-HT slide scanner (Meyer Instruments, Houston TX) and read using NDP.com software (Hamamatsu Corp., Bridgewater, NJ). Images were numbered and their identity concealed during analysis. A blinded technician randomly selected five ×400 images from each ×40 slide. All ×40 and ×400 images were converted into JPEGs and imported into Adobe photoshop (Adobe Systems Inc., San Jose, CA). Two blinded researchers manually measured nerve cross-sectional area from ×40 images and counted axons from each ×400 image. Total counts were entered into a randomization Web site (randomizer.org) to obtain 50 random numbers. Numbered axons were then identified on each ×400 image, from which fiber and axon diameters were measured. This provided measurements for 250 axons per distal nerve section.

Statistical Analysis

Statistical analysis was performed using KaleidaGraph for Windows v4.1 (Synergy Software, Reading, PA). Testing between experimental groups was achieved using analysis of variance (ANOVA) and the posthoc Bonferroni test. A repeated measures ANOVA was applied specifically to SFI data to detect the existence of significant differences over time. Statistical significance was set at $p < 0.05$.

Results

Sciatic Nerve Reconstruction

Gross Observation following Sacrifice

There were no cases of nerve dehiscence in either ANA group and no animals suffered from foot ulceration or automutilation. In those ANAs repaired using light-activated sealing, cross-linked amnion wraps were still present at the repair site as evidenced by RB staining (►**Fig. 2**). Extraneural scar tissue formation was obvious in those nerves repaired using conventional suture and was qualitatively less in photochemically bonded nerves (►**Fig. 2**). Qualitatively, nerve caliber was reduced in sutured ANA in comparison to photochemically bonded ANA, a suggestion that regeneration was less successful.

Sciatic Function Index and Gastrocnemius Muscle Mass Retention

At the 5-month time point, SFI was 80.3 ± 4.2 in the ANA = suture group and 78.3 ± 5.0 in the ANA + PTB group (mean ± standard deviation [SD]; ►**Table 1**). These results were not significantly different. No statistically significant difference

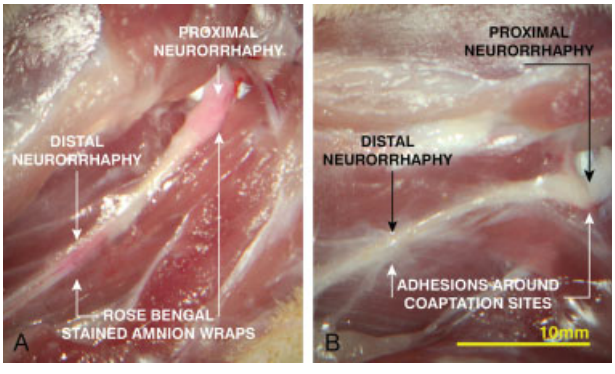

Fig. 2 Gross observations following sacrifice. All acellular nerve allografts were found to be intact and showed evidence of regeneration. Qualitatively, sutured repairs had more extraneural scar tissue formation surrounding coaptation sites in comparison to photochemical repairs. Cross-linked amnion nerve wrap still present at the repair site after 5 months, as evidenced by pink staining of Rose Bengal. (Sigma-Aldrich, Co., St. Louis, MO).

Table 1 Mean SFI for ANA treatment groups over 5-month follow-up period

Experimental group	Mean SFI				
	1 mo	2 mo	3 mo	4 mo	5 mo
ANA + suture	−95.4 ± 2.5	−90.3 ± 10.6	−87.9 ± 4.0	−84.1 ± 3.2	−80.3 ± 4.2
ANA + PTB	−93.4 ± 3.4	−91.1 ± 5.4	−88.9 ± 5.4	−83.4 ± 4.8	−78.3 ± 5.0

Abbreviations: ANA, acellular nerve allograft; PTB, photochemical tissue bonding; SFI, sciatic function index.
Note: At each time point throughout recovery, no statistically significant difference existed between ANA + suture and ANA + PTB. All data expressed as mean ± SD. Analysis performed using repeated measures ANOVA and posthoc Bonferroni test

Table 2 Gastrocnemius muscle mass retention and nerve histomorphometry for ANA treatment groups

Muscle mass retention and nerve histomorphometry 5 mm distal from ANA							
Experimental group	Muscle mass retention (%)	Total axon count (×0.001)	Axon density (mm^2 × 0.001)	Nerve fiber diameter (μm)	Axon diameter (μm)	Myelin thickness (μm)	G ratio
ANA = suture	52.9 ± 4.8	5.04 ± 2.57	21.50 ± 2.56	5.26 ± 1.29	3.30 ± 1.15	1.76 ± 0.86	0.62 ± 0.12
ANA + PTB	55.2 ± 5.5	6.04 ± 3.20	22.03 ± 5.15	5.38 ± 1.22	3.41 ± 0.99	1.97 ± 0.69	0.63 ± 0.11

Abbreviations: ANA, acellular nerve allograft; ANOVA, analysis of variance; PTB, photochemical tissue bonding; SD, standard deviation.
Note: Muscle mass retention was not significantly different between sutured and photochemically sealed ANA. With the exception of G ratio, no significant differences existed between ANA + suture and ANA + PTB for all remaining histomorphometric parameters. All data expressed as mean ± SD. Analysis performed using ANOVA and posthoc Bonferroni test; $p < 0.05$.

existed between groups over the duration of follow-up when assessing for the effects of time. Gastrocnemius muscle mass retention was not significantly different between ANA + suture and ANA + PTB (52.9 ± 4.8% vs. 55.2 ± 5.5%; $p = 1$; ►**Table 2**).

Nerve Histomorphometry

Axon counts in the distal nerve stump were not significantly different between ANA + suture and ANA + PTB (5.04 ± 2.57 vs. 6.04 ± 3.20 [actual count ×0.001]). No significant differences were detected between ANA + suture and ANA + PTB for nerve fiber diameter (5.26 ± 1.29 μm vs. 5.38 ± 1.22 μm), axon diameter (3.30 ± 1.15 μm vs. 3.41 ± 0.99 μm), myelin thickness (1.76 ± 0.86 μm vs. 1.97 ± 0.69 μm) or G ratio (0.621 ± 0.12 vs. 0.631 ± 0.11). All results expressed as mean ± SD; ►**Table 2**.

Discussion

This study has detected no statistically significant differences between light-activated sealing and conventional suture when applied to ANA. This represents the second phase of a two-phase experiment investigating the application of light-activated sealing when applied to nerve gap repair. In phase 1, light-activated sealing of isograft coaptation sites with cross-linked amnion nerve wraps resulted in superior outcomes in comparison to conventional suture.[20] The seemingly attenuated effect of light-activated sealing when applied to ANA suggests that the mechanism of effect may be reliant on the presence of SCs and growth-promoting factors typically absent in ANA. Following injury, neurotrophic rich fluid leaks from nerve ends and can be physically collected.[22–24] Early techniques that captured and enclosed this fluid at the repair site resulted in superior outcome.[22] It is possible that PTB helps seal in beneficial cellular elements such as SCs and neurotrophic factors, improving the longevity of their effect and therefore maintaining a growth permissive environment for longer. This protective barrier may prevent the infiltration of extraneural scar and the extrafascicular loss of axons.

The beneficial effects of PTB observed in phase 1 may also relate to the effects of suture reduction. Suture material causes foreign body reaction, granuloma formation, and the formation of intra- and extraneural scar.[11] Although insufficient data was collected to allow robust, quantitative assessment, a reduction in extraneural scarring is consistent with previous studies.[19,20] The relative absence of suture associated with PTB may lead to a less tumultuous repair environment, expediting the regeneration of axons across coaptation sites. The use of six 10–0 epineurial sutures for sutured repairs in this study may be considered excessive for a 1 to 2 mm nerve but was chosen deliberately to ensure a considerably greater suture burden at the repair site in comparison to light activated repairs. Although it is possible that any beneficial effect observed may be due exclusively to reduced suture burden, previous studies comparing sutured neurorrhaphy with and without photochemically sealed amnion wraps showed a significant benefit with photochemical sealing.[16,19] In addition, photochemically sealed cross-linked amnion wraps in phase 1 led to significantly greater fiber diameter, axon diameter, and myelin thickness in comparison to cross-linked amnion secured with fibrin glue.[20] Both of these groups had nerve ends "tacked" with two 10–0 epineurial sutures, suggesting that an effect independent of suture-induced inflammation and scarring is occurring. Furthermore, phototherapy has been shown to inhibit fibroblast and myofibroblast activity and causes massive neurite sprouting and SC proliferation in vitro.[25–27] This effect may

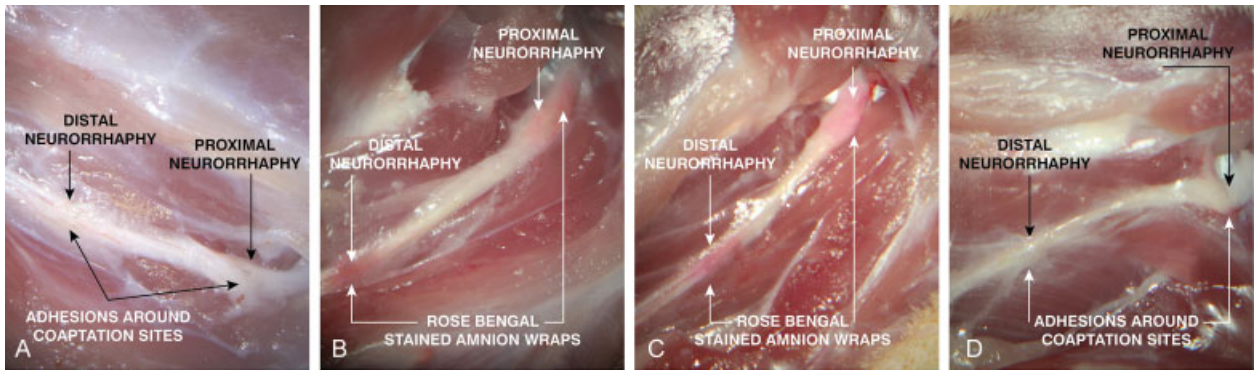

Fig. 3 Gross observations following sacrifice: comparison between isograft and acellular nerve allograft. Qualitatively, ANA diameters (C + D) were noticeably reduced in comparison to isograft (A + B), an indication that regeneration through these grafts was less successful. (Isograft sacrifice images reproduced with permission from: Fairbairn et al. Light-activated sealing of nerve graft coaptation sites improves outcome following large gap peripheral nerve injury. Plast Reconstr Surg 2015;136(4):739–750.)

partly explain recently demonstrated reductions in implant capsule formation and capsular contracture by tissues pretreated with photochemical tissue passivation.[28] The antifibrotic effects of transplanted amnion have also been well reported.[29,30] All of these potential mechanisms remain unsubstantiated.

In addition to assessing the efficacy of light-activated sealing against conventional suture when applied to ANA, it was also of interest to assess the performance of ANA repairs against isografts. Using data from phase 1, a comparative analysis was performed between ANA groups and sutured and photochemically sealed isografts. Qualitatively, isografts were of larger diameter reflecting superior regeneration across these grafts (►**Fig. 3**). Photochemically sealed isografts recovered significantly greater SFI (►**Tables 3** and **5**, ►**Fig. 4**), muscle mass (►**Tables 4** and **5**, ►**Fig. 5**), fiber diameter, axon diameter, myelin thickness and G ratio (►**Tables 4** and **5**, ►**Fig. 6**) in comparison to photochemically sealed ANA. Likewise, sutured isografts recovered significantly greater SFI (►**Tables 3** and **5**, ►**Fig. 4**), muscle mass (►**Tables 4** and **5**, ►**Fig. 5**), fiber diameter and axon diameter in comparison to sutured ANA (►**Tables 4** and **5**, ►**Fig. 6**). These findings are consistent with the clinical observation that cellularized autograft supports regeneration better than decellularized allograft.

While ANA + suture had significantly poorer outcomes in comparison to isograft + suture, the greater mean values observed in the ANA + PTB group were statistically comparable to isograft + suture, the current standard of care. Although the beneficial effect of photochemical sealing is attenuated when applied to ANA, this small increase toward significance may translate clinically into improved rates of regeneration that can rival that of the current standard of care. This may have important clinical applications when severe injury, complicated by limb loss, precludes the use of autograft.

The poorer performance of ANA + suture compared with isograft + suture over a 15-mm nerve gap is not consistent with other studies. Whitlock et al reported no significant difference in outcome between isograft and rodent allograft across a 14-mm sciatic nerve gap after 12 weeks. However, a significant difference was detected after 16 weeks when the gap was extended to 28 mm.[31] The

Table 3 SFI data for ANAs and isografts from phase 1

Experimental group	Mean SFI				
	1 mo	2 mo	3 mo	4 mo	5 mo
Isograft + suture	−87.6 ± 5.0	−81.1 ± 4.5	−71.8 ± 7.3	−74.7 ± 6.3	−71.7 ± 4.8
Isograft + PTB	−88.2 ± 3.9	−80.3 ± 3.5	−67.2 ± 3.3	−71.6 ± 5.5	−67.9 ± 5.1
ANA + suture	−95.4 ± 2.5	−90.3 ± 10.6	−87.9 ± 4.0	−84.1 ± 3.2	−80.3 ± 4.2[a]
ANA + PTB	−93.4 ± 3.4	−91.1 ± 5.4	−88.9 ± 5.4	−83.4 ± 4.8	−78.3 ± 5.0[a]

Abbreviations: ANA, acellular nerve allograft; ANOVA, analysis of variance; PTB, photochemical tissue bonding; SFI, sciatic function index.
Source: Isograft group data of phase 1 experiments reproduced with permission from: Fairbairn et al. Light-activated sealing of nerve graft coaptation sites improves outcome following large gap peripheral nerve injury. Plast Reconstr Surg 2015;136(4):739–750.
Note: Isograft + PTB from phase 1 recovered greatest SFI. This was statistically significant in comparison to ANA groups although not significant in comparison to isograft + suture Table 3 and ►**Table 4**; ►**Fig. 3**). ANA + suture performed statistically poorer than isograft + suture ($p < 0.001$; Table 3 and ►**Table 4**; ►**Fig. 3**). SFI was also statistically less for ANA + PTB in comparison to isograft + suture and isograft + PTB (Table 3 and ►**Table 4**; ►**Fig. 3**). All data expressed as mean ± SD.
[a]Denotes significant difference in comparison to isograft + suture. Analysis performed using repeated measures ANOVA and posthoc Bonferroni test; $p < 0.05$.

Table 4 Muscle mass retention and nerve histomorphometry for ANA and isograft groups from phase 1

Muscle mass retention and nerve histomorphometry 5 mm distal from graft							
Experimental group	Muscle mass retention (%)	Total axon count (×0.001)	Axon density ($mm^2 \times 0.001$)	Nerve fiber diameter (μm)	Axon diameter (μm)	Myelin thickness (μm)	G ratio
Isograft + suture	60.0 ± 5.2	7.61 ± 3.42	29.36 ± 18.10	5.47 ± 1.70	3.50 ± 1.44	1.96 ± 0.47	0.62 ± 0.08
Isograft + PTB	67.3 ± 4.4[a]	9.66 ± 3.08	30.73 ± 14.73	6.87 ± 2.23[a]	4.51 ± 1.83[a]	2.35 ± 0.64[a]	0.64 ± 0.08
ANA + suture	52.9 ± 4.8	5.04 ± 2.57	21.50 ± 2.56	5.26 ± 1.29	3.30 ± 1.15	1.76 ± 0.86	0.62 ± 0.12
ANA + PTB	55.2 ± 5.5	6.04 ± 3.20	22.03 ± 5.15	5.38 ± 1.22	3.41 ± 0.99	1.97 ± 0.69	0.63 ± 0.11

Abbreviations: ANA, acellular nerve allograft; ANOVA, analysis of variance; PTB, photochemical tissue bonding; SFI, sciatic function index.
Source: Isograft group data of phase 1 experiments reproduced with permission from: Fairbairn et al. Light-activated sealing of nerve graft coaptation sites improves outcome following large gap peripheral nerve injury. Plast Reconstr Surg 2015;136(4):739–750.
Note: Isograft + PTB recovered significantly greater muscle mass in comparison to isograft + suture ($p = 0.01$) and remaining groups. Muscle mass retention was significantly poorer in the ANA + suture group in comparison to isograft + suture ($p = 0.02$). Retention in the ANA+PTB group was statistically comparable to isograft + suture ($p = 0.22$). Isograft + PTB recovered significantly greater fiber diameter, axon diameter, and myelin thickness than all other groups (Table 4 and ►**Table 5**; ►**Fig. 5**). ANA + suture recovered significantly less fiber diameter and axon diameter than isograft + suture. No difference in axon count, myelin thickness, and G ratio existed between these two groups (Table 4 and ►**Table 5**; ►**Fig. 5**). In comparison to sutured ANA, photochemically sealed ANA resulted in small increases in fiber diameter and axon diameter that approached significance ($p = 0.07$ and 0.06, respectively; Table 4 and ►**Table 5**). ANA + PTB was statistically comparable to isograft + suture for all histomorphometric parameters. (Table 4 and ►**Table 5**; ►**Fig. 5**). All data expressed as mean ± SD. Analysis performed using ANOVA and posthoc Bonferroni test; $p < 0.05$.

lack of significant difference between sutured and photochemically sealed ANA may have been related to insufficient gap size coupled with the large regenerative potential of rodents, although the 15 mm gap used was sufficient to detect significant differences between isograft and rodent ANA. Further studies using larger nerve gaps are planned.

Although the presence of basal lamina elements such as fibronectin and laminin in ANA can promote neurite outgrowth and support axonal regeneration in the absence of SCs,[32–39] with increasing graft length, successful regeneration is reliant on graft repopulation by resident SCs. Studies have shown diminishing regenerative return with increasing graft length.[1] Evidence suggests a finite migratory and proliferative capacity of SCs and shows that repopulation of increasingly long ANAs by recipient SCs can lead to SC senescence.[40] The current study did not assess SC

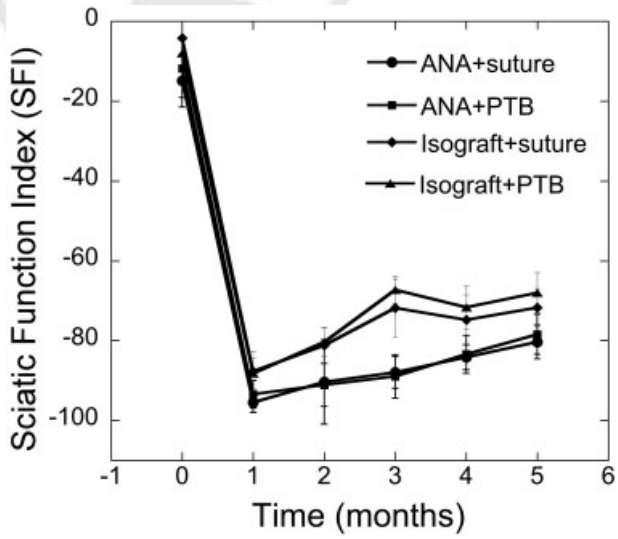

Fig. 4 SFI of ANA and isograft-treated groups. After 5-months follow-up, no significant difference existed within either isograft or ANA groups. ANA = suture and ANA + PTB groups recovered significantly less SFI in comparison to isograft + suture and isograft + PTB groups, respectively. ANA, acellular nerve allograft; SFI, sciatic function index. (Isograft SFI data reproduced with permission from: Fairbairn et al. Light-activated sealing of nerve graft coaptation sites improves outcome following large gap peripheral nerve injury. Plast Reconstr Surg 2015;136(4):739–750.)

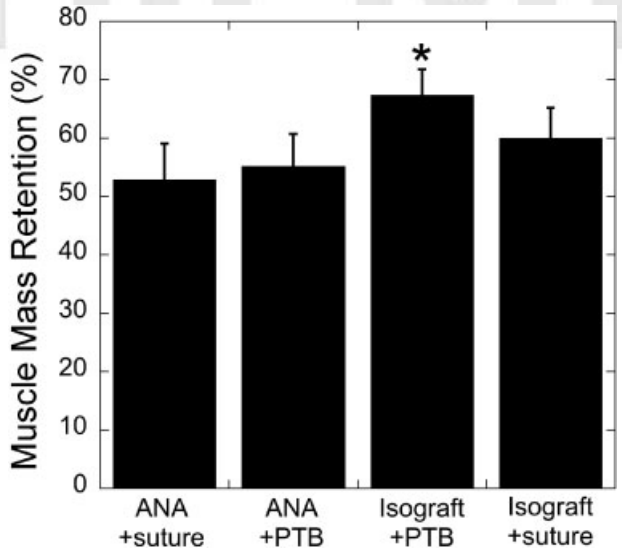

Fig. 5 Gastrocnemius muscle mass retention for ANA and isograft-treated groups. Isograft + PTB achieved significantly better outcomes in comparison to all other groups. No significant difference existed between ANA + suture and ANA + PTB. ANA + suture recovered significantly less muscle mass than isograft + suture but there was no significant difference between isograft + suture and ANA + PTB. Graphical data expressed as mean ± SD. Analysis performed using ANOVA and posthoc Bonferroni test. *Denotes statistical significance in comparison to isograft + suture ($p = 0.01$). ANA, acellular nerve allograft; PTB, photochemical tissue bonding. (Isograft gastrocnemius muscle mass retention data reproduced with permission from: Fairbairn et al. Light-activated sealing of nerve graft coaptation sites improves outcome following large gap peripheral nerve injury. Plast Reconstr Surg 2015;136(4):739–750.)

Table 5 Bonferroni all-pairs comparison for all treatment groups

Group comparison	SFI (5 mo)	Muscle mass	Axon count	Fiber diameter	Axon diameter	Myelin thickness	G ratio
Isograft + suture vs. isograft + PTB	0.59	0.01	0.90	< 0.0001	< 0.0001	< 0.0001	< 0.0001
Isograft + suture vs. ANA + suture	0.002	0.02	0.47	< 0.0001	< 0.0001	1	1
Isograft + suture vs. ANA + PTB	0.03	0.22	1	0.27	0.08	1	0.21
Isograft + PTB vs. ANA + suture	< 0.0001	< 0.0001	0.02	< 0.0001	< 0.0001	< 0.0001	< 0.0001
Isograft + PTB vs. ANA + PTB	0.0002	< 0.0001	0.08	< 0.0001	< 0.0001	< 0.0001	0.0005
ANA + suture vs. ANA + PTB	1	1	1	0.07	0.06	1	0.0062

Abbreviations: ANA, acellular nerve allograft; PTB, photochemical tissue bonding; SFI, sciatic function index.
Source: Isograft group data of phase 1 experiments reproduced with permission from: Fairbairn et al. Light-activated sealing of nerve graft coaptation sites improves outcome following large gap peripheral nerve injury. Plast Reconstr Surg 2015;136(4):739–750.
Note: In comparison to isograft + suture, isograft + PTB results in statistically significant improvements in muscle mass retention, fiber diameter, axon diameter, and myelin thickness. ANA + suture had significantly poorer recovery of SFI, muscle mass retention, fiber diameter, and axon diameter. With the exception of G ratio, there was no significant difference between ANA + suture and ANA + PTB for any of the outcomes measured. There was no significant difference in muscle mass retention, axon count, fiber diameter, axon diameter, myelin thickness, and G ratio between ANA + PTB and isograft + suture.

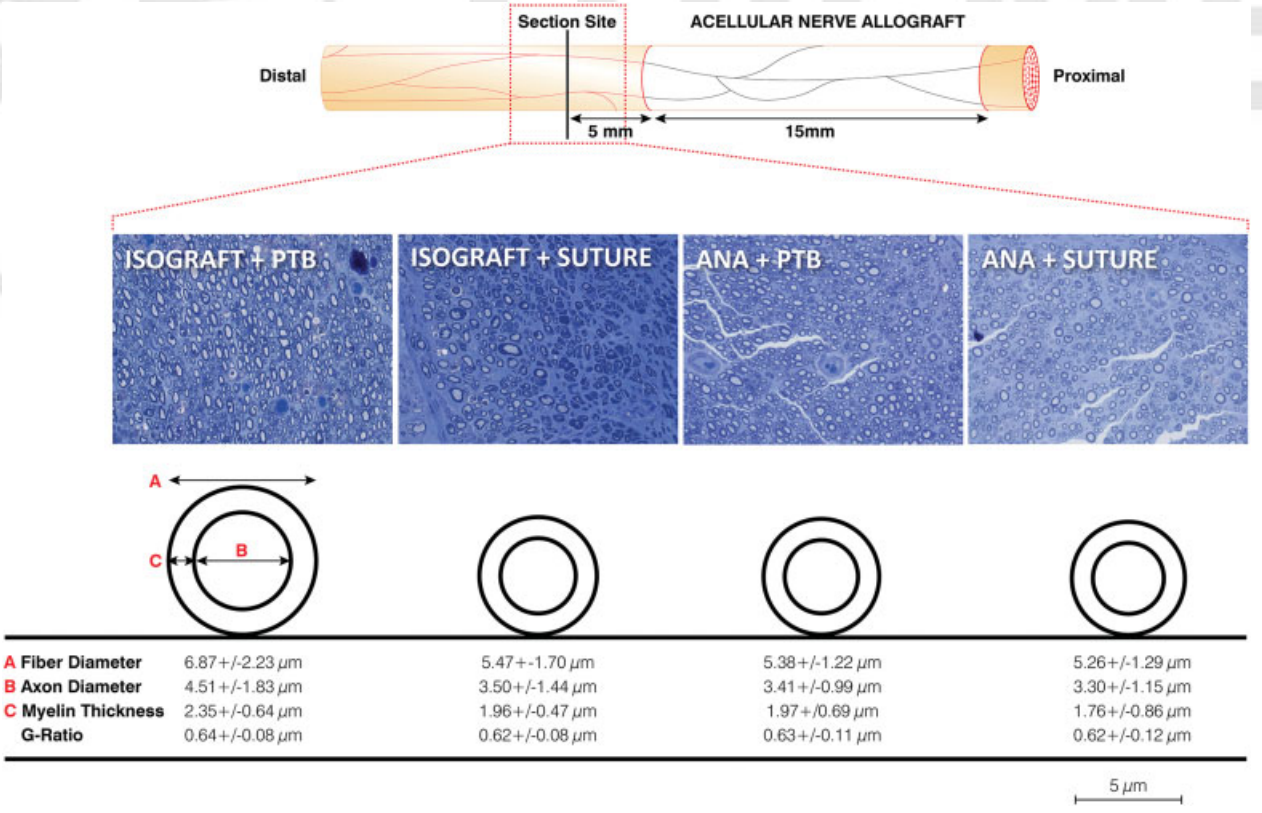

Fig. 6 Examples of distal nerve histology from all groups and schematic representation of histomorphometry. Isograft + PTB recovered significantly greater fiber diameter, axon diameter, and myelin thickness in comparison to remaining groups. Histomorphometric outcomes were not significantly different between ANA + PTB and isograft + suture, the current standard of care. ANA, acellular nerve allograft; PTB, photochemical tissue bonding. (Isograft histomorphometric data reproduced with permission from: Fairbairn et al. Light-activated sealing of nerve graft coaptation sites improves outcome following large gap peripheral nerve injury. Plast Reconstr Surg 2015;136(4):739–750.)

repopulation but it is possible that photochemical sealing of the intraneural mileu may augment SC migration and regeneration through ANAs. Assessing SC repopulation in ANAs of varying length may form the basis of future study. Perhaps combining this approach with cell-based therapy may have a synergistic effect.

The method of ANA decellularization can influence outcome.[41] Comparative analysis between allografts and xenografts from various animal species has also detected significant differences in outcome.[42] Although the use of human cadaveric Avance would have had greater clinical relevance, investigators have shown that in rodent models regeneration through Avance is inferior to rodent ANA.[43] This is believed to be due to a xenograft-induced subclinical inflammatory response. The use of Sprague–Dawley ANA in favor of Avance in the current study aimed to reduce any detrimental effect of cross-species immunoreactivity.

A limitation of this study is the use of phase 1 data as historical controls for comparative analysis and the selection bias this incurs. Isograft + PTB was the "optimal" repair method from phase 1 and an assumption has been made that the outcomes in both isograft groups would have been replicated had they been repeated. The use of this data was justified in light of the fact that the same surgeons performed all experiments, the same methods of repair were used (other than the use of ANA in place of isograft in phase 1), the same researchers were involved in outcome assessment and the animals received the same postoperative care by the same animal facility team. The experiments also took place sequentially with very little delay between phases 1 and 2. Although methodologically "cleaner," the inclusion of new isograft groups would have resulted in unnecessary animal morbidity and cost.

Conclusion

Recent work has shown that light-activated sealing of 15 mm rodent isografts results in superior outcomes in comparison to conventional suture. This study has been unable to detect any significant difference between light-activated sealing and suture when applied to 15 mm rodent ANA. However, while sutured ANA performed statistically poorer than sutured isografts, outcomes following photochemically sealed ANA were comparable to sutured isografts, the current standard of care. Light-activated sealing has the potential to improve the performance of ANA, a finding that has important clinical implications, particularly following severe trauma when the use of nerve autograft is not possible.

Acknowledgments

The authors are grateful for excellent histological support from the Photopathology core at the Wellman Center for Photomedicine. This study was funded by the U. S. Army Medical Research Acquisition Activity W81XWH-12–1-0511. The content of this article does not necessarily reflect the position or the policy of the U. S. Government, and no official endorsement should be inferred.

References

1 Gulati AK. Evaluation of acellular and cellular nerve grafts in repair of rat peripheral nerve. J Neurosurg 1988;68(1):117–123
2 Hudson TW, Liu SY, Schmidt CE. Engineering an improved acellular nerve graft via optimized chemical processing. Tissue Eng 2004; 10(9–10):1346–1358
3 Hudson TW, Zawko S, Deister C, et al. Optimized acellular nerve graft is immunologically tolerated and supports regeneration. Tissue Eng 2004;10(11–12):1641–1651
4 Sondell M, Lundborg G, Kanje M. Regeneration of the rat sciatic nerve into allografts made acellular through chemical extraction. Brain Res 1998;795(1–2):44–54
5 Brooks DN, Weber RV, Chao JD, et al. Processed nerve allografts for peripheral nerve reconstruction: a multicenter study of utilization and outcomes in sensory, mixed, and motor nerve reconstructions. Microsurgery 2012;32(1):1–14
6 Giusti G, Willems WF, Kremer T, Friedrich PF, Bishop AT, Shin AY. Return of motor function after segmental nerve loss in a rat model: comparison of autogenous nerve graft, collagen conduit, and processed allograft (AxoGen). J Bone Joint Surg Am 2012;94(5): 410–417
7 Cho MS, Rinker BD, Weber RV, et al. Functional outcome following nerve repair in the upper extremity using processed nerve allograft. J Hand Surg Am 2012;37(11):2340–2349
8 Rinker BD, Ingari JV, Greenberg JA, Thayer WP, Safa B, Buncke GM. Outcomes of short-gap sensory nerve injuries reconstructed with processed nerve allografts from a multicenter registry study. J Reconstr Microsurg 2015;31(5):384–390
9 Boyd KU, Nimigan AS, Mackinnon SE. Nerve reconstruction in the hand and upper extremity. Clin Plast Surg 2011;38(4):643–660
10 Fowler JR, Lavasani M, Huard J, Goitz RJ. Biologic strategies to improve nerve regeneration after peripheral nerve repair. J Reconstr Microsurg 2015;31(4):243–248
11 Myles LM, Gilmour JA, Glasby MA. Effects of different methods of peripheral nerve repair on the number and distribution of muscle afferent neurons in rat dorsal root ganglion. J Neurosurg 1992; 77(3):457–462
12 Chan BP, Hui TY, Chan OC, et al. Photochemical cross-linking for collagen-based scaffolds: a study on optical properties, mechanical properties, stability, and hematocompatibility. Tissue Eng 2007;13(1):73–85
13 Kochevar IE, Redmond RW. Photosensitized production of singlet oxygen. Methods Enzymol 2000;319:20–28
14 Balasubramanian D, Du X, Zigler JS Jr. The reaction of singlet oxygen with proteins, with special reference to crystallins. Photochem Photobiol 1990;52(4):761–768
15 Webster A, Britton D, Apap-Bologna A, Kemp G. A dye-photosensitized reaction that generates stable protein-protein crosslinks. Anal Biochem 1989;179(1):154–157
16 Henry FP, Goyal NA, David WS, et al. Improving electrophysiologic and histologic outcomes by photochemically sealing amnion to the peripheral nerve repair site. Surgery 2009;145(3): 313–321
17 Johnson TS, O'Neill AC, Motarjem PM, et al. Photochemical tissue bonding: a promising technique for peripheral nerve repair. J Surg Res 2007;143(2):224–229
18 O'Neill AC, Randolph MA, Bujold KE, Kochevar IE, Redmond RW, Winograd JM. Preparation and integration of human amnion nerve conduits using a light-activated technique. Plast Reconstr Surg 2009;124(2):428–437
19 O'Neill AC, Randolph MA, Bujold KE, Kochevar IE, Redmond RW, Winograd JM. Photochemical sealing improves outcome following peripheral neurorrhaphy. J Surg Res 2009;151(1):33–39
20 Fairbairn NG, Ng-Glazier J, Meppelink AM, et al. Light-Activated Sealing of Nerve Graft Coaptation Sites Improves Outcome following Large Gap Peripheral Nerve Injury. Plast Reconstr Surg 2015; 136(4):739–750

21 Bain JR, Mackinnon SE, Hunter DA. Functional evaluation of complete sciatic, peroneal, and posterior tibial nerve lesions in the rat. Plast Reconstr Surg 1989;83(1):129–138
22 Demirkan F, Snyder CC, Latifoglu O, Siemionow M. A method of enhancing regeneration of conventionally repaired peripheral nerves. Ann Plast Surg 1995;34(1):67–72
23 Longo FM, Manthorpe M, Skaper SD, Lundborg G, Varon S. Neuronotrophic activities accumulate in vivo within silicone nerve regeneration chambers. Brain Res 1983;261(1):109–116
24 Lundborg G, Longo FM, Varon S. Nerve regeneration model and trophic factors in vivo. Brain Res 1982;232(1):157–161
25 Rochkind S. Phototherapy in peripheral nerve regeneration: From basic science to clinical study. Neurosurg Focus 2009;26(2):E8
26 Van Breugel HH, Bär PR. He-Ne laser irradiation affects proliferation of cultured rat Schwann cells in a dose-dependent manner. J Neurocytol 1993;22(3):185–190
27 Wollman Y, Rochkind S, Simantov R. Low power laser irradiation enhances migration and neurite sprouting of cultured rat embryonal brain cells. Neurol Res 1996;18(5):467–470
28 Fernandes JR, Salinas HM, Broelsch GF, et al. Prevention of capsular contracture with photochemical tissue passivation. Plast Reconstr Surg 2014;133(3):571–577
29 Fairbairn NG, Randolph MA, Redmond RW. The clinical applications of human amnion in plastic surgery. J Plast Reconstr Aesthet Surg 2014;67(5):662–675
30 Mamede AC, Carvalho MJ, Abrantes AM, Laranjo M, Maia CJ, Botelho MF. Amniotic membrane: from structure and functions to clinical applications. Cell Tissue Res 2012;349(2):447–458
31 Whitlock EL, Tuffaha SH, Luciano JP, et al. Processed allografts and type I collagen conduits for repair of peripheral nerve gaps. Muscle Nerve 2009;39(6):787–799
32 Hall SM. Regeneration in cellular and acellular autografts in the peripheral nervous system. Neuropathol Appl Neurobiol 1986; 12(1):27–46
33 Ide C. Nerve regeneration and Schwann cell basal lamina: observations of the long-term regeneration. Arch Histol Jpn 1983;46(2): 243–257
34 Ide C, Tohyama K, Yokota R, Nitatori T, Onodera S. Schwann cell basal lamina and nerve regeneration. Brain Res 1983;288(1–2):61–75
35 Fawcett JW, Keynes RJ. Muscle basal lamina: a new graft material for peripheral nerve repair. J Neurosurg 1986;65(3):354–363
36 Keynes RJ, Hopkins WG, Huang LH. Regeneration of mouse peripheral nerves in degenerating skeletal muscle: guidance by residual muscle fibre basement membrane. Brain Res 1984; 295(2):275–281
37 Bryan DJ, Miller RA, Costas PD, Wang KK, Seckel BR. Immunocytochemistry of skeletal muscle basal lamina grafts in nerve regeneration. Plast Reconstr Surg 1993;92(5):927–940
38 Glasby MA, Gilmour JA, Gschmeissner SE, Hems TE, Myles LM. The repair of large peripheral nerves using skeletal muscle autografts: a comparison with cable grafts in the sheep femoral nerve. Br J Plast Surg 1990;43(2):169–178
39 Akers RM, Mosher DF, Lilien JE. Promotion of retinal neurite outgrowth by substratum-bound fibronectin. Dev Biol 1981; 86(1):179–188
40 Saheb-Al-Zamani M, Yan Y, Farber SJ, et al. Limited regeneration in long acellular nerve allografts is associated with increased Schwann cell senescence. Exp Neurol 2013;247:165–177
41 Moore AM, MacEwan M, Santosa KB, et al. Acellular nerve allografts in peripheral nerve regeneration: a comparative study. Muscle Nerve 2011;44(2):221–234
42 Kvist M, Sondell M, Kanje M, Dahlin LB. Regeneration in, and properties of, extracted peripheral nerve allografts and xenografts. J Plast Surg Hand Surg 2011;45(3):122–128
43 Wood MD, Kemp SW, Liu EH, Szynkaruk M, Gordon T, Borschel GH. Rat-derived processed nerve allografts support more axon regeneration in rat than human-derived processed nerve xenografts. J Biomed Mater Res A 2014;102(4):1085–1091